UNIVERSIDADE DE LISBOA
FACULDADE DE CIÊNCIAS
DEPARTAMENTO QUÍMICA E BIOQUÍMICA

Organotypic brain slice cultures as a model to study supressors of amyloid-β toxicity relevant in Alzheimer's disease

Francisco Filipe Terra Silveira Schäller Dias

Mestrado em Bioquímica
Especialização em Bioquímica Médica

Dissertação orientada por:
Professor Doutor Cláudio M. Gomes
Professora Doutora Adelaide Fernandes

2020

Agradecimentos

Em primeiro lugar, gostaria de expressar o meu profundo agradecimento aos meus orientadores, Professor Doutor Cláudio Gomes e Professora Doutora Adelaide Fernandes, que demonstraram uma paciência inesgotável para me guiar pelo caminho certo, explicando sempre de forma clara quais os aspetos a melhorar. Sem o seu trabalho incessante este projeto não teria sido completado. Agradeço especialmente à Professora Adelaide por me esclarecer todas as dúvidas da forma mais calma e clara que eu poderia imaginar.

A ambos, expresso a minha enorme gratidão por me terem aceitado nos vossos laboratórios, introduzindo-me assim à verdadeira ciência por detrás das doenças neurodegenerativas. A ambos, um enorme obrigado.

Agradeço aos colegas do laboratório Protein Misfolding and Amyloids in Biomedicine. Os primeiros meses do mestrado conseguem ser os mais assustadores, principalmente as primeiras semanas a purificar proteínas, mas o ambiente acolhedor e espírito de entreajuda com que me receberam fez com que olhasse para esta etapa com outros olhos. Um obrigado em especial ao Guilherme por toda a ajuda nas diversas técnicas laboratoriais.

Agradeço também aos colegas do grupo Neuron-Glia Biology in Health and Disease por tudo o que me ensinaram ao longo deste percurso, desde a entediante extração de proteínas até à fascinante imunohistoquímica. A partilha das vossas várias ideias e opiniões ensinaram-me a olhar para os dados de outra forma e foram fundamentais para a escrita deste trabalho. Um obrigado em especial ao Alexandre por me aturar durante as longas horas de espera dos Western!

Não poderia deixar de agradecer aos meus amigos – Sofia, João e António que fizerem deste ano atípico uma experiência que nunca irei esquecer. As diversas conversas, jogos, almoços e tudo o mais foram indispensáveis para aliviar o stress da escrita da tese. Convosco a seu lado, qualquer um poderia concluir o mestrado!

Por fim, agradeço à minha mãe e irmãs por me terem acompanhado durante todo o percurso universitário, apoiando-me em todos os momentos de dúvidas e indecisões e celebrando sempre as conquistas das várias etapas.

Abstract

The accumulation of the amyloid-β peptide and its subsequent aggregation is followed by an initial neuroinflammatory response, thought as one of the driving processes leading to neurodegeneration in AD. Rising evidence describe this disease as an evolving two-stage inflammatory process, where early stages involve glial ability to regulate AD related mechanisms, maintaining an homeostatic environment prior to plaque formation, whilst late stages are characterized by an amyloid plaque-associated exacerbated neuroinflammation and consequent neurodegeneration. The proinflammatory protein S100B is one of the glial response alarmins upregulated in AD, thought to play an important, although unclear role during the early stages of the disease. S100B has been known for its role as an inflammatory inducer in other neurodegenerative disorders, yet recent *in vitro* approaches established a new chaperone-like function for this protein, as a suppressor of Aβ aggregation. Therefore, we here investigated whether S100B plays a neuroprotective or disease-aggravating role against Aβ-induced toxicity in a hippocampal organotypic slice culture model. First, S100B and $A\beta_{42}$ were recombinantly purified in *E. coli*. Then, tissue slices were incubated with the recombinant proteins to mimic the AD environment and explore the dual role of S100B. In these conditions, our results suggest that in the dentate gyrus region, S100B is able to partially prevent microglia reactivity induced by $A\beta_{42}$. Also, it seems to regulate the $A\beta_{42}$ induced expression of inflammatory genes, such as IL-1β, without affecting neuronal death. Although these initial studies suggest that S100B might play a neuroprotective role against Aβ-induced neuroinflammation, further studies are needed to better ascertain whether the interplay between these two biomolecules can be used as potential therapeutic approach to ameliorate AD pathology.

Keywords: Alzheimer, Amyloid β_{42}, S100B, Neuroinflammation, Neurodegeneration

Resumo

Os eventos que levam à acumulação do péptido Beta Amiloide (Aβ) e à sua subsequente agregação são seguidos por uma resposta neuro inflamatória, num estágio inicial da doença de Alzheimer (AD), que se pensa ser um dos principais processos conducentes à neurodegeneração observada nesta doença. De facto, descobertas recentes descrevem esta doença como um processo neuroinflamatório bifásico em constante evolução, cujos estados iniciais são caracterizados pela regulação de processos relacionados com AD pelas células gliais, mantendo assim um ambiente homeostático precedente à formação de placas amiloides, enquanto estados mais tardios são caracterizados por uma exacerbada neuroinflamação relacionada com estas placas, conduzindo assim à neurodegeneração característica desta doença. A proteína pró-inflamatória S100B é uma das alarminas provenientes desta resposta glial aumentada em AD, que se pensa ter um papel importante, embora pouco claro, durante os estados iniciais da doença. Esta proteína tem vindo a ser conhecida pela sua função como indutora inflamatória noutras doenças neurodegenerativas, contudo uma recente abordagem *in vitro* estabeleceu uma nova função para esta proteína, semelhante a uma chaperona, capaz de suprimir a agregação do péptido Aβ. Deste modo, foi investigado neste projeto se a S100B assume uma função neuro protetora ou agravadora da toxicidade imposta pelo péptido Aβ no modelo de culturas organotípicas de hipocampo. Primeiramente, a proteína S100B e o péptido $A\beta_{42}$ foram purificados de forma recombinante a partir de *E. coli*. De seguida, as culturas organotípicas foram incubadas com ambas as proteínas de forma a mimetizar o ambiente proteico de AD e para explorar esta dupla função da S100B. Nestas condições, os resultados obtidos sugerem que na região do Dentate Gyrus, a S100B consegue prevenir, de forma parcial, a reatividade da microglia induzida pelo péptido $A\beta_{42}$. Além disso, parece regular a expressão inflamatória de genes induzida pelo $A\beta_{42}$, como por exemplo a expressão da citocina IL-1β, sem afetar a viabilidade neuronal. Embora estes resultados preliminares possam indicar que a S100B desempenha uma função neuro protetora face à neuroinflamação induzida pelo péptido Aβ, estudos adicionais são necessários para melhor confirmar se a interação entre estas duas biomoléculas pode ser usada como uma eventual abordagem terapêutica para melhorar a patologia de Alzheimer.

Palavras-chave: Alzheimer, Beta amiloide 42, S100B, Neuroinflamação, Neurodegeneração

Index

Figure Index

Table Index

Abbreviations

AD	Alzheimer's Disease
ADP	Adenosine diphosphate
AIF	Apoptosis inducing factor
ALS	Amyotrophic Lateral Sclerosis
APOε4	Apolipoprotein E4
APP	Amyloid precursor protein
AQ	Aquaporin
ATP	Adenosine triphosphate
Aβ	Amyloid-beta
BACE1	β-site APP cleaving enzyme 1
BBB	Blood brain barrier
CAA	Cerebral amyloid angiopathy
CA	Cornus Ammonis
CD	Cluster of differentiation
CMA	Chaperone mediated autophagy
CNS	Central nervous system
CSF	Cerebrospinal fluid
CX3CR1	CX3C chemokine receptor 1
DAM	Disease associated microglia
DAMPs	Damage associated molecular patterns
DG	Dentate Gyrus
DNA	Deoxyribonucleic acid
EEAT	Excitatory amino acid transporter
E-NMDA	Excitatory NMDA
FAD	Familial AD
FTD	Fronto-temporal dementia
GABA	γ-aminobutyric acid
GFAP	Glial fibrillar acidic protein
GLT1	Glutamate receptor 1
GSK-3β	Glycogen synthase kinase 3β
HIC	Hydrophobic interaction chromatography
HMGB1	High mobility group box 1
HSC	Hippocampal slice cultures
Iba	Ionized calcium binding adaptor molecule
IDE	Insulin degrading enzyme
IDP	Intrinsically disordered protein
IDR	Intrinsically disordered region
IL	Interleukin
iNOS	induced Nitric Oxide synthase
iPSCs	Induced pluripotent stem cells
LOAD	Late onset AD
LPS	Lipopolysaccharides
LRP1	Low density lipoprotein receptor related protein 1
MAPK	Mitogen activated protein kinase
MAP	Microtubule associated protein
MMP	Matrix metalloproteinases
mRNA	Messenger ribonucleic acid
mtDNA	Mitochondrial DNA
NEP	Neutral endopeptidase
NFT	Neurofibrillary tangles
NF-κB	Nuclear factor-kappaB
NLRP3	NOD-like receptor family pyrin domain containing 3
NMDA	N-methyl D aspartate

NO	Nitric oxide
NT	Neuropil threads
OBSC	Organotypic brain slice cultures
OHSC	Organotypic HSC
P2Y12R	G-protein coupled purinergic receptor for ADP
P^{75NTR}	p75 neurotrophin receptor
PAMPs	Pathogen associated molecular patterns
PD	Parkinson's Disease
P-gp	P-glycoprotein
PICALM	Phosphatidyl inositol binding clathrin assembly protein
PRRs	Pattern recognition receptors
PSD95	Postsynaptic density protein 95
PSEN	Presenilin protein
PTM	Post translational modification
RAGE	Receptor for advanced glycation end-products
RNA	Ribonucleic acid
ROS	Reactive oxygen species
SEC	Size exclusion chromatography
S-NMDA	Synaptic NMDA
SP	Senile plaques
SR	Scavenger receptor
TLR	Toll like receptors
TNF	Tumor necrosis factor
TREM2	Trigerring receptor expressed on myeloid cells 2
UPS	Ubiquitin proteasome system

1.Introduction

1.1.Alzheimer's Disease

Between diseases that cause dementia, such as Lewy Bodies dementia or Frontotemporal dementia, Alzheimer's Disease (AD) is the most common one. This disease is characterized by being mostly sporadic (95%), although around 1% of AD patients have inherited mutations in genes associated with amyloid-beta (Aβ) processing, leading to Aβ aggregation and deposition, which precedes neurofibrillary and neuritic changes with an apparent origin in the frontal and temporal lobes, hippocampus and limbic system [10, 13-15].

1.1.1.Pathology, Progression and Staging

According to some authors [6, 16], the pathology of AD can be diagnosed using a combination of features, both macroscopic and microscopic which alone are not specific of AD, but rather their combination strongly supports the AD diagnosis. Moving deeper into the macroscopic features, many authors reported most cases of AD brains, after a post mortem analysis, show clear signs of cerebral cortical atrophy involving the frontotemporal cortex [17], accompanied by posterior cortical atrophy, resulting in the typical brain shrinkage know to affect AD brains, which is followed by the enlargement of frontal and temporal horns of the lateral ventricles (Fig. 1.1). Other macroscopic features found in AD are the hippocampus and amygdala atrophy, also accompanied by the temporal horn enlargement [18] and loss of pigmentation [19]. Despite none of these features being unique to AD, when observed along with the microscopic features, their presence strongly suggests is an AD brain.

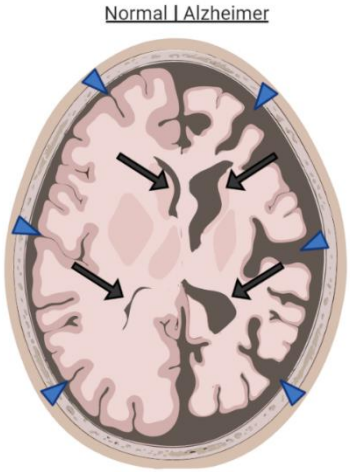

Figure 1.1 Macroscopic features of Alzheimer's Brain. Alzheimer's brain shrinkage is characterized by the widening of sulci and narrowing of gyri (blue arrow heads) compared to the normal brain. Brain atrophy is followed by the enlargement of frontal and temporal horns of the lateral ventricles (black arrows). Adapted from [6].

These microscopic pathological features of AD can be separated in three different parts: one related to molecular aggregation, other related with cellular loss and the last one related with inflammatory processes. The first part, directly linked with disease diagnosis, is comprehended by the accumulation of both Aβ and Tau, responsible for the two main lesions found in AD: senile plaques (SPs) and neurofibrillary tangles (NFTs), respectively. These legions, given enough time, slowly promote microglial activation (and consequently neuroinflammation), neuronal death, and synaptic loss through a series of processes, ultimately resulting in dementia. [6, 17, 19].

Many authors have tried to characterize the progression of the AD pathology in the brain since early times. In 1991, Braak and Braak observed a characteristic pattern of NFT and neuropil threads (NT) – composed of unmyelinated axons, dendrites and glial cells - throughout the brains of AD patients and

were thus able to propose a detailed scheme for the progression of NFT changes in AD – Six Stages of Braak (Fig. 1.2) [2]. Stage **I** and **II** are referred as "transentorhinal stages", since the neurons from this region are generally the firsts to develop NFT and NT. In these stages there is also a mild involvement of the hippocampus, while only a few NFT are visible in isocortical areas. The two "limbic stages", Stage **III** and **IV**, are characterized by a severely affected entorhinal region and the appearance of the first "ghost tangles"- extraneuronal NFT, released upon neuronal death, and by the presence of a moderate number of NFT in the hippocampus, while the isocortical region remains mildly affected. Stages **V** and **VI**, as the name "isocortical stages" suggests, show a progressive spread of NFT and NT to the isocortical regions in stage V, ending up as one of the severely affected regions in stage VI, along with the entorhinal region and hippocampus, accompanied by a large number of "ghost tangles" in the entorhinal region.

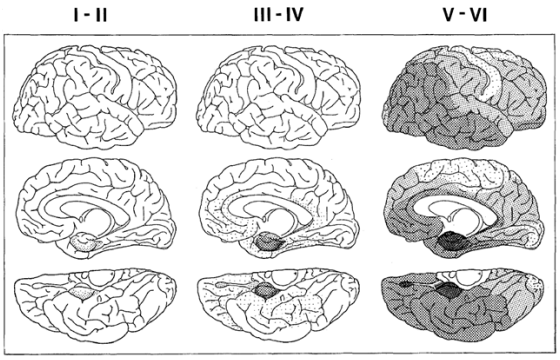

Figure 1.2 Braak stages in Alzheimer. Spreading of NFT is illustrated by a system of 6 stages. Extracted from [2].

To enlighten the progression of Aβ deposition in the brain, Thal et al. studied the formation of Aβ deposits in brains from demented and non-demented patients with AD-related pathology and patients with any relation with AD, proposing a five-phase system describing Aβ deposition in the brain [20]. Brains in phase 1 show Aβ deposits only in neocortical regions, appearing as small diffuse plaques, while no other brain region is affected. Phase 2 is characterized by the spread of the previous Aβ deposits to the allocortex, including the entorhinal region, while other areas remain devoid of Aβ deposits. From the allocortex, Aβ then spreads to the diencephalic nuclei and striatum in phase 3, while the previous regions show increased Aβ deposition. Phase 4 is characterized by the first involvement of several brainstem nuclei, with only a few plaque-like formations and finally in phase 5 the spreading of Aβ deposits reaches the cerebellum, as well as the remaining brainstem nuclei. Bearing these phases in mind, it is possible to establish a hierarchically involvement of brain regions, with Aβ deposition starting in the outer regions of the brain - neocortex, and progressively spreading to the adjacent, inner regions. Furthermore, and interestingly, the phases of Aβ deposition correlate with those of NFT progression proposed by Braak, specifically, AD brains exhibiting Aβ phases from 3 to 5 also show NFT stages from III to VI, whereas non-demented patients showed Aβ phases from 0 (meaning no Aβ deposition) to 3 and NFT stages ranging from 0 to III.

1.1.2.Molecular hallmarks - Tau and Aβ aggregation

The formation of intraneuronal filaments, or NFT, due to Tau aggregation is not only found in AD, but also in various neurodegenerative diseases, such as Fronto-temporal Dementia (FTD), Parkinson's Disease (PD), Amyotrophic Lateral Sclerosis (ALS), among others. Thus, it is imperative to understand the role of Tau and which processes promote Tau aggregation and toxicity [21].

Since the microtubules have a key role in neuronal structure and function, Tau (Fig. 1.3A), as a microtubule-associated protein (MAP), is predominantly expressed in these cells of the central nervous system (CNS). Early studies [22] have shown most of Tau to be found inside axons, promoting the assembly of microtubules, acting as their stabilizers and regulating motor proteins binding to microtubules [23, 24], thus having an important role in axonal transport of material from the neuronal cell body to the synapses.

In AD, the decreased Tau affinity for microtubules is one of the processes responsible for NTF formation, and a few post translational modifications (PTM) can modulate this affinity [25], the most common one being phosphorylation (Fig. 1.3B). Indeed, it has been shown Tau hyperphosphorylation to be correlated with AD. The majority of the sites phosphorylated in Tau flank the microtubule binding domains of the protein [26], decreasing the aggregation preventive effect of these regions, allowing the microtubule binding domains to self-aggregate into protofilaments [27]. Thus, phosphorylation of Tau by kinases, such as Glycogen synthase kinase 3β – GSK3β and mitogen-activated protein kinases – MAPKs [28, 29] decrease Tau affinity for microtubules, destabilizing them and freeing Tau (Fig. 1.3C). Unbound Tau, being an intrinsically disordered protein (IDP), adopts a random coiled structure and with its microtubule binding domain exposed, is then one step closer to the beginning of the aggregation process.

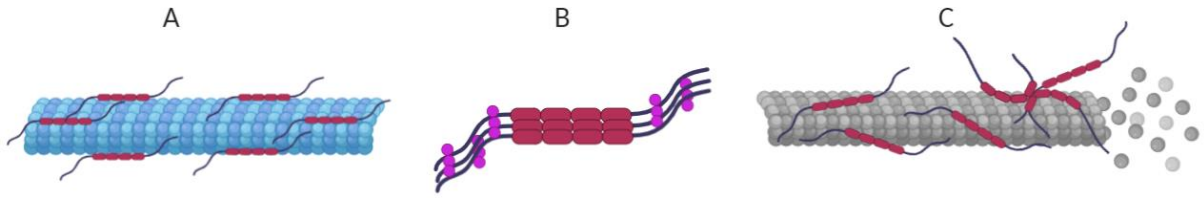

Figure 1.3 Tau as a microtubule binding protein. Tau is found bound to microtubules, stabilizing them (A). The progression of AD leads to Tau hyperphosphorylation, depicted as purple dots (B), freeing it from the microtubules, who start to disrupt (C).

The amyloid precursor protein (APP) is a transmembrane protein expressed in various tissues and is located around the synapses of neurons. This protein can be processed along two major pathways (Fig. 1.4): the α-secretase and β-secretase pathways. In the α-secretase pathway, this enzyme cleaves the Aβ region in the middle, releasing a large soluble APP fragment, α-APP, and the leftover is later processed by γ-secretase into p3 ($A\beta_{17-42}$) [30]. In the β-secretase (BACE1) pathway, this enzyme cleaves the protein before the Aβ region, releasing a long, but shorter than in the α pathway, soluble fragment, β-APP. The resulting peptide is then processed by γ-secretase, which cleaves it in several regions, forming the abundant $A\beta_{40}$ and the amyloidogenic $A\beta_{42}$, which differs in two amino acids, Ile41 and Ala42.

Some heritable mutations result in an accumulation of Aβ, like APP mutations and PSEN1/PSEN2 mutations. These mutations will increase β-secretase cleavage or γ-secretase cleavage, respectively, leading to early-onsets of AD, the familiar cases [14, 15].

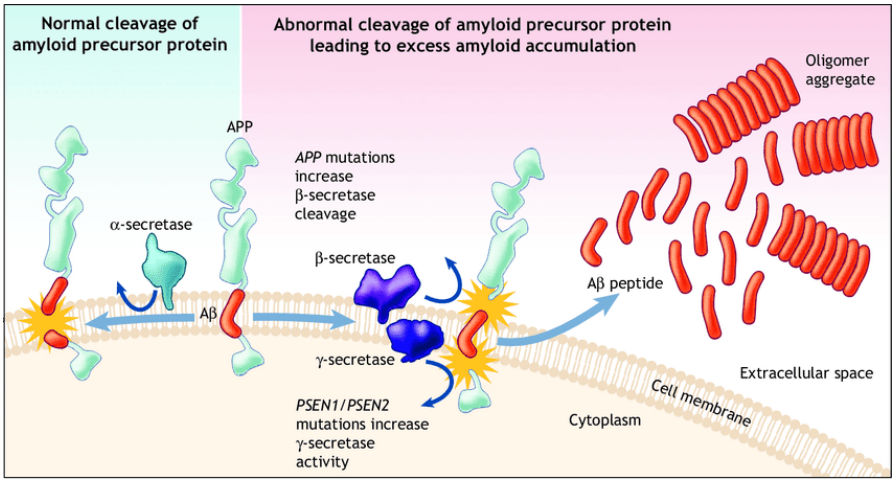

Figure 1.4 Proteolytic cleavage of APP. APP sequential cleavage by β-secretase and γ-secretase originates the amyloidogenic peptide-amyloid beta, which after aggregation, deposits in the extracellular space as fibrils, forming amyloid plaques. Extracted from [10].

The Aβ peptide, being an IDP, does not fold into a defined tertiary structure and has an intrinsically disordered region (IDR). This region can mediate some interactions, can adopt different conformations

when binding to different molecules and can be modified by post translational modifications, allowing different interactions depending on its chemical composition. However, this region contains a higher proportion of polar or charged amino acids, has a lack of tertiary structure and forms different conformations in dynamic equilibrium with each other [31].

The aggregation propensity of every protein is encoded in its sequence, being called aggregation prone region. This region is typically composed of 5-15 amino acids, has high hydrophobicity and low net charge and has a high tendency to form β-strands that can interact with each other (via strong backbone hydrogen bonds), forming a β-sheet structure.

Thus, between conformational changes, and due to the lack of a defined tertiary structure, the aggregation prone region of Aβ and Tau are exposed, which promotes their aggregation and amyloid fibril formation, a favorable energetic state. These amyloid fibrils have a rigid and well-defined cross-β structure: various cross-β protofibrils linked to other protofibrils by side-chain interactions, and each protofibril is composed by a super molecular stack of β-sheets. Thereby, the formation of amyloid plaques, as the ones seen in AD, are the direct consequence of amyloid fibrils assembly [32].

With this in mind, understanding the formation of these aggregates is of the utmost importance. To this end, the amyloid aggregation mechanism must be analyzed and separated in simpler molecular events that allows us to start from the protein monomer, follow its aggregation steps into oligomers and reach the endpoint, the mature amyloid fibrils.

These molecular events can be separated in two major categories: one responsible for the formation of new aggregates and other responsible for an increase of aggregate mass. The first category is composed of two distinct pathways leading to fibrils formation (Fig. 1.5). The first pathway, or primary nucleation, occurs directly, and solely, from monomer spontaneous aggregation in solution (when the aggregation prone regions are exposed) into oligomers, and is the first step in the aggregation process, hence being the limiting step of amyloid aggregation. In the presence of a surface, monomer assembly can also be facilitated, thus promoting primary nucleation and fibril formation [32-34]. The second pathway is composed of two different molecular events, which depend on the existence of pre-formed fibrillar material: fibril fragmentation and surface-catalyzed secondary nucleation. In the fragmentation process, the existing amyloid fibrils can break at any given location, forming two new protofibrils, independently of the presence of monomers. In the secondary nucleation, the surface of existing fibrils serves as a catalyst for the formation of new aggregates depending on monomer concentration. However, is worth noting this secondary nucleation is different from the surface catalyzed primary nucleation, since in primary nucleation, any external surface, like lipid vesicles, can promote monomer assembly, yet in secondary nucleation, aggregates formation occurs directly in the surface of existing fibrils, therefore, the number of existing fibrils, and catalytic surfaces, increase over time, which in turn will promote the formation of new aggregates, as long as there are enough monomers in solution (autocatalytic feedback loops) [32, 34]. According to some authors [35], here lies the difference between the two major forms of Amyloid-β peptide linked to AD, $A\beta_{40}$ and $A\beta_{42}$. As stated previously, $A\beta_{42}$ has two additional amino acids, Ile41 and Ala42, that by being hydrophobic can decrease the "kinetic barriers of aggregation" imposed by primary nucleation, promoting monomer assembly. However, after fibril formation, the residue interaction weakens and loose some of its relevance in the secondary nucleation. Other authors have also shown that the aggregates formation is derived predominantly by secondary nucleation, although the $A\beta_{40}$ secondary nucleation is highly dependent on monomer concentration, and the primary nucleation has less prevalence to the overall $A\beta_{40}$ aggregation process than to the $A\beta_{42}$ aggregation process [34].

The second category is also composed of two distinct molecular events, responsible for the increase in aggregate mass, fibril elongation and monomer dissociation, being as simple as the addition of monomers to fibril ends or removal of individual monomers from fibril ends, respectively [32].

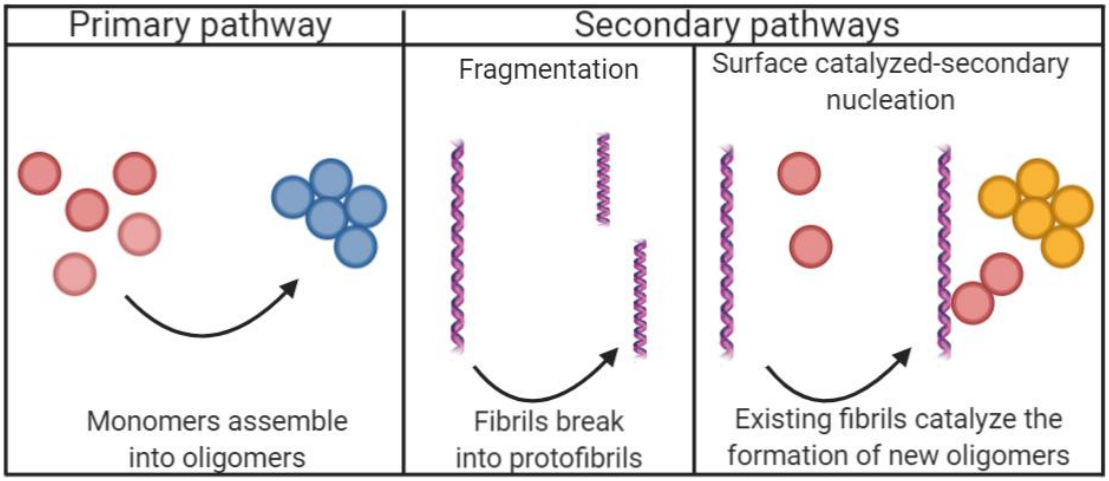

Figure 1.5 Amyloid aggregation mechanism. The primary nucleation, being the limiting step of the reaction, is responsible for the lag phase seen in amyloid aggregation kinetics. To notice, oligomers formed from the surface catalyzed-secondary nucleation are different than those from primary nucleation. Adapted from [7].

There is also another way of forming amyloid fibrils, as well as spreading them, known as seeding, where the addition of small, preformed aggregates induces the aggregation and misfolding of the soluble peptide by secondary nucleation, reducing the lag phase of the aggregation process [34, 36].

As discussed previously, these mature amyloid fibrils can propagate through the brain and act as catalysts for amyloid plaque formation in other areas of the brain, thus spreading the pathology phenotype [37].

1.1.3.Amyloid Cascade Hypothesis

The amyloid cascade (Fig. 1.6) is a hypothesis first presented in 1992 [38], proposing the idea that the accumulation of Aβ peptide, and the concomitant formation of neuritic plaques (mostly constituted by Aβ fibrils), may be the trigger for a collection of symptoms that ultimately leads to dementia, being the Aβ accumulation the primary cause of AD. Thus, the first event of the cascade would be the accumulation of Aβ peptide in the extracellular space, due to regulation of APP processing by APP/PSEN mutations, leading to abnormal production of the peptide. Furthermore, the ε4 allele of the Apolipoprotein E gene (ApoEε4) was shown to be a risk factor for AD by promoting Aβ accumulation [39]. Due to their characteristics, the Aβ peptides would then aggregate into oligomers, as well as assemble into extracellular, insoluble deposits, which can relocate in the synapses between neurons, disrupting neurotransmitter signaling between neurons and impairing the brain function. The continuation of the aggregation process (Aβ continues to aggregate into protofibrils and mature amyloid fibrils) activates the surrounding microglia and astrocytes, forming the amyloid plaques (deposits of aggregated Aβ surrounded by activated microglia and astrocytes) and gives rise to an inflammatory response which can damage surrounding neurons and alter their homeostasis [14, 40]. Although still not understood, it is thought this process initiates neuronal pathways leading to the activation of kinases targeting Tau (for example GSK3β and MAPKs), promoting the disassembly of Tau from the microtubules and facilitating its aggregation into NFTs. Aggregated Tau,

Figure 1.6 Amyloid Cascade hypothesis. Extracted from [5].

by not being bound to microtubules, leads to their destabilization, impairing the axonal transport to and from the synapses, resulting in synapse dysfunction and degeneration. Furthermore, NFTs themselves can be prejudicial to neurons through a toxic gain of function, for instance, by blocking axonal transport, resulting in neuronal dysfunction, degeneration and even apoptosis [21, 41]. As neurons continue to degenerate and die, the brain atrophy spreads through all the brain and it starts to shrink, resulting in dementia [6, 19].

1.1.4.Amyloid aggregation and clearance

The Aβ monomers formed by cleavage of APP can be exported to the cerebrospinal fluid (CSF) and to the blood circulation through the Blood Brain Barrier (BBB) (Fig. 1.7) [42]. Extracellularly, some Aβ monomers aggregate into oligomers and fibrils which can then be phagocyted by microglia, as well as astrocytes and can be degraded by proteases secreted from both neurons and astrocytes (Fig. 1.7) [43].

Intracellularly, unfolded Aβ monomers can be marked to degradation in the Ubiquitin-Proteasome System (UPS) through sequential conjugation of ubiquitins or can be degraded by Chaperone-Mediated Autophagy (CMA) through the hydrolases in the lysosomes. However, once large aggregates start to form, the proteolytic activity of these two pathways becomes impaired, as the large aggregates cannot be degraded, blocking proteasomes and affecting CMA, also impairing the clearance of other damaged/abnormally folded proteins, which is toxic to the cell and can even lead to apoptosis [44, 45]. As AD progresses, compensatory mechanisms start to function – macroautophagy – aiming to degrade large oligomeric species. Nevertheless, macroautophagy dysfunction is correlated with disease progression since the maturation and transport of autophagosomes are known to be impaired in AD due to reasons still not well understood [45]. In fact, Simonovitch et al. showed autophagy to be inhibited in Apoε4 astrocytes, resulting in a less efficient Aβ degradation [46].

Extracellular Aβ can be degraded by proteases expressed from neurons and astrocytes, some of the most studied ones being neprilysin and insulin-degrading enzyme (IDE). Neprisylin, or neutral endopeptidase (NEP), is a membrane-bound zinc metalloendopeptidase and was found to be the major Aβ catabolic pathway in the brain [47]. In the scope of AD, NEP mRNA and protein levels were found decreased in the hippocampus and temporal gyrus, areas vulnerable to plaque development [48], while studies using AD animal models observed the NEP knockout [49], or its administration [50] resulted in amyloid-like deposits and behavioral deficits or lowered the Aβ levels and plaque load, respectively. IDE, a zinc endopeptidase, despite its putative role in insulin degradation, can also degrade extracellular Aβ, probably due to the enzyme specificity towards cross-β structures [51], and indeed, various studies correlate either IDE knockout in mice, or decreased levels in AD brains with losses in Aβ degradation and consequent Aβ accumulation [52, 53]. Moreover, other peptidases, such as endothelin-converting enzyme, and matrix metalloproteinases (MMP), can also degrade extracellular Aβ [42].

Microglia, called “the macrophages of the brain”, express many of the surface receptors that recognize Damage Associated Molecular Patterns (DAMPs), such as Aβ, called Pattern Recognition Receptors (PRR). Upon Aβ binding to receptors, a series of signaling cascades will lead to microglial activation and consequent secretion of proinflammatory mediators, contributing to the inflammatory status characteristic of AD (to be discussed later) [8, 54]. Among these receptors are Complement receptors, Scavenger receptors, Toll-Like receptors (TLR), Receptor for Advanced Glycation End products (RAGE) and NLRP3 (which is not a surface receptor but also recognizes Aβ in the cytoplasm) [8, 55]. Furthermore, triggering receptor expressed on myeloid cells 2 (TREM2, - also a microglial surface receptor), is known to regulate the phagocytic clearance of Aβ by microglia and regulate pro-inflammatory cytokine production [56]. In 2013, Jonsson et al. analyzed genome variants from an Iceland population and associated them with the genome of the participant AD patients, having found the mutation R47H in TREM2 [57], which decreases microglial response to amyloid deposition (resulting in defective Aβ clearance, increased amyloid plaque toxicity and neuronal dystrophy) [58], presents a significant risk factor of AD. Other molecules, such as CD33 and copper can also influence microglia phagocytic activity [42].

There are also evidences of RAGE being responsible for Aβ uptake in neurons [59, 60]. Some authors showed a co-localization of extracellular Aβ to the intracellular space and mitochondria using

Aβ antibodies and intracellular neuronal markers. However, when blocking RAGE, or in RAGE deficient neurons, intracellular Aβ was diminished, and neurons presented a reduced mitochondrial dysfunction [61].

Besides these degradation pathways, extracellular Aβ can also be exported from the brain to the blood via BBB or CSF absorption, which in fact represents the clearance of half of the Aβ in the human brain [42]. Due to the BBB selectivity, for the transport from brain to blood occur, specific transporter proteins are required. Two of them, the first being phosphatidylinositol-binding clathrin assembly protein (PICALM), is known to promote the internalization of the low density lipoprotein receptor related protein 1 (LRP1), an astrocytic membrane receptor which recognizes Aβ, and since astrocytes are in contact with blood-vessels, it plays a major role in Aβ clearance from the brain [62]. Interestingly, the authors also found PICALM to be reduced in the endothelium of AD brains, which was correlated with an increased Aβ accumulation. Additionally, other transporter known to take part in Aβ clearance through the BBB, P-glycoprotein (p-gp), was shown to have its expression and function reduced in late onset AD [63], thus resulting in a less efficient Aβ clearance. Another receptor reported to regulate the clearance of Aβ from the brain was RAGE [64]. Some of the receptors present in the BBB-astrocyte vicinity, such as LRP1, P-gp and RAGE are also present in the Blood-CSF Barrier, mediating the absorption of Aβ from the CSF to the blood [42].

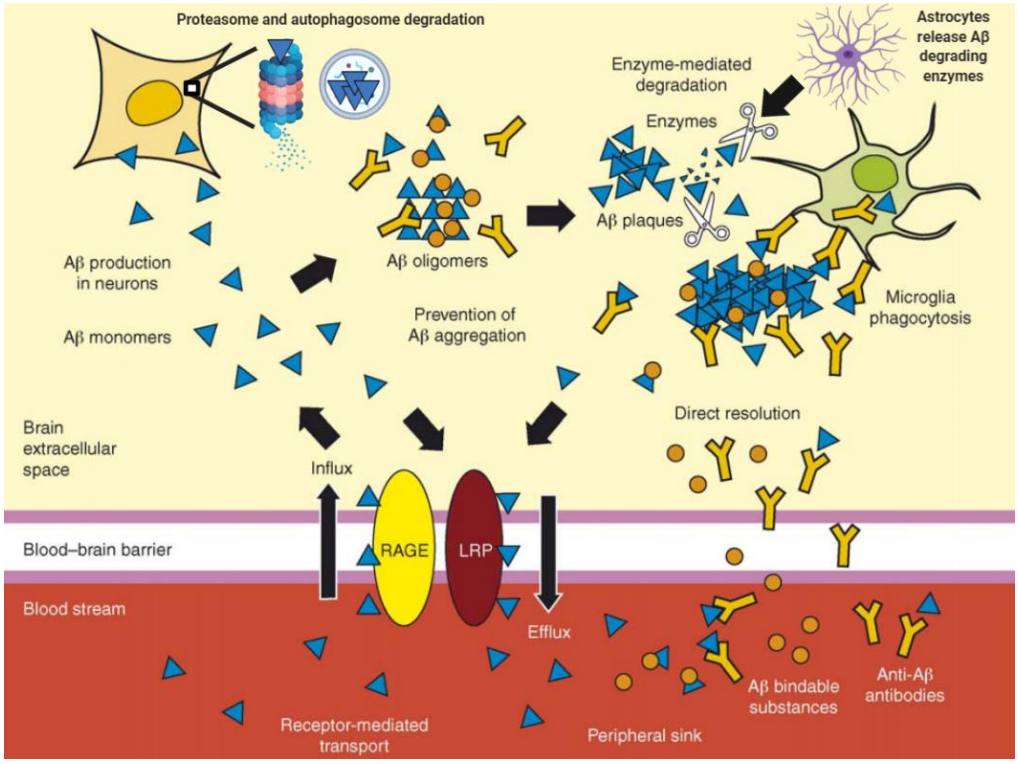

Figure 1.7 Principal Aβ clearance pathways. The amyloid-beta peptide, produced in neurons, can be degraded intracellularly by the UPS or the autophagy system. Once in the extracellular space, Aβ either travels across the BBB through RAGE and LRP to the blood or starts the aggregation process. Extracellular proteases can degrade Aβ, while microglia phagocytes both Aβ monomers and oligomers, delaying aggregation. Meanwhile, some peripheral anti-Aβ antibodies and molecules are also able to enter the brain and delay the amyloid aggregation process. Adapted from [9].

1.1.5.Cellular and Molecular Processes Altered in AD

As stated by the Amyloid Cascade Hypothesis, for AD to develop, a genetic/sporadic alteration resulting in the accumulation of Aβ must be present in the brain. However, apart from the events following Aβ aggregation described by the hypothesis, such as neuronal atrophy and synaptic dysfunction, this peptide's aggregation has other consequences at the cellular level.

Protein sequestration, a process in which endogenous proteins are sequestered by Aβ and Tau oligomeric species during their aggregation, is known to happen *in vivo* [65]. In fact, as shown in Olzscha et al. this event represents one of the proteotoxic pathways involving amyloidogenic proteins,

since the sequestered and impaired proteins were found to possess vital roles in a variety of essential cellular functions [66], such as transcription, translation [67] and cell architecture. Additionally, the protein quality control can also be impaired by these aggregates, thus being unbale to perform its function, resulting in the accumulation of other misfolded proteins.

Early studies involving the effect of Aβ oligomeric species in neuronal cells showed the peptide could induce oxidative stress and impair Ca^{2+} homeostasis [68, 69], triggering apoptotic pathways leading to neuronal death [70]. Since then, various authors provided insight about the initial mechanisms which ultimately result in neuronal apoptosis. These studies showed Aβ oligomers were able to interact with neuronal surface receptors, such as the p75 neurotrophin receptor ($p75^{NTR}$) [71] and APP itself [72], generating apoptotic signals. In fact, neurons expressing $p75^{NTR}$ in AD are preferentially affected by aggregated Aβ. However, on cell lines lacking this receptor, almost no Aβ toxic effect was observed [71]. Additionally, Aβ can also be recognized by RAGE at the neuronal surface, promoting the formation of free radicals, which will lead to oxidative stress [73, 74]. Furthermore, microglial Aβ-RAGE dependent activation releases tumor necrosis factor α (TNF-α), which is recognized by neurons via a TNF-α receptor, which in turn can also promote free radical formation and oxidative stress [75].

Mitochondrial dysfunction, a phenomenon also seen in AD neurons, is believed to arise from mitochondrial DNA (mtDNA) damage by both Aβ, resulting in defective mitochondrial respiratory chain proteins, specifically complexes I, IV and V, and decreased membrane potential [76, 77], which leads to reduced ATP production and formation of reactive oxygen species (ROS) causing mitochondrial and cellular damage [78]. Additionally, mtDNA damage can also arise from hyperphosphorylated Tau, as defective mitochondrial transport across the microtubules to and from the synapses impairs ATP production and promotes ROS formation [79]. Due to this dysfunction phenomenon, mitochondria lose their Ca^{2+} buffering ability and membrane potential, which initiates a cascade of events leading to the release of apoptotic factors to the cytoplasm, such as cytochrome *c* and apoptosis-inducing factor (AIF) [80].

Another pathway from which Aβ can induce neuronal and synaptic dysfunction is through excitotoxicity, involving the release of neurotransmitters such as glutamate from pre-synaptic to postsynaptic neurons. Early findings report the glutamate in the synaptic cleft can be taken up by surrounding astrocytes and converted into glutamine [81] and in fact, the presence of astrocytes surrounding the synapses is vital to neuronal survival [82]. In AD, Aβ was shown as able to induce extracellular glutamate concentration, either through an increased release of glutamate from neurons and astrocytes, or through decreasing the expression of astrocytic receptors responsible for glutamate uptake [83]. From the pool of receptors which glutamate binds to, the N-methyl-D-aspartate (NMDA) have a key role in the process of excitotoxicity. During normal signal transmission, synaptic (S)-NMDA receptors allow the entrance of calcium into the neuron, promoting anti-apoptotic and antioxidant signals, leading to neuronal survival. However, there are extra synaptic (E)-NMDA receptors, requiring high glutamate concentrations and glycine as co-agonist to function [84, 85], that impair S-NMDA signaling, promoting high concentrations of calcium to enter the neuron and activating various enzymes, such as calpain, resulting in neuronal and synaptic dysfunction through cell damage pathways [85]. Thus, the Aβ deposition seen in the synapses of AD brains results in an increased glutamate concentration in the synaptic cleft, which promotes the overactivation of E-NMDA receptors, ultimately leading to neuronal dysfunction and neurodegeneration (Fig. 1.8). Furthermore, some studies even suggest Aβ might interact with the NMDA receptors directly or through the synaptic protein PSD-95 [86, 87], worsening the excitatory effects of these receptors.

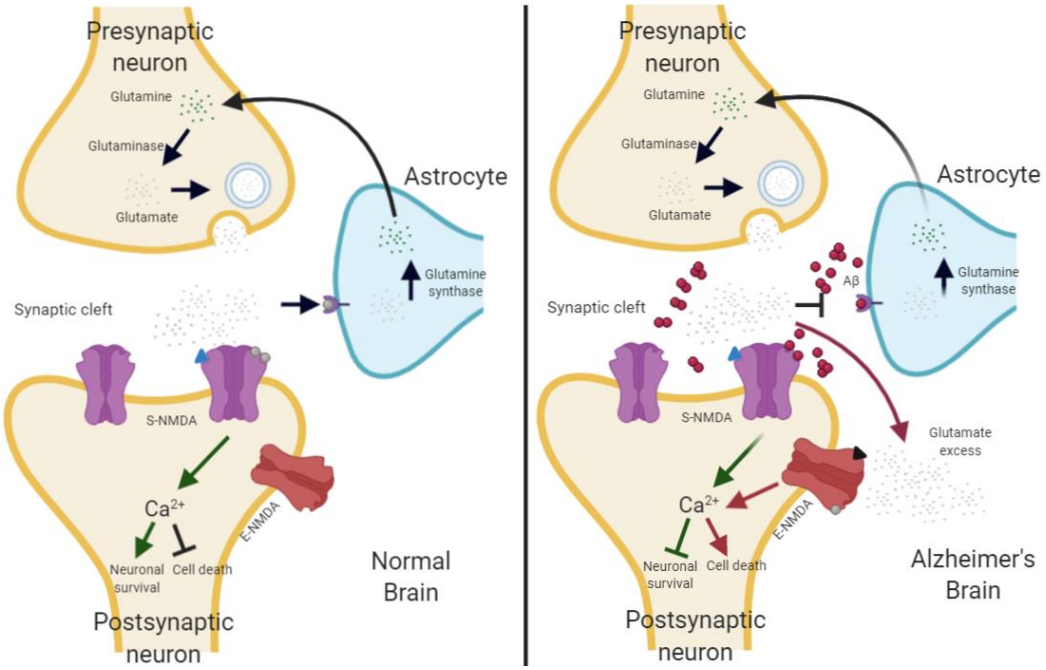

Figure 1.8 Excitotoxicity in Alzheimer. During normal brain function, Glutamate (grey) released from presynaptic neurons binds to S-NMDA receptors in the surface of postsynaptic neurons, in conjunction with its co-agonist D-serine (blue triangle), increasing intracellular calcium, promoting neuronal survival pathways. Astrocytes regulate synaptic glutamate concentrations through receptors - excitatory amino acid transporters (EEATs), converting it into glutamine (green), which is again converted into glutamate in neurons. In AD, Aβ binds both EEATs and S-NMDAs, leading to an excess of synaptic glutamate. This glutamate in excess, in turn, binds to E-NMDA in conjunction with its co-agonist glycine (black triangle), which blocks S-NMDA signaling and results in high intracellular calcium levels, promoting cell damage pathways. Adapted from [12].

Similarly, to the calcium dysregulation seen in AD, other metal ions, such as iron, copper and zinc are also dysregulated, presenting neurotoxic effects in the brain of AD patients. In the case of iron, a tight regulation is necessary, as a deficiency in this metal leads to neuronal under development, yet excessive levels result in increased ROS production [88]. Early reports have shown increased iron levels in AD brains [89], later being co-localized around senile plaques [90], increasing the expression of APP (and consequently Aβ) through inhibition of APP mRNA repressors [91]. Additionally, some authors suggested iron could bind Aβ and influence the formation of toxic species (or oligomers) *in vitro* [92].

Copper is required for the synthesis of neurotransmitters, and when present in low concentrations, development and maintenance of the myelin surrounding neurons is impaired, resulting in neuronal degeneration. However, as also happens with iron, when present in high enough concentrations in the brain, ROS production is enhanced [93]. In the scope of AD, recent evidences demonstrate that copper concentration increases with disease progression [94], while others suggest copper binds to Aβ and promotes the formation of toxic oligomeric species, exacerbating Aβ cytotoxicity [95].

Although primarily located between synapses, modulating the nerve impulse and promote the normal development and function of the brain, early findings report a zinc colocalization with senile plaques of AD brains [96], suggesting a role for zinc in senile plaque formation. Indeed, clinical studies have detected increased zinc in the brains of AD patients compared to age-matched controls, also correlated with increased ROS production [97]. Later findings provided insight about this role of zinc, having found that zinc not only binds Aβ, but also promotes its aggregation [98], forming aggregates with increased cytotoxicity [99, 100]. In addition to facilitating Aβ aggregation, zinc binding to the peptide also increases its resistance against degradation from NEP and IDE [101], increasing the overall amount of Aβ in the brain, and impairing synaptic signaling due to zinc scavenging. Moreover, a high zinc diet in an AD mouse model was shown to increase the expression of APP, regulate APP processing by inhibition of the α-secretase cleavage and promotion of the amyloidogenic β- and γ- secretase cleavage, increasing the amount of Aβ in the brain, as well as promoting its deposition [102].

In semblance to Aβ plaques and NFT, chronic inflammation, followed by neurodegeneration is also a hallmark of AD.

1.2.Neuroinflammation in AD

During the last decades, a sustained immune response, responsible for the chronic inflammation, has been highly accepted as a link between Aβ and Tau pathologies, exacerbating their neurotoxic effects. Furthermore, an increasingly number of studies have found an inflammatory response in both AD models and post mortem AD brains [103].

1.2.1.Inflammatory stages in AD

It is widely known that Aβ aggregation and plaque formation processes occur decades before the appearance of the first symptoms. In fact, the first occurring events would be the accumulation of intraneuronal toxic oligomeric species, which would then evolve to the extracellular deposits seen in AD [104]. The intraneuronal Aβ accumulation causes the release of inflammatory molecules from neurons, which are sensed by microglial cells (Fig. 1.9). Microglia would then become intermediately activated, also releasing inflammatory molecules that recruit yet more microglia to Aβ-burdened neurons [4]. This inflammatory response from glial cells and neurons is thought to contribute to homeostasis. However, when these mechanisms turn into pathological processes, both chronic and irreversible, the homeostasis status is disrupted, giving rise to the chronic neuroinflammation characteristic of AD [105].

Some of the currently available techniques detect Aβ and Tau when the respective aggregates are deposited at high concentrations in the brain, which is only detected during the later stages of preclinical AD [4], thus, cannot account as evidence for the early inflammatory response thought to precede aggregate deposition. This early inflammatory response is believed to start even before the formation of amyloid plaques, deriving from the accumulation of oligomeric species, evolving as a "disease aggravating" process as the disease progresses, ultimately leading to a cellular immune response. Indeed, some clinical studies found activated microglia and astrocytes in the brains of AD patients with low Braak scores [106], while other studies found astrocytes to be activated before the accumulation of Aβ plaques [107]. Additionally, an increased "pro-inflammatory" profile and a dysfunctional adaptive immune response was seen in the hippocampus of AD patients in an early stage of dementia [108]. Hereupon, the majority of evidence of this early inflammation rely on the enhanced amyloid burden in the CNS, thus one can presume the beginning of both Aβ and Tau aggregation is able to trigger a proinflammatory response prior to the appearance of the first symptom. Several studies with AD transgenic mice were performed to attest this possibility. Some found an upregulation of inflammatory cytokines, such as TNF-α, during the early stages of amyloid formation, which increased throughout disease progression [109]. Others found sites of glial activation, and consequent up-regulation of inflammatory markers, even before amyloid deposition, accompanied by an increased activity of the β-secretase enzyme, which all together lead to amyloid plaque formation in aged transgenic mice [110]. Additionally, a proinflammatory reaction in the hippocampus and cerebral cortex of AD transgenic mice, prior to amyloid plaque formation was also observed [111]. The upregulation of microglial activation markers, such as iNOS, was seen in pathological stages as early as

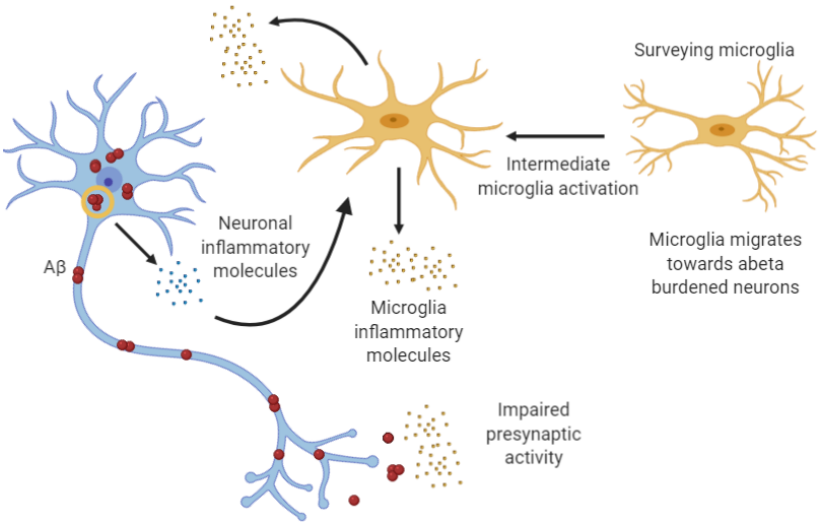

Figure 1.9 Early inflammatory stage of Alzheimer. Aβ-burdened neurons release inflammatory molecules that signal surveying microglia, which became reactive and release their own inflammatory molecules, recruiting more microglia to Aβ-burdened neurons and starting the inflammatory process. Adapted from [4].

intraneuronal Aβ accumulation, while microglia itself was being recruited to Aβ-burdened neurons, adopting an intermediate activated phenotype and releasing inflammatory markers, such as TNF-α and IL-1β during a pre-plaque stage, giving rise to the idea that Aβ-burdened neurons play a role as inflammatory agents in the early stages of preclinical AD [112]. As disease progresses, glial cells would be recruited to these neurons, increasing the production of proinflammatory molecules, and aggravating the toxic response to Aβ, leading to both the inflammation and immune response seen in the later stages of the disease.

These later stages, occurring during the symptomatic clinical phase, are usually characterized as an amyloid plaque associated process [4]. Early reports describe these structures as sites of persistent inflammation [113] and in fact, several studies over the decades allowed us to understand this inflammatory process. At this stage, microglia surrounding extracellular amyloid deposits are fully active, performing the phagocytosis of Aβ fragments and releasing inflammatory molecules, such as cytokines and ROS [114]. Certainly, the pronounced Aβ phagocytosis would control amyloid load and lessen neuronal damage. However, excessive exposure of microglia to Aβ and increasingly inflammatory mediators seems to lead to functional impairment [115]. Working together with microglia are activated astrocytes, located in the periphery of amyloid plaques [116], releasing their own inflammatory molecules, as well as chemokines to recruit yet more microglia to the amyloid plaques, exacerbating the inflammatory response, while sustaining functional impairment.

An inflammatory response is usually followed by a resolution process, in which homeostasis is recovered through phagocytic clearance of debris or clearance of apoptotic cells. However, the chronic neuroinflammation seen in the later stages of AD suggests these inflammatory-resolving mechanisms are dysfunctional [117]. Thus, both microglial and astrocytic atrophy results in a defective Aβ clearance, as well as an increased neuronal degeneration, and since both glial cells lose their ability to support neurons and maintain synaptic connections, neurodegeneration starts to spread [115, 118].

1.2.2.Altered Cellular Reactivity

As previously stated, both activated microglia and reactive astrocytes are found within and in the periphery of amyloid plaques, respectively, meaning this glial response is initiated due to the formation and deposition of Aβ. Furthermore, some reports state this glial response to also be triggered by NFT burden [19]. However, both astrocytes and microglia have various basal functions, which are essential to the homeostasis of the brain, and respond differently to the pathological aggregates formed in AD.

Microglia, as the resident immune cells of the brain, are in constant motion, utilizing their surface receptors to scan the surrounding areas for something that could be harmful to the brain. Upon recognition of an injury site, microglia migrate towards it and releases chemokines, recruiting yet more microglia, which then begin performing their housekeeping functions [118]. Such functions consist of synaptic remodeling through classical complement proteins and fractalkine receptor CX3CR1 [119, 120], as well as phagocytosis of dead or dying cells and even debris through scavenger receptors and Trem2 [121]. Additionally, when microglia recognize pathological agents, such as virus, bacteria and disease related self-aggregating proteins through their surface receptors, an inflammatory reaction is triggered, thus beginning the production of inflammatory cytokines, as well as chemokines that attract more microglia to the site where the pathological molecule was recognized [122], therefore, brain homeostasis is maintained. Nevertheless, aberrant housekeeping functions can easily lead to neurodegeneration. In AD, various genetic mutations can not only impair microglia response towards amyloid plaques but also its housekeeping functions [122], leading to an increased amyloid load and a defective clearance of debris as well as synaptic remodeling. Indeed, Grabert et al. found a correlation between downregulation of microglial genes related with environmental scanning and aging in the hippocampus, thus leaving this area susceptible to aging and protein deposition, as well as the neuroinflammation that follows, while young brain microglia appeared to have an increased response towards amyloid deposition [123].

Hereupon, not only genetic mutations, such as Apoε4 or Trem2 variants, influence microglial functions, but the microglial itself undergoes a gain and loss of functions during AD (Fig. 1.10) [124]. As described previously, microglia gain of function, in response to Aβ accumulation, is mostly associated with neuroinflammation, being the production of inflammatory cytokines the major

characteristic of this response, which involves the activation of the NLRP3 inflammasome, resulting in the production and secretion of IL-1β. Early findings showed that the increase of microglial IL-1β induces a reactive phenotype in the astrocytes of AD brains [125], followed by an increased S100B and GFAP expression. Additionally, Heneka et al. found increased levels of caspase-1 in the brains of AD patients, associated with NLRP3 activation and IL-1β production [126]. However, recent findings were able to detect an interaction between Aβ oligomers or fibrils and NLRP3, yet only the oligomers induced IL-1β secretion [55], thus the direct association between Aβ and NLRP3 remains unclear.

Regarding this gain and loss of function, a recent study indeed found a new distinctive type of microglia in both AD mouse models and postmortem tissue from AD patients, defined as disease-associated microglia (DAM) [127]. In this study, microglia demonstrated a transition between homeostatic microglia to DAM, with a significant increase of phagocytic and endocytic pathways, as well as increased immune response. This transition, which correlated with disease progression, was characterized by a downregulation of various homeostatic genes, such as P2Y12R and the CX3CR1, involved in microglia migration and neuron-microglia signaling, respectively, as well as upregulation of known AD risk factors, such as ApoE and Trem2. Furthermore, DAM was found localized in the vicinity of amyloid plaques and was shown to participate in Aβ phagocytosis, thus contributing to plaque dismantling and digestion [127].

Concerning astrocytes, their importance in the maintenance of brain homeostasis has increased significantly over the years. Several studies have unveiled the role of these glial cells in neurodevelopment, as was shown that astrocytes are not only required for synapse pruning (in conjunction with microglia), but also for synapse formation, maintenance and maturation [128]. Astrocytes also have a trophic supportive role, as they produce enough trophic factors required for neuronal and microglia maintenance, such as cholesterol, also vital for synaptogenesis [105, 129]. Additionally, astrocytes, through their end feet, participate in structures such as synapses and BBB, connecting various cellular components of the brain, creating the neurovascular unit [105]. This neurovascular unit is comprised of a capillary vessel surrounded by astrocytic end feet, while other end feet of the astrocyte are associated with synapses, forming a "tri-partite synapse". Astrocytes can then coordinate the neuronal activity from the synapses, with the blood flow within the capillaries – neurovascular coupling [130] – as well as regulate the water flux circulating across the brain through expression of aquaporins (AQ), which are also involved in the clearance of toxic solutes [131]. Moreover, since the BBB is one of the major amyloid beta clearance pathways, astrocytes, along with other cell types, contribute to the clearance of this peptide [132]. Interestingly, both human and mice carrying the APOE4 mutation were shown to be prone to BBB injury, leading to reduced Aβ clearance [133].

Due to being in proximity of synapses, astrocytes have a key role in synapse formation and maintenance. During neuronal activity, various neurotransmitters are released to the synaptic cleft, such as glutamate or gamma-amino butyric acid (GABA), among others, that are recognized by their respective receptors in the post-synaptic neuron, propagating the nerve pulse. Astrocyte also possess surface receptors that recognize these neurotransmitters, such as glutamate transporter-1 (GLT-1), controlling their concentration in the synaptic cleft [105]. As is now known, a deficiency in the re-uptake of glutamate leads to the over-activation of NMDA neuronal receptors, which causes neuronal excitotoxicity [84, 85]. Additionally, astrocytes release "gliotransmitters" to the synaptic cleft that serve as modulators of neuronal receptor activity, such as D-serine, ATP and even calcium, mediating synaptic transmission [134]. Another way the astrocyte is involved in this process is via release of the complement protein C3, which once recognized by the microglia C3 receptor, C3R, drives synapse elimination, a process also upregulated in the presence of Aβ [135].

In semblance to microglia, astrocytes also undergo a gain and loss of function in AD (Fig. 1.10). Indeed, due to being located in the vicinity of amyloid plaques, astrocytes not only engulf dystrophic neurites [136], but also prevent the diffusion of Aβ toxic species from the amyloid plaques [131]. However, to perform these neuroprotective functions, astrocytes need to become reactive, which not only alters their morphology (processes hypertrophy), but also changes their transcriptome. In fact, various studies showed reactive astrocytes to have a neurotoxic role in AD, as was the case of reactive astrocytes isolated from an AD mice model, which presented less neuronal neurotrophic support when compared with astrocytes isolated from healthy mice. Additionally, these isolated astrocytes also had presented a reduced uptake of Aβ when compared to wild-type astrocytes, as well as increased GFAP

expression [137], possibly linked to a downregulation of LRP1 [138]. Additionally, the role of astrocytes in Aβ degradation is diminished in AD patients with the APOε4, and mice expressing these allele presented less astrocyte mediated degradation of Aβ than those expressing other alleles [46]. On the other hand, some reports suggest that reactive astrocytes may also be involved in AD progression trough up-regulation of BACE1 and APP, thus increasing amyloid production, originating a positive-feedback loop [139, 140]. Furthermore, transcriptomic studies revealed aged astrocytes to down regulate neurotrophic factors (mainly cholesterol synthesis), while the synaptic elimination and innate immune response were up regulated both in mice [141, 142] and in humans [143]. These findings led to the classification of distinct reactive astrocytes types, A1 and A2, the first being neurotoxic and the latter neuroprotective [144]. Indeed, these A1 neurotoxic astrocytes were recently shown to loose neurotrophic, synaptic maintenance and phagocytic functions *in vitro*, while A2 reactive astrocytes had a reparative function, up regulating neurotrophic factors, promoting the survival and growth of neurons [145].

Besides the loss of neuroprotective functions and gain of neurotoxic ones in AD, reactive astrocytes also lose their ability to regulate synaptic transmission. Apart from the Aβ-induced impairment of glutamate transport, another way the astrocyte can inhibit synaptic transmission in AD is through Nuclear Factor κB - NF-κB activation. Studies using transgenic mice (IκBα knockout, an inhibitor of NF-κB) found an increased NF-κB activity in astrocytes [146], which interestingly was correlated with an increased complement protein C3 expression in the hippocampus, shown to have a role in neurogenesis [147]. Other studies correlated increased levels of C3 in neurons surrounded by astrocytes with reduced synaptic density, dendritic length and increased intracellular calcium [146]. Similarly, increased C3 levels were also found in primary astrocyte cultures treated with Aβ, or in both AD mice models and post mortem AD brains [148], therefore, since synaptic elimination is driven by C3R activated microglia [135], one can presume the increased C3 secretion from astrocytes to the extracellular space would activate microglia, mediating synapse elimination. Finally, the excess of calcium in the brain leads to calcineurin activation, a phosphatase seen to have increased activity in the hippocampus of both AD patients and mice models [149, 150], that is correlated with an increased astrocytic immune response and hypertrophy [151].

Various studies over the years suggest a correlation between the impairment of the BBB integrity and AD [131], and since astrocytes compose one of the main components of the BBB, reactive astrocytes may also have a role in this phenomenon. Due to having the same pathological protein in common, Cerebral Amyloid Angiopathy (CAA) is usually present in AD brains, although its only usually diagnosed during autopsy. While the $A\beta_{42}$ peptide mainly aggregates in the extracellular space, the $A\beta_{40}$ tends to accumulate in the blood vessels walls of the BBB, originating CAA, characterized by hemorrhages in the brain [19]. Nevertheless, in AD and CAA mouse models, and human AD brains, some authors found not only a disrupted blood flow associated with vascular Aβ accumulation, but also a distinct astrocytic reaction, prior to extracellular amyloid deposition [152]. Additionally, morphological and biochemical alterations of the BBB were found in these models [153] - mainly water and potassium channels downregulation, along with an increase in S100B-positive astrocytes [154], and the downregulation of astrocytic AQ in these models was shown to impair the drainage of solutes from the aging brain, such as Aβ [155], thus impairing Aβ clearance and contributing to its accumulation. Indeed, a study using an AD mouse model showed that AQ4 deficiency increased Aβ accumulation, promoted CAA, exacerbated astrocyte hypertrophy and aggravated cognitive impairment [156]. Therefore, adding up, the BBB disruption, the altered blood flow, both impaired solute drainage and impaired nutrient signaling lead to neuronal impairment.

Thus, these glial cells have a key role in CNS homeostatic maintenance and defense, ensuring a normal brain function. However, once dysregulated, these cells are tightly correlated with brain dysfunction and neuropathological processes, ultimately leading to neuronal and synaptic loss, as is the case of AD (Fig. 1.10) [157].

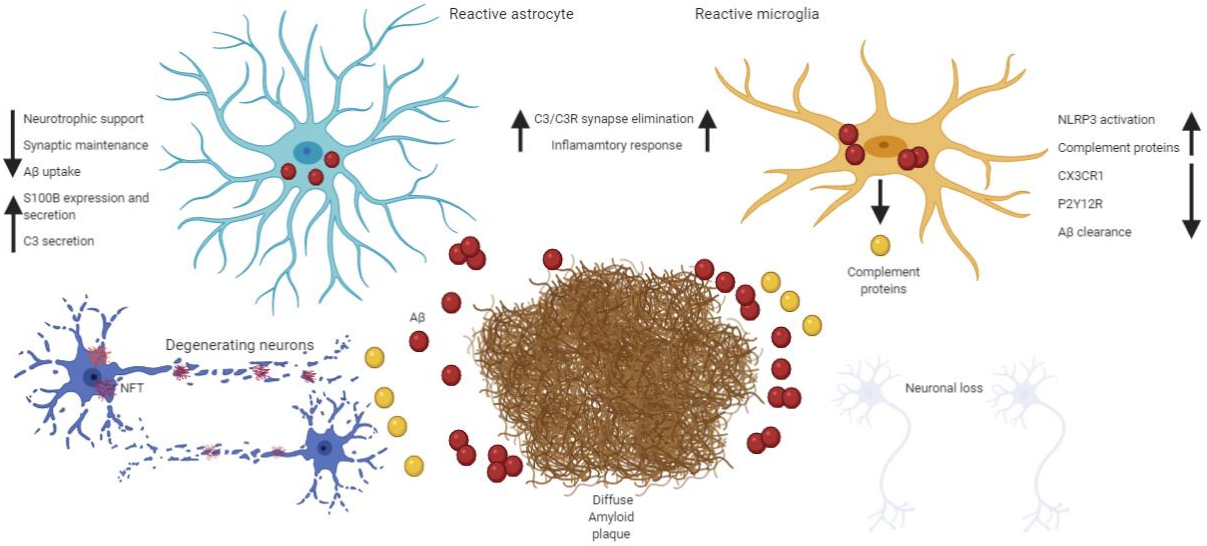

Figure 1.10 Altered cellular reactivity in Alzheimer. Altogether, the downregulation and upregulation of homeostatic and toxic functions, specifically, from glial cells lead to neuronal and synaptic loss.

1.2.3.Inflammatory processes in neurodegeneration

Initially, the chronic inflammation seen in AD was suspected to arise from the neuronal damage following Aβ deposition. However, it is now known the interaction of Aβ with microglial cells results in their activation, followed by a release of various pro-inflammatory cytokines. It is from the imbalance between the two types of cytokines (pro- and anti-inflammatory) that neuroinflammation arises [103, 115]. As stated previously, the interaction between Aβ and microglial surface receptors, the PPRs, would trigger Aβ phagocytosis and microglial activation, which would then release cytokines, neurotoxins and chemokines to the extracellular space, recruiting yet more phagocytic microglia to the surrounding Aβ plaque, therefore, the continuous secretion of proinflammatory cytokines and neurotoxins would only contribute to the aggravation of the neuroinflammation, which in turn is prejudicial to neuronal survival, resulting in neurodegeneration [119, 158]. Furthermore, the disassembly of Tau from microtubules due to Tau hyperphosphorylation can induce abnormal microglial activation and proinflammatory cytokine production, also giving rise to a pathologic cycle of aberrant Tau production, neurotoxicity and neuroinflammation [119].

In addition to the previously described microglial phagocytic activity mediated by TREM-2, several other microglial surface receptors can bind and internalize Aβ.

From these surface receptors, the two scavenger receptors, SR-A and CD36, can bind Aβ and initiate an inflammatory response [159-161]. Some findings show a direct association between SRA-I, an isoform of SR-A, and the internalization (and clearance) of Aβ [162, 163]. In the first study, mice treated with anti-SRI-I antibodies showed a reduction in clearance and internalization of Aβ, while in the second study, longer periods of microglial activation led to a reduced SR-I expression and consequent reduced Aβ clearance. Concerning CD36, CD36-deficient mice exposed to fibrillar Aβ showed a decreased proinflammatory cytokines expression (Il-1β and TNF-α) and ROS production [164], thus suggesting a role for CD36 in microglia activation in response to fibrillar Aβ. Interestingly, there are also reports of higher expression of CD36 in human AD brains or brains with Aβ plaques, while no CD36 was detected in healthy brains [165]. Furthermore, a surface receptor composed of CD36, $\alpha_6\beta_1$-integrin and CD47 was found capable of recognizing fibrillar Aβ, mediating its phagocytosis, ROS production and cytokine expression [166]. Besides this complex, there is evidence about the formation of a heterotrimeric

complex comprising CD36, TLR4 and TLR6 [167]. The recognition of Aβ by CD36 triggers a signal that induces TRL4-TLR6 heterodimerization, leading to microglia activation and production of proinflammatory mediators, such as IL-1β.

The membrane proteins TLRs were also shown to recognize Aβ on their own. In spite of TLR4 main role being the recognition of lipopolysaccharides (LPS) [168], it can also be involved in Aβ mediated clearance and microglia activation. In particular, the activation, and internalization of the fibrillar forms of the peptide by microglia is dependent on the interaction between TLR4 and its coreceptor CD14 [169, 170]. This was shown through usage of antibodies against TLR4, which resulted in a reduced TNF-α and IL-6 expression, as well as phagocytic clearance, after exposure to fibrillar Aβ [171]. In addition to TLR4, TLR2 has also been associated to Aβ mediated response, as knocking down microglial TRL2 resulted in a reduced expression of TNF-α, IL-1β, IL-6 [172] and microglia presented a reduced Aβ clearance when exposed to the fibrillar form of the peptide [173].

NLRP3, a major component of the NLRP3 inflammasome, is part of the family of NOD (nucleotide binding domain)-like receptors and can be activated by diverse molecules, such as ATP, bacterial toxins and Aβ, among other DAMPs. In 2008, it was shown that microglial caspase-1 activation requires the activation of this inflammasome [174]. Aβ, recognized by CD36 complex, is phagocyted and later internalized by the lysosomes, destabilizing them, resulting in the release of cathepsin B - a lysosomal protease acting as a signal for NLRP3 activation and IL-1β production and secretion. In fact, as also shown that the recognition of Aβ by CD36 promotes the dimerization of TLR4 and TLR6, originating a signal for NRLP3 transcription and activation [167, 175].

RAGE, a multiligand surface receptor of the immunoglobin superfamily, not only binds AGE, but also S100 proteins, High mobility group box 1 (HMGB1), Aβ and other molecules [73, 163, 176]. Various authors showed the Aβ-RAGE interaction increases Aβ load in the brain and promotes NF-kB activation [73, 176, 177], mediating the expression of proinflammatory cytokines that might cause the neuronal damage and learning/memory deficits characteristic of AD [178].

Thus, exists a cooperation between microglial surface receptors to internalize and degrade Aβ (Fig. 1.11), resulting in the activation of microglia and production of proinflammatory mediators, giving rise to the neuronal inflammation present in AD.

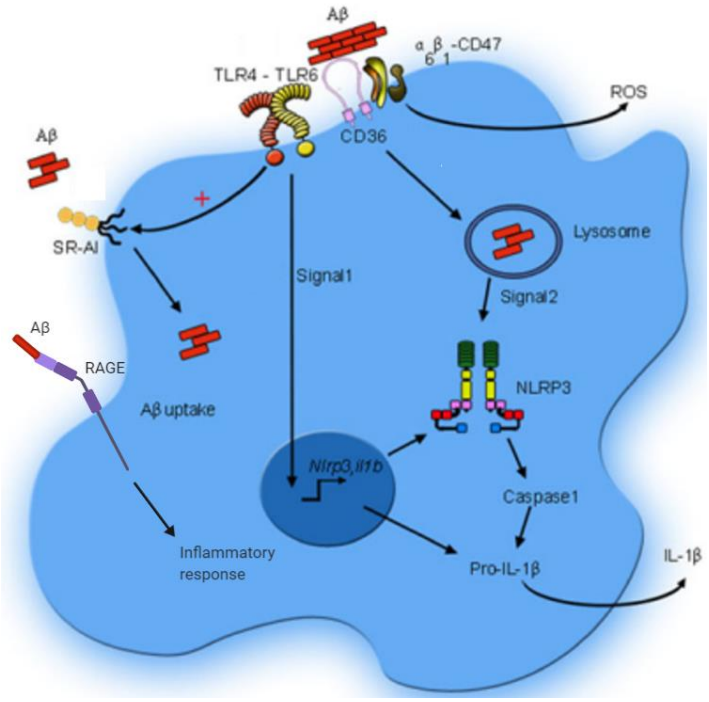

Figure 1.11 Cooperation of microglial receptors in response to Aβ. The recognition of oligomeric forms of Aβ by the scavenger receptor complex triggers a signaling cascade leading to Aβ clearance and NLRP3 activation. The recognition of Aβ by RAGE also triggers an inflammatory response from microglia. Adapted from [8].

Similarly to microglia, it has been shown that Aβ was able to activate astrocytes in the AD brain [116], through usage of confocal microscopy and an anti-glial fibrillar acidic protein (GFAP) antibody (specific for activated astrocytes), showing that reactive astrocytes surround and penetrate Aβ plaques. When activated, astrocytes overproduce proinflammatory cytokines, such as IL-1β, IL-6 and S100B, which could be involved in the inflammatory process characteristic of AD [179], and indeed early evidence shows that Aβ induces cytokine expression by astrocytes, particularly, IL-1β and S100B [180, 181], which in turn can promote APP mRNA expression in neurons, leading to an increased Aβ production [182]. Furthermore, one of the most important astrocytic functions is the release of chemokines, which regulate microglial migration towards regions with neuroinflammation [115].

Additionally, the Apolipoprotein gene, predominantly expressed in astrocytes, also influences Aβ mediated degradation and internalization by these cells [46, 183].

Besides the microglial receptors and astrocytes responsible for the initiation of an immune response in the brain, other risk factors related to AD, such as diabetes, cardiovascular disorders, traumatic brain injury and age are also capable of inducing an immune response [103]. Additionally, a previous study had shown patients with said risk factors, containing the Apo-ε4 allele were more susceptible to cognitive decline when compared with healthy subjects or patients without the Apo-ε4 allele [184]

1.2.4.Alarmins

Alarmins are endogenous proteins/peptides with immune activating properties, released upon immune induction or cell death/injury [185], acting as danger signal molecules in response to tissue damage, exacerbating the inflammatory response, thus are also known as damage-associated molecular patterns-DAMPs, and differ from pathogen-associated molecular patterns-PAMPs, since the latter only stimulates the inflammatory response in the presence of exogenous pathogens [186]. Alarmins are characterized by diverse groups of peptides, metabolic products and proteins expressed in different cell types and different cellular compartments, such as Aβ, HMGB1, ROS, S100 proteins, among others, and their recognition by the pattern recognition receptors-PRR, such as TLRs, triggers various signaling cascades that ultimately lead to immune system activation and initiation of the inflammatory response [187]. Furthermore, although being a diverse group of molecules, alarmins have a few common characteristics: have, for the most part, non-immunological functions inside the cells, are released in response to traumatic injury, have cytokine-like and chemotactic functions and take part in the resolution of inflammation [186]. Additionally, certain receptors, such as RAGE, can also recognize some alarmins and mediate diverse cellular pathways resulting in NF-κB activation.

In order to initiate the inflammatory response, alarmins first activate leukocytes (corresponding to microglial cells in the brain), leading to the production of inflammatory mediators, both cytokines and chemokines that end up recruiting more microglial cells to the sites of injury [188], with alarmins also contributing to the chemoattractive process, originating a cycle of microglia activation and recruitment until the inflammation is resolved [185]. Furthermore, while the majority of alarmins induces the release of pro-inflammatory cytokines through binding to microglial surface receptors, such as TLRs, RAGE and CD36, once in the intracellular space, some alarmins such as fibrillar Aβ or ATP can trigger the NLRP3 inflammasome activation, activating caspase-1 and promoting the production and release of active IL-1β and IL-18, both with key roles in the immune response [185, 187]. Indeed, brains from AD patients were shown to have higher amounts of active caspase-1 than age-matched controls [189]. On the other hand, AD mouse models deficient in NLRP3 or caspase-1 were found to be protected from AD pathology, due to decreased fibrillar Aβ-induced IL-1β production, whilst NLRP3 deficiency also improved microglial -mediated Aβ clearance and reduced Aβ deposition, preventing spatial memory dysfunction [189] Interestingly, NLRP3 impairment in aged wild type mice was shown to have a neuroprotective effect, as the mice brains were protected from age-related cognitive decline, even in the absence of Aβ pathology, thus suggesting the NLRP3 inflammasome has a key role in brain inflammation [190].

Apart from Aβ, the alarmins represented by the S100 protein family have also been implicated in AD. The S100 family of calcium-binding proteins is comprised of low molecular (9-14 kDa) monomeric subunits with tendency to form (usually) dimers or oligomers of higher molecular mass [191]. More specifically, the S100 protein family belongs to the EF-hand superfamily, characterized by a helix-loop-helix domain, which contains ligands that bind the calcium ions in the loop, thus these proteins function as calcium sensors inside the cell [186]. Although being expressed in a wide variety of tissues, each member of the S100 protein family has a distinct expression pattern and possess several characteristics of alarmins [192]. These proteins are constitutively expressed in various tissues, regulating various cellular functions, such as cell growth and differentiation, protection from oxidative damage, protein phosphorylation and secretion, among others [193]. However, upon brain injury, such as in Aβ pathology, reactive microglia release chemokines which mediate the migration of surrounding astrocytes to the Aβ plaques, where S100 proteins expression and secretion is rapidly induced, regulating the immune response through RAGE and TLRs binding, acting as DAMPs [185].

1.2.5.S100 Proteins in AD

Considering the inflammation stages seen in AD, the early stages are characterized by the release of inflammatory mediators from reactive glial cells, including S100 proteins, that in low concentrations contribute to homeostasis prior to amyloid plaque formation, thus having a neuroprotective role against Aβ pathology [105]. However, at later disease stages, the Aβ-mediated up-regulation of inflammatory molecules from glial cells exacerbates neuroinflammation through diverse cellular pathways in a concentration-dependent manner, leading to neuronal degeneration and synaptic loss [4]. Therefore, in AD, S100 proteins may exert a variety of functions depending on their concentrations. Indeed, over the years several studies linked different S100 proteins to different pathological processes, either exacerbating or ameliorating AD pathology, ranging from APP processing (S100B, S100A1, S100A7, S100A9), modulation of Aβ levels (S100B, S100A1, S100A6, S100A8, S100A9), Tau post translational modifications (S100B, S100A1, S100A6) and protein inclusions to calcium dysregulation [191]. In fact, these proteins ability to sense and bind calcium is not only vital for calcium homeostasis (through modulation of calcium release and uptake), but also for conformational changes that expose a hydrophobic cleft in the proteins, allowing the interaction of S100 with their respective targets, and some S100 proteins also have the ability to bind both zinc and copper, metals found elevated in AD senile plaques [191].

Specifically, from the S100 family, S100B is the most studied in AD. This protein, mostly secreted by astrocytes [194, 195], was shown to have both neurotrophic and toxic effects in the brain, depending on its concentration [196]. Low levels of S100B, at the nanomolar range (Fig. 1.12), promote neuronal survival and dendrite extension [197, 198] via S100B-RAGE dependent NF-κB activation [199, 200]. Additionally, nanomolar levels of S100B were shown to protect LAN-5 neuroblastomas from $A\beta_{25-35}$ -induced toxicity, also in a RAGE-dependent manner [201]. However, when at the micromolar range, S100B was shown to have a toxic effect (Fig. 1.12), leading to an increased cellular death, increased release of proinflammatory mediators [202, 203] and leading to oligodendrogenesis and myelination impairment during neuronal development [204], all of these effects through a RAGE-dependent binding. Moreover, as a calcium-sensor, intracellular S100B regulates the calcium levels of CNS cells [205-207]. Indeed, astrocytes from S100B knockout mice present a reduced calcium handling capacity, whereas neurons from the same culture do not [206]. Furthermore, Aβ-induced calcium dysregulation in isolated astrocytic cultures was followed by S100B up-regulation, suggesting a protective mechanism against calcium dyshomeostasis [208]. Recent studies demonstrated that S100B also acts as a zinc scavenger in the brain, regulating its levels, which indirectly affects calcium levels and inhibits excitotoxicity, giving rise to a new neuroprotective role of S100B through this metal-buffering activity [209].

In the context of AD, various studies found elevated S100B levels in the hippocampus, temporal lobe and cortex of AD patients [195, 210], mainly surrounding amyloid plaques, although elevated S100B levels were also found in the CSF of AD patients, which was correlated with increased brain atrophy [211]. Recent findings also corroborate these findings in mice. Increased levels of S100B were

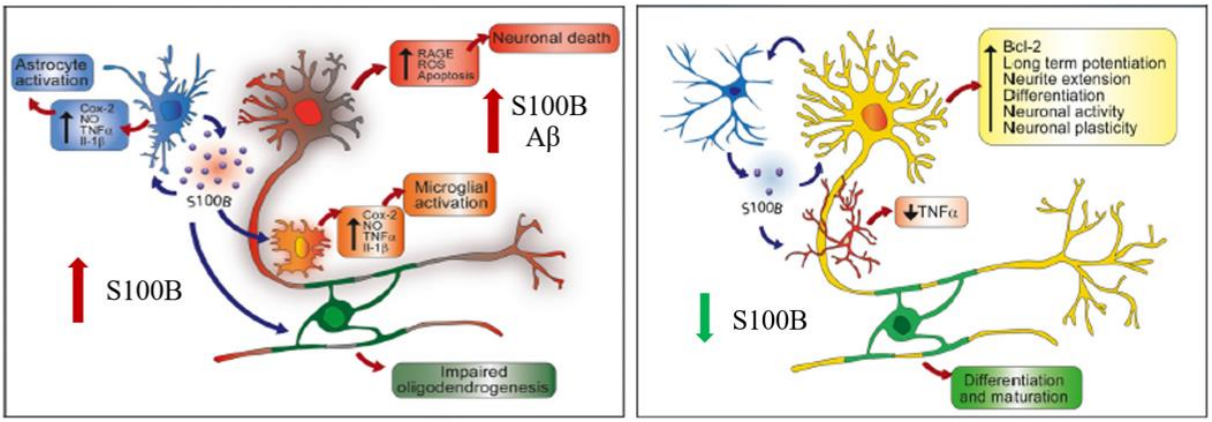

Figure 1.12 Differential effects of S100B concentrations in the CNS. When at nanomolar concentrations (right), S100B promotes neuronal survival and oligodendrocyte differentiation and maturation. However, when at micromolar concentrations (left), such as in AD due to the increased Aβ load, S100B acts as an alarmin, mediating several inflammatory processes leading to neuronal loss. Adapted from [11]

detected in the cortex of APP23 mice and localized in the border zone of amyloid plaques [192]. Indeed, the Aβ-induced release of TNF-α and IL-1β was suggested to activate astrocytes and induce the expression and secretion of S100B (Fig. 1.12) [212-214], and this S100B overexpression was thought as being responsible for the evolution of diffuse, non-fibrillar amyloid deposits into dystrophic neuritic plaques [215-217], which was later supported by two studies: one in PSAPP AD mice models knocked out for S100B, where removal of S100B resulted in a reduction of plaque load, GFAP-positive astrocytes, phosphorylated Tau and Iba-1 positive microglia [218], and other in a transgenic AD mice model overexpressing human S100B, where S100B overexpression resulted in an increase of both Aβ levels and deposits number, along with increased astrogliosis and microgliosis [219]. Furthermore, S100B is thought to not only promote APP mRNA and Aβ production in neurons [182], but was also shown to increase BACE1 activity, leading to higher levels of β-APP and C-terminal fragments, including β-CTF or C99, an amyloidogenic fragment, promoting Aβ-mediated neuroinflammation [219]. Additionally, S100B binding to RAGE and TLRs induces the production of proinflammatory cytokines, such as TNFα and IL-1β, in several cell types, as well as mediating both microglial and astrocytic migration [196], thus confirming its role as an alarmin.

In the scope of Tau pathology, the high levels of S100B in the AD brains also correlated with Tau tangles [194]. Previous *in* vitro studies have also shown that S100B binds Tau in a calcium or zinc dependent process, inhibiting its phosphorylation [220]. S100B levels were found upregulated in mouse models expressing Tau, along with increased GFAP expression and decreased proteins involved in glutamate metabolism [221]. However, the knockout of S100B in PS/APP AD mice showed a decrease in dystrophic neurons positive for phosphorylated Tau [218]. Accordingly, S100B was demonstrated to promote tau hyperphosphorylation through GSK-3β activation, and this activation was RAGE dependent [222] Therefore, although the influence of S100B in tau pathology is still unclear, S100B has key roles in several other AD-related processes, having both protective and toxic functions depending on its concentration [191].

Since activated astrocytes overexpressing S100B were found in the periphery of amyloid plaques, some authors proposed S100B could interact with the Aβ peptide [1], which was confirmed *in vitro*. Through a calcium-dependent conformational change, a hydrophobic cleft is formed in S100B allowing the interaction between the protein and both the peptide monomers and its oligomeric and fibrillar forms, which was capable of suppressing $A\beta_{42}$ aggregation in a calcium-dependent manner (Fig. 1.13). Furthermore, S100B was also able to rescue the cellular viability of SH-S5Y5 cells exposed to $A\beta_{42}$, supporting a neuroprotective role for S100B in AD [1].

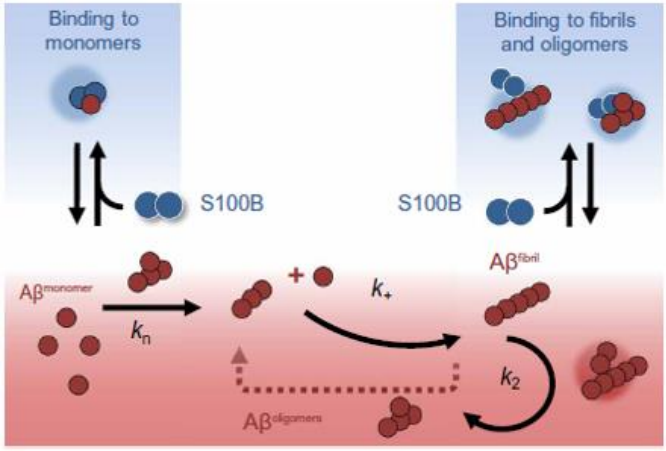

Figure 1.13 S100B interference in the amyloid aggregation mechanism. S100B binds both Aβ monomers and oligomers/fibrils, thus delaying the amyloid aggregation by suppressing the primary nucleation and interfering with secondary nucleation. Extracted from [1]

1.2.6.Models to study AD

The unique neurological changes occurring during AD progression are initiated several decades prior to the disease clinical diagnosis [6], thus being nearly impossible to study during the early stages of the disease. Hence, experimental models of AD are crucial means to achieve a complete understanding of AD pathophysiology, as well as to devise and evaluate possible treatments for this disease (Fig. 1.14) [3]. However, these models have their own drawbacks and limitations, since none of the available models can accurately replicate all of AD unique pathological features and their crosstalk, such as extracellular amyloid plaques, intracellular NFT and the neuronal and synaptic loss that follows [223].

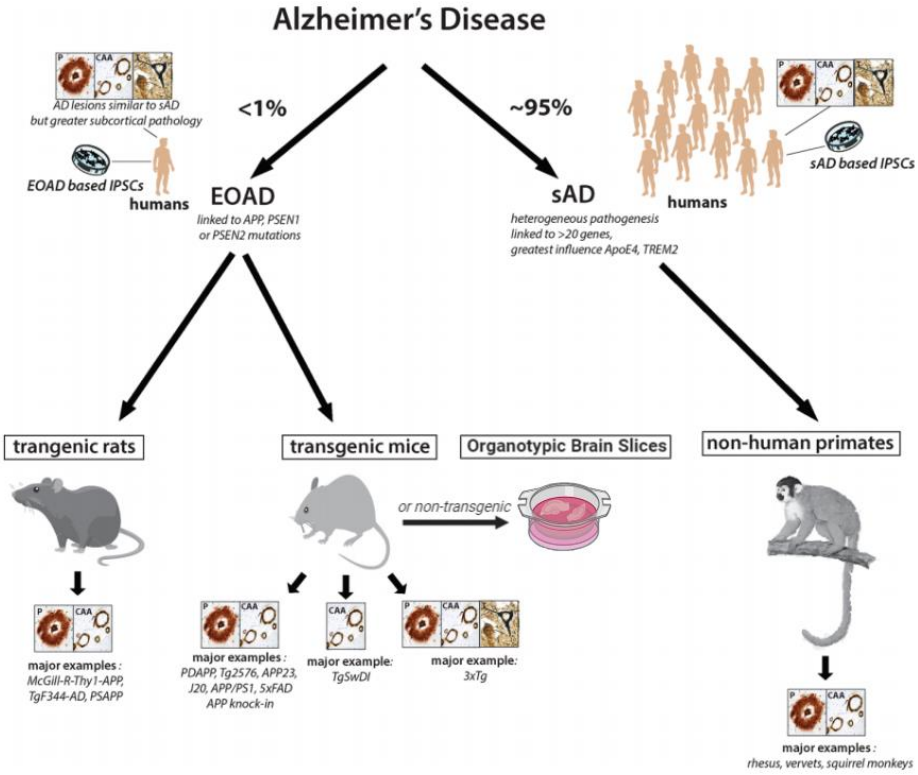

Figure 1.14 Experimental models in AD. In addition to non-human primates, dogs also develop AD-like pathology with age, thus also being an experimental model of sporadic AD. Adapted from [3].

1.2.7.*In vitro* Cell Models

In vitro cell cultures have been extensively used to study AD. This experimental model allows for rapid and direct interpretation of the pathological changes occurring in the various CNS cell types when in the presence of AD pathological agents, such as Aβ and Tau, which otherwise would be difficult to access *in vivo*, thus reducing experimental costs. Additionally, the screening of possible AD treatments is first performed in these models, as they enable the study of conserved molecular and cellular pathways, providing crucial information at a cellular level [223]. This is only possible due to the isolation of distinct cell types from their normal biological environment, which reduces the complex interactions between CNS cells.

Human neuroblastoma cell lines are frequently used as *in vitro* models to study AD since they have the capacity to differentiate into more neuron-like phenotypes after treatment with retinoic acid [224], allowing the identification of underlying mechanisms of key AD processes, such as APP processing, as well as showing the effect of compounds on Aβ production and oligomer formation, thus modulating Aβ toxicity and subsequent cell viability. Nevertheless, human neuroblastomas have their own limitations as an AD model. In spite of their human origin, these cell models do not mimic the cellular

interactions between neurons and glia occurring in the CNS during AD, thus inter-cellular pathological or neurological changes are not detected in these models [223].

Similarly, primary cultures of CNS cells from various species are extensively used to study the AD pathology. Specifically, primary rat hippocampal neurons are phenotypically closer to aged or adult neurons, in addition to being sensitive to chemical changes, thus providing a good model to study the pathophysiological processes occurring in neurons related to AD, such as the neuronal response to inflammatory markers and possible treatments to Aβ-induced toxicity [225], although as is the case of neuroblastomas, these cell models do not replicate the cellular environment of the CNS, neither its biochemical interactions. Furthermore, glia cell lines from rat, mouse or even humans are also used to ease the investigation of AD-related inflammatory processes and cellular pathways [226], such as glial-response upon Aβ induction. However, these experimental models have their own drawbacks, besides the ones previously described. Microglial cultures may suffer phenotypic changes upon viral infection, and their phenotype does not replicate that of aged microglia [226]. Additionally, recent findings detected differences at genetic [227] and functional [228] levels of microglia cell lines when compared to primary or *ex vivo* microglia.

Induced pluripotent stem cells (iPCSs), as their name suggests, can be differentiated into all cell types, including neurons and glia (Fig. 1.15). Several IPCS-derived neurons have been generated from both familiar and sporadic AD patients (sAD) [229], having shown increased Aβ production and Tau phosphorylation when compared with control iPCS-derived neurons, confirming the similar genetic background between iPCSs and donors [3]. Indeed, the identification of several AD related genes in iPCSs-derived neurons support these cells as a strategy to study underlying mechanisms of AD and disease modeling [230]. Additional advantages of this model compared to the previous ones comprise the detection of phosphorylated tau and amyloidosis [223], some of the unique AD pathological features, yet are not the ideal model to represent the normal brain environment in which neurons reside, surrounded by glia and the vascular system [230]. Moreover, iPCS might need extended culture times so that iPCS-derived neurons can be representative of mature neurons from aged patients. In addition, the epigenetic modifications of different donors can contribute to different phenotypes of iPCS-derived neurons [230].

Therefore, this typical cell cultures provide lack of insight about the complexity of the cellular and molecular mechanism that lead to the development of AD, thus a more complex, 3D model that recapitulates these cellular mechanisms occurring in the AD brain is needed to better model this disease [231].

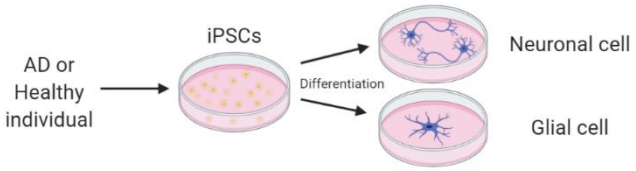

Figure 1.15 Representative image of iPSCs differentiation.

1.2.8.*Ex Vivo* Cell Culture Models – Organotypic Brain Slice Cultures

Organotypic Brain Slice Cultures (OBSCs) (Fig. 1.16) have the advantages of preserving the original tissue architecture and connections, as well as supporting all the central nervous system cell types [232], while being a relatively simple and inexpensive method. Between these cell types are microglia, astrocytes, oligodendrocytes and neurons [233], which are involved in the neuroinflammation process, thus representing a good model to study neuroinflammatory cascades in AD. Another major advantage of this model, in comparison with free cell models, is their ability to survive for longer periods of time, thus reducing culture costs [234]. Although the blood brain barrier, which plays a major part in Aβ clearance, is absent in this experimental model, this provides the ability to manipulate with relative ease the contents of the culture medium, which by being in direct contact with the slice cultures, allows the study of specific conditions, such as the excess of S100B in the medium, and how they affect the slice cultures [204, 235]. Additionally, due to its simple handling, OBSCs not only facilitate biochemical studies, such as immunohistochemistry, RT-PCR and Western Blot, but also ease the screening of possible treatments of neurodegenerative disorders [235].

The most commonly used brain region in the preparation of OBSCs is the hippocampus, as its neuronal loss and pathological changes are associated with various neurodegenerative diseases, including AD [235]. Indeed, in OBSCs from neonatal mice, both glial cells and neurons have been described as being representative of the corresponding cell type in the *in vivo* brain [236-238], and recent studies using human brain derived slice cultures showed this model was able to reproduce the neuronal activity and cell-to-cell connections of the brain [232], therefore, OBSCs serve as a model to study neurodegeneration, oxidative stress, neurotoxicity, neuroinflammation, neuroprotection and neurogenesis, among others [234].

In the context of AD, OBSCs have been extensively used to study this disease. Exposure of hippocampal slices to Aβ revealed neuronal damage and plaque-like deposits, with the consequent activation of microglia and peripheric astrocytes [239]. Thioflavin S staining also showed amyloid plaques surrounded by reactive microglia and reactive astrocytes in OBSCs [231]. Additionally, an increased caspase activity and increased cell death were detected in hippocampal slices exposed to high concentrations of Aβ [240]. The effect of GFAP absence was also investigated in hippocampal slices from transgenic mice exposed to Aβ. In this study, astrocytic processes were less organized in the periphery of amyloid plaques and could not cover them completely, thus suggesting GFAP might play an important role in the astrocytic response to Aβ [116, 239, 241]. Furthermore, it was demonstrated that microglia from OBSCs contribute to amyloid plaque clearance, thus representing that of the *in vivo* brain, and that young microglia might stimulate Aβ clearance in old tissues [242].

Nevertheless, although OBSCs represent a better model to study neurodegenerative diseases than free cell models, it also has its own limitations. Most of the OBSCs used to study AD originate from mouse models, either transgenic or non-transgenic, thus having the same limitations-to be discussed later [235]. In addition, this model cannot represent the neurological changes undergoing in AD, since the cultured slices, despite surviving long culture periods, still do not mimic the mature situation of the brain [234]. Furthermore, the presence of a blood brain barrier, which this model lacks, is of vital importance for the development of pharmacologic compounds, thus the screening of possible AD treatments is limited to alterations in the culture medium [235].

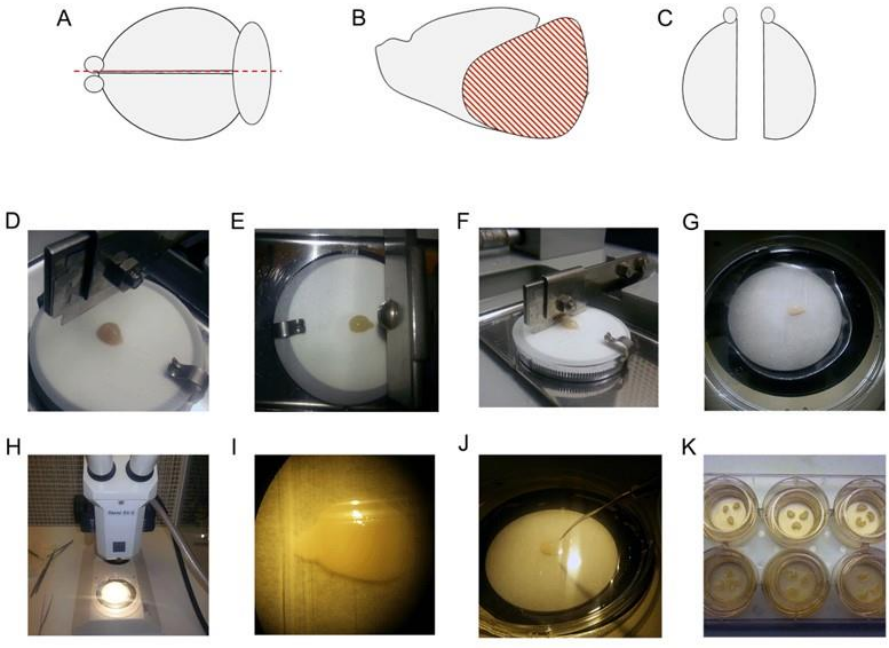

Figure 1.16 Representative image of the hippocampal brain slice cultures preparation process. (A) After mice decapitation, brains are removed and both hemispheres are separated. **(B)** Cerebellum and hindbrain are removed leaving the forebrain, **(C)** from where the hippocampus is removed. **(D-F)** Hippocampal slices are obtained using a McIlwain tissue chopper, **(G-J)** being then separated under a microscope and **(K)** placed into membrane culture inserts. Extracted from [272]

Therefore, a new model, mimicking both the complex brain cellular environment, the unique AD pathological features and the blood brain barrier is needed to find suitable therapeutic molecules against this disease [243].

1.2.9. *In Vivo* Models for AD

Various *in vivo* models, from several organisms, have been used to study the AD pathology. Simple organisms, such as yeast, worm and fly, although lacking some aspects of the normal human biology, namely a complex nervous system and adaptative immune system, provide a faster and less expensive model to not only study highly conserved molecular pathways related to AD, but also to screen AD ameliorating compounds [244], whereas more complex organisms, such as primates, dogs and rodents can recapitulate the majority of human pathological phenotypes, thus being primarily used in preclinical studies before human clinical trials [3].

Some of these models lack homologues for APP and β- and γ- secretases, as is the case of yeast, lack a sequence region homologous to human Aβ and the β-secretase activity to process full-length APP, as is the case of worms, or others, such as fly models, although having low levels of β-secretase activity also lack a sequence region homologous to human Aβ [244], thus in order to obtain a better *in vivo* model to study AD, one can create transgenic models expressing human genes related to this neurodegenerative disease, such as human Aβ (in the case of yeast models), human Tau, human APP, or even genes that regulate APP processing [244]. On other hand, more complex *in vivo* models, such as primates and dogs, share their Aβ sequence with that of human Aβ and also develop amyloid plaques and CAA with age, albeit these plaques have some differences when compared with that of aged-human AD plaques, as they are more diffuse and less abundant [3], thus these animals serve as models to study sporadic AD. Furthermore, behavioral tests can be performed in these models, and indeed those that develop amyloid plaques with age presented some, although few, behavioral abnormalities [3]. In addition, despite their Tau sequence being similar to human Tau, both primates and dogs do not usually develop severe tauopathy, therefore, although some phosphorylated Tau is detected, the absence of NFT and dystrophic neurites hinders the study of the specific molecular pathways leading to this disease hallmark [243], thus representing one of the limitations of these models. Other limitations include the lack of a complex nervous system (as is the case of yeast, worms and flies), the lack of standardized protocols for cognitive performance, and for non-human primates and dogs, their long lifespan and inter-individual variations also represent major drawbacks, as experiments are expensive and time-consuming [3].

On other hand, rodent models (Fig. 1.17) are easily accessible, easy to manipulate, have relatively short life-spans and the cognitive protocols are well defined [243]. In fact, rodent models, specifically transgenic mice, are one of the most used models in the study of AD pathology. Although wild-type mouse APP has a 97% sequence homology with human APP, this difference results in different amino acids in the Aβ sequence, which were shown to impair both Aβ aggregation and amyloid plaques formation in wild-type mice [3]. Indeed, various transgenic mice lines have been created, each with different mutations conferring both different phenotypes and pathological changes, such as plaque morphology, different APP processing and thus variable $A\beta_{40}$ and $A\beta_{42}$ production, as well as affected regions [244]. Usually, transgenic models are based on mutations in genes correlated with familiar forms of the disease (FAD), such as APP mutants, which normally increase the production of $A\beta_{42}$. One of the models based on APP overexpression is the Tg2576 mouse, which was shown to develop dense amyloid plaques, as well as dystrophic neurites, reactive glia and cognitive deficits starting at 11 months of age [245]. PSEN1/2 mutants, which modify mouse APP processing, increase $A\beta_{42}$ production without leading to amyloid deposition [243], therefore, double mutants of human APP/PSEN expression are used to highly accelerate both amyloid deposition and biochemical changes, as is the case of the 5xFAD mouse, developing amyloid plaques as early as 2-4 months of age, which were also surrounded by reactive glia. Additionally, neuronal loss, degeneration and impaired memory were observed at 4-6 months of age. However, no Tau pathology or NFTs were observed [246]. In fact, most APP overexpression models do not recapitulate the Tau pathology seen in human AD, thus several mutants expressing human Tau have been created, from yeast to rodents. In the case of rodents, the majority of models that develop tauopathy are based on FTD-linked mutations and have overt neurodegenerative

changes, such as reactive astrocytes and apoptotic neurons. However, it remains unclear whether these Tau aggregates and Tau-induced neurological changes are relevant to those of AD [243]. Nevertheless, the creation of double and triple mutants of human APP, PSEN1/2 and Tau overexpression provided a good platform to understand how Aβ and Tau crosstalk leads to neurodegeneration. A frequently used model is the triple mutant 3xTg-AD mouse, which was shown to develop extracellular amyloid plaques in the cortex at 6 months of age, surrounded by reactive astrocytes. Additionally, Tau pathology was only observed after amyloid deposition, starting at 12 months in the hippocampus and spreading to other regions in an age-dependent fashion [247], which correlates with the progression of Tau pathology in humans. Interestingly, both Aβ and Tau co-localized with the same neurons, suggesting that intracellular Aβ might influence Tau pathology. Furthermore, the presence of intracellular Aβ was also correlated with synaptic deficits at 6 months in the hippocampus [247].

Although these rodent models provide answers to vital questions about AD pathology, they still do not recapitulate all the unique features of the disease. Apart from lack of Tau pathology (possibly due to differences in the Tau sequence) in most of APP/PSEN mutants, these mutations represent those of familiar AD, characterized by the overexpression of Aβ, whereas the most common, sporadic form of the disease is attributed to deficits in Aβ clearance [3], thus transgenic animals are a poor model to represent sporadic AD. On the other hand, non-transgenic rodents (Fig. 1.17) have been shown to develop AD-like pathology and suffer from cognitive impairment during advanced stages of the disease, similar to that of late-onset human AD and other non-transgenic models (primates and dogs). However, similarly to the latter, no Tau pathology was observed in these models [223]. Additionally, endogenous proteins may behave differently in the presence of non-physiological levels of human proteins, resulting in reactions that may not be representative of what happens inside the human brain. Furthermore, one cannot accurately confirm that pathology derives from the expression of human APP, PSEN or Tau, since other APP products also possess amyloidogenic properties, thus promoting toxicity independently of Aβ [3]. Finally, the pathological processes leading to cognitive impairment in transgenic mice might be different than those of humans, since cognitive deficits occur in different disease stages in mice, namely prior or at the same time as amyloid plaque formation, whereas the human cognitive impairment is only detected many decades after plaque formation.

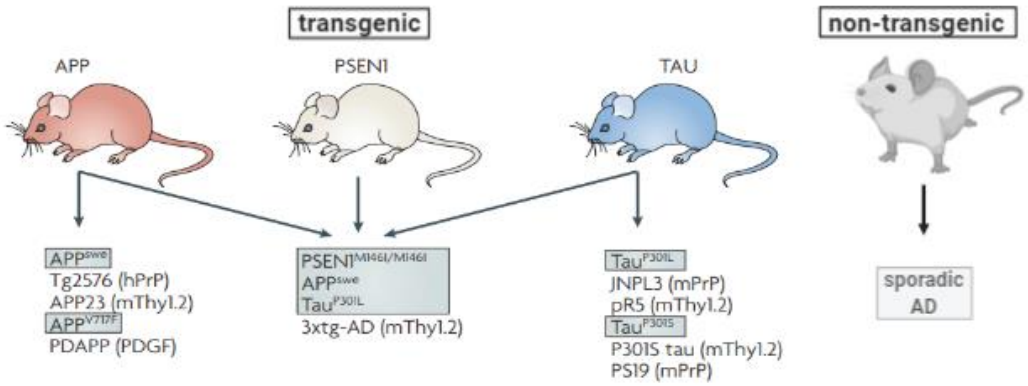

Figure 1.17 Representative image of in vivo rodent models to study AD. Adapted from [273]

Therefore, each model offers its own advantages whilst having disadvantages. Nevertheless, the combined use of *in vitro*, *ex vivo* and *in vivo* models contributed greatly to the understanding of AD pathophysiology.

2.Motivation

Since Alzheimer's neurodegenerative disease was first described by Alois Alzheimer over a 100 years ago, many of the underlying mechanisms leading to dementia and neurodegeneration have been elucidated, yet some remain unclear. As our lifespan grows, so does the likeliness of developing AD. However, over the past decades various attempts to find a preventive treatment to this disease have failed, despite passing preclinical testing in AD models. Researchers attribute this failure to the unique pathological features of AD in humans, which several animal models lack [223]. Indeed, extracellular deposits of insoluble Aβ, intracellular Tau aggregates and consequent overt neuroinflammation are unique features of human AD, having vital roles in the neurodegenerative process [38]. S100B, a pro-inflammatory calcium-binding protein is chronically up-regulated in AD, being mainly expressed by astrocytes surrounding the extracellular amyloid plaques. Recent studies found that S100B not only colocalizes with these extracellular deposits [192], but also binds $A\beta_{42}$ *in vitro*, suppressing its aggregation mechanism and toxicity [1]. Additional studies also associated the S100B metal-buffering activity to neuroprotective functions [209]. However, due to its pro-inflammatory role, S100B also takes part in neuroinflammation and several cellular processes, thus having a neurotoxic function when up-regulated [11]. Therefore, the dual role of S100B, as a neuroprotector suppressing Aβ aggregation, and as a pro-inflammatory cytokine remains to be investigated in more complex cellular models.

3.Objectives

The main goal of the present work was to investigate whether S100B could prevent $A\beta_{42}$ neurotoxicity or further potentiate it in Organotypic Hippocampal Slice Cultures.

To achieve this goal, we developed the following Tasks:

- Recombinant S100B and $A\beta_{42}$ were expressed in *E. coli* and purified using a previously established protocol;
- Organotypic hippocampal brain slices, prepared from neonatal wild-type mice, were exposed to different concentrations of $A\beta_{42}$ and S100B. An overall assessment of $A\beta_{42}$ and S100B levels in slices and media, glia reactivity, neurotoxicity and gene expression of inflammation markers was performed.

All together, these experimental approaches provided some insight on whether S100B ameliorates amyloid pathology or exacerbates it in this slice model.

4.Materials and Methods

4.1.S100B expression and Purification

S100B was expressed and purified following a previously established protocol (Botelho, Fritz et al. 2012). Chemically competent *E. cloni* express BL21 (DE3) cells from Lucigen (Wisconsin, EUA) were transformed with 1 µL of pGEMEX-2 S100B. Cells were then left on ice for 30 min and rapidly heated at 42°C for 45 s, having returned to ice for 2 min). 960 µL of LB were added to the previous mixture, being incubated afterwards for 1 h at 37 °C, 250 rpm (INCU-Line ILS6). Cells were then plated in LA containing 100 µg/mL ampicillin and were left to grow overnight at 37 °C. A pre-inoculum was made from an *E. coli* colony in 100 mL LB with 100 µg/mL ampicillin and was left overnight at 37 °C, 150 rpm. A scale-up was performed adding 10 mL of the pre-inoculum to 500 mL LB with 100 µg/mL ampicillin at 37 °C, 150 rpm until OD_{600nm} = 0.7 - 1. Then, cells were induced with 1 mM IPTG and left to grow at 37 °C, 150 rpm for 4 to 5 h before being harvested by centrifugation at 8000 rpm for 10 min at 4 °C (Beckman Coulter J2-21 M/E, rotor JA-14). After this step, cell pellet was stored at -20 °C. Afterwards, cell pellet was thawed and resuspended in 50 mM Tris-HCl pH 7.6 with 5 mM $MgCl_2$ and was later added DNase and 0.5 mM PMSF. Cells were ruptured in a French Press using 14500 PSI and were later centrifuged at 42000 rpm for 1 h, at 4 °C (Beckman L8-70M, rotor 45 Ti). The supernatant was then diluted 2x in phenylsepharose buffer A – 50 mM Tris-HCl pH 7.6 with 5 mM $CaCl_2$. 0.5 mM DTT were added to both buffer A and supernatant. Protein sample was filtered through a 0.45 µM PVDF membrane (FILTER-LAB) and concentrated in amicons (Millipore) - cut off = 3 kDa, in cycles of 9 min at 4 °C and 4400 rpm (Eppendorf centrifuge 5702 R), until a final volume of 35 to 40 mL. The sample was again filtered through a 0.45 µm PVDF membrane and loaded (15 mL) in a Phenylsepharose column (HiPrep Phenyl Fast-Flow 16/10, GE Healthcare) mounted in an ÄKTA purifier system, previously equilibrated in phenylsepharose buffer A, with a flow rate of 2 mL/min. S100B was eluted after switching buffer A for phenylsepharose buffer B – 50 mM Tris-HCl pH 7.6 with 10 mM EDTA, with a flow of 5 mL/min. Fractions containing S100B were then concentrated in amicons (Millipore) - cut off = 3 kDa, in cycles of 9 min at 4°C and 4400 rpm, until a final volume of 10 mL. Dimer form of S100B was obtained when loading (5 mL) the sample in a HiLoad Superdex 75 16/600prep grade (GE Healthcare) with a flow of 1 mL/min, previously equilibrated in 20 mM Tris-HCl pH 7.6 with 150 mM NaCl and 0.5 mM DTT to promote dimer peak appearance. The fractions containing S100B dimers were collected, concentrated in amicons (Millipore) - cut off = 3 kDa, in cycles of 9 min at 4°C and 4400 rpm until a final concentration of 538 µM (measured spectrophotometrically (SPECTROstar nano, BMG LABTECH) using $\varepsilon_{S100B}^{280nm}$ = 2980 M^{-1} cm^{-1}) and flash-frozen in liquid nitrogen and stored at -20 °C. Apo S100B was prepared by thawing the S100B dimers obtained previously and adding 0.5 mM EDTA, up to 300 fold excess of DTT and incubation for 2 h at 37 °C. Afterwards the samples were centrifuged 10 min at 14800 rpm before being loaded (1 mL) into a Tricorn Superdex 75 (GE Healthcare) previously equilibrated in 50mM Tris-HCl pH 7.4 in H_2O Chelex with a flow of 1 mL/min. The fractions containing the protein were concentrated in amicons (Millipore) with a cut off of 3 kDa, for 8 min at 4 °C, 4400 rpm until a final concentration of 374.5 µM and were flash-frozen in liquid nitrogen and stored at -20 °C. All purifications steps were followed with SDS-PAGE 12% Tris-Tricine gel analysis.

4.2.Aβ expression and purification

Aβ was expressed and purified following a previously established protocol [249]. Chemically competent *E. cloni express* BL21 pLysS Lucigen cells were transformed with 1 µL of pET-SAC – Aβ1-42. Cells were then left on ice for 30 min and rapidly heated at 42°C for 45 s, having returned to ice for 2 min). 900 µL of LB were added to the previous mixture, being incubated afterwards for 1 h at 37°C,

250 rpm. Cells were then plated in LA containing 50 µg/mL ampicillin and 30 µg/mL chloramphenicol and were left to grow overnight at 37 °C. A pre-inoculum was made from 500 µL of the transformed cells in 80 mL LB with 50 µg/mL ampicillin and 30 µg/mL chloramphenicol, and was grown overnight at 37 °C, 150 rpm. A scale-up was performed adding 20 mL of the pre-inoculum to 500 mL M9 medium with 50 µg/mL ampicillin 30 µg/mL chloramphenicol at 37°C, 150 rpm until OD_{600nm} = 0.6-0.8. Then, cells were induced with 1 mM IPTG and left to grow at 37°C, 150 rpm for 4 to 5 h before being harvested by centrifugation at 8000 rpm for 10 min, 4°C (Beckman Coulter J2-21 M/E, rotor JA-14). Cell pellet was resuspended in 100 mM Tris-HCl pH 8 with 10 mM EDTA and stored at -20°C. After thawing the cells, 0.5 mM PMSF and DNase were added (in a Potter homogenizer), followed by sonication at 65% amplitude, cycle 0.5, 3 min (Up200S – Ultrasonic Processor) and centrifugation at 14000 rpm, 20 min, 4°C (Beckman Coulter J2-21 M/E, rotor JA-20). Pellet was dissolved in 10 mM Tris-HCl pH 8 with 1 mM EDTA (in a Potter homogenizer) and sonicated at 65 amplitude, cycle 0.5, 3 min, followed by centrifugation at 14000 rpm, 20 min, 4°C. Pellet was dissolved in 8M Urea in 10 mM Tris-HCl pH8 and 1 mM EDTA (in a Potter homogenizer) and left on ice, gently mixing for 1 h. The protein sample was diluted 4-fold to 2M Urea in 10 mM Tris-HCl pH 8 with 1 mM EDTA and was separated in an ion exchange chromatography (DEAE Sepharose Fast-Flow GE Heatlhcare), mounted with a Buchner funnel, previously equilibrated in 10 mM Tris-HCl pH 8 with 1 mM EDTA. Proteins were eluted with the addition of increasing salt concentrations. First the column was washed with 10 mM Tris-HCl pH8 with 1 mM EDTA, followed by 10 mM Tris-HCl pH8 with 1 mM EDTA and 25 mM NaCl. The Aβ peptide was eluted with 10 mM Tris-HCl pH8 with 1 mM EDTA and 125 mM NaCl, being later concentrated in amicons (Millipore) - cut off = 30000 kDa, for 13 min at 4°C 4400 rpm. The Flow Through was recovered and concentrated in amicons (Millipore) - cut off = 3 kDa, for 10 min at 4°C and 4400 rpm until a final concentration of 287.9 µM (measured spectrophotometrically (SPECTROstar nano, BMG LABTECH) using $\varepsilon_{A\beta}^{280nm}$ = 1424 M^{-1} cm^{-1}). Proteins were then stored at -20°C and lyophilized. All the purifications steps were followed by SDS-PAGE 12% Tris-Tricine gel analysis.

4.3.*Ex Vivo* model - Organotypic Hippocampal Slice Cultures

Parasagittal hippocampal slices were prepared from the brains of neonatal mice at post-natal day 10. After removal of the brains, the cerebellum and hindbrain were separated from the forebrain, from where the hippocampus was removed. Hippocampal slices of 400 µm were obtained using McIlwain tissue chopper, being placed into membrane culture inserts, in a number of four slices per insert, (BD Falcon, #353493, Lincoln Park, NJ, USA) in a 6-well cell culture plate in an air-liquid interface at 37 °C in 5% CO_2. Slices were kept in culture for 6 days. Culture medium consisted of 50% (v/v) minimal essential medium (MEM-Gibco, Life Technologies, Inc., Grand Island, USA), 25% (v/v) heat inactivated horse serum (Gibco), 25% (v/v) Earl's balanced salt solution (SIGMA - St. Louis, Missouri, USA), 1% (v/v) antibiotic-antimycotic - 100 U/mL penicillin, 0.1 mg/mL streptomycin and 0.25 µg/mL amphotericin B (SIGMA), 2 mM L-Glutamine (SIGMA), 25 mM HEPES, 6.5 mg/mL Glucose (SIGMA), 0.02 mg/mL insulin and 0.016 mg/mL ascorbic acid. Half of culture medium was changed every day. After 72 h, culture medium was changed to 98% (v/v) Neurobasal (Gibco) supplemented with 2% (v/v) B-27 (Gibco), 2 mM L-Glutamine, 36 mM Glucose, 1% (v/v) antibiotic-antimycotic and 25 mM HEPES. At 5 days-in-vitro (DIV), slices were incubated for 24 h with different concentrations of Aβ and S100B, originating 8 conditions (Fig. 4.1): Control, S100B 5 µM, Aβ 0.5 µM, Aβ 1 µM, Aβ 2 µM, Aβ 0.5 µM + S100B 5 µM, Aβ 1 µM + S100B 5 µM and Aβ 2 µM + S100B 5 µM.

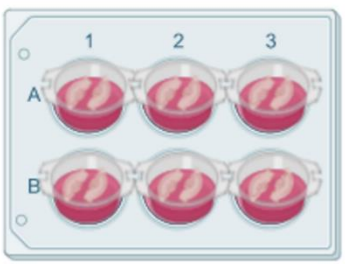

Duplicates

Control	S100B 5 µM
Aβ 0.5 µM	Aβ 0.5 µM + S100B 5 µM
Aβ 1 µM	Aβ 1 µM + S100B 5 µM
Aβ 2 µM	Aβ 2 µM + S100B 5 µM

Figure 4.1 Experimental Conditions. Organotypic Hippocampal Slices were exposed to increasing concentrations of Aβ42 and to S100B.

At 6 DIV, culture medium was collected. Three slices per condition were kept in TRIzol® reagent (Invitrogen - Carlsbad, California, USA) at -20°C for mRNA and protein extraction, and the remaining four were fixed with 1 mL 4% PFA for 1 h, washed 3x with PBS and stored in PBS at 4°C for immunohistochemistry studies.

4.4.mRNA Extraction from slice cultures and RealTime PCR analysis

mRNA was extracted from frozen slices kept in 100 µL TRIzol®. Slices were homogenized by using a pestle motor for pellet pestle mixers for 1 min, the membrane in which slices were cultured was removed, and slices were homogenized for an additional 1 min. Then, 20 µL of chloroform was added, followed by 15 s shaking in the vortex and incubation at RT for 3 min. Samples were centrifuged at 12000g for 15 min, 4°C (Eppendorf Centrifuge 5810 R). The upper aqueous phase containing the RNA was transferred to a new tube and 50 µL of isopropanol were added, followed by a 10 min incubation at RT and centrifugation at 12000g for 15 min, 4°C. RNA pellet was washed with 100 µL 75% ethanol, vortexed 10 s and centrifuged at 12000g for 15 min at 4°C. Pellet was air-dried (not completely) and dissolved in 20 µL of RNase free water (QIAGEN - Hilden, Germany). RNA concentration was determined using Nanodrop ND-100 Spectrophotometer (NanoDrop Technologies, Wilmington, DE, USA).

RNA was diluted in RNase free water to get a 500 ng/µL concentration for each sample. The samples were reversibly transcribed into complementary DNA (cDNA) using Xpert cDNA Synthesis Mastermix kit (GRiSP – Porto, Portugal). In brief, RNA samples were mixed with 10 µL of Xpert cDNA Mastermix (Grisp), incubated in a thermocycler for 5 min at 65°C and then placed on ice for 2 min. Afterwards, 1 µL of Xpert RTase (200U/µL) enzyme was added to each sample, the mixture was homogenized and incubated at 25°C for 10 min, followed by 50°C for 15 min and 85°C for 5 min in the thermocycler. cDNA samples were then diluted to a final concentration of 250 ng/µL and cDNA amplified using the Xpert Fast SYBR Mastermix (GRiSP) Kit on the QuantStudio™ 7 Flex Real-Time PCR (Applied Biosystems) under optimized conditions of 50ºC for 2 min, 95ºC for 10 min followed by 40 cycles at 95ºC for 5 s and 62ºC for 30 s. The PCR was performed in 384-well plates with each sample being performed in duplicate. The genes and respective sequences used as primers are listed in Table 1, with β-actin gene being used as an endogenous control to normalize the expression levels. The NTC wells contain only RNase free water and the Mastermix with primers. Results were analyzed as previously reported by Santos, Barateiro [204]. Briefly, relative mRNA concentration was calculated using the Pfaffl modification of the $\Delta\Delta C_T$ equation, where C_T represents the cycle number at which fluorescence passes the threshold level of detection, considering the efficiency values of individual genes. The initial amount of template for each sample was determined as relative expression by the formula $2^{-\Delta\Delta CT}$. ΔC_T is given by the difference between the mean C_T value of each gene and the mean C_T of β-Actin for each individual sample, and $\Delta\Delta C_T$ is given as the difference between the ΔC_T of each sample and the mean ΔC_T of β-Actin.

Table 4.1 List of primers used in RealTime-PCR

Gene	Forward	Reverse
TNF-α	agcttacaacaggccaggtttc	cggctggcgacatacagtac
IL-1β	cagagctgcgcttgcagag	gtcagcagccggttaccaag
IL-10	cctggaggaggtgatgcccca	cctgctccacggccttgctc
S100B	acccacatctggcagaatgag	agccatgacctttcgcattag
RAGE	tgggcaccatcttcatcattc	ggtcacccagcacaccactt
β-Actin	gctccggcatgtgcaa	aggatcttcatgaggtagt

4.5.Protein extraction from slice cultures

The lower phases obtained from the first step of RNA extraction were used for protein extraction. First, to precipitate DNA, 30 µL of ethanol 100% were added, followed by homogenization (by inversion), incubation at RT for 3 min and samples centrifuged at 2000g for 5 min at 4°C. The supernatant was transferred to a new tube and proteins were precipitated with 150 µL of isopropanol, along with 15 s in vortex, followed by incubation at RT for 10 min and centrifugation at 12000g for 10 min at 4°C. The pellet was washed 3 times with 0.3 M Guanidine HCl in 95% ethanol by adding 200 µL of the guanidine solution, homogenized by inversion and incubated at RT for 20 min followed by centrifugation at 7500g for 5 min at 4°C. Afterwards, the pellet was washed with 200 µL of ethanol 100%, incubated at RT for 20 min and centrifuged at 7500g for 5 min at 4°C. Pellet was air-dried for 10 min and resuspended in 500 µL of 8M Urea (in Tris-HCl pH 8), 500 µL of 1% SDS and 20 µL of protease inhibitors. The samples were then sonicated 2 to 3 times for 15 s, with amplitude 100%, cycle 1 and centrifuged for 10 min at 3200g, 4°C. Supernatant was stored at -80°C until used in Western Blot.

4.6.Protein extraction from medium of slice cultures

Culture medium proteins were extracted using 10% trichloroacetic acid (TCA) in acetone. 100 µL of TCA were added to 900 µL of culture medium followed by homogenization and incubation overnight at -20°C. Samples were then centrifuged at 15000g for 10 min, 4°C. The pellet was resuspended in 100 µL of acetone with 20 mM DTT, homogenized, incubated 10 min at -20°C and centrifuged at 15000g for 10 min at 4°C and the supernatant was removed. The pellet was resuspended and additional time in 100 µL of acetone with 20 mM DTT, homogenized, incubated 10 min at -20°C and centrifuged at 15000g for 10 min at 4°C and the supernatant was removed. Finally, the pellets were air-dried for 45 min to 1 h, dissolved in 50 µL of the solution 1:1 8M Urea (in Tris-HCl pH 8), 1% SDS and 1:25 of protease inhibitors and resuspended by sonication (cycles of 0.5 at 100% amplitude during 40 s) followed by centrifugation at 14000 g for 10 min at 4° C to remove insoluble particles. Supernatants containing the proteins were stored at -80°C until used in Western Blot.

4.7.Western Blot analysis of slice cultures

Protein concentrations (both from the medium and slices) was measured using the Bradford method (Bio-Rad's Protein Assay Reagent, Bio-Rad Laboratories and GloMax Multi Detection System, Promega). For each experimental condition, at least 3 µg from the slices and 100 µg of proteins from the culture medium were prepared together with 1:1 8M Urea (in Tris-HCl pH 8), 1% SDS and 1:25 of protease inhibitors until a final volume of 50 µL, followed by the addition of 25 µL of denaturing buffer 2x [0.25 M Tris-HCl (pH 6.8); 4% (w/v) SDS; 40% (v/v) glycerol; 0.2% (w/v) bromofenol blue and 1% (v/v) β-mercaptoethanol]. Prior to being loaded into the gel, samples were denatured by incubation for 10 minutes but only at 60°C since at higher temperatures, the bands that should represent the Aβ peptide are lost. Proteins were separated electrophoretically for about 1h and 30 min at 200 V and 50 mA per gel and were transferred to a nitrocellulose membrane for 1 h and 30 min at 200V, 300 mA. The membrane was washed with Tris-buffered saline (TBS) for 5 to 10 minutes, followed by AmidoBlack solution stain to detect the total amount of protein in each sample. To serve as a normalization control for the relative band intensity, the membrane containing the proteins detected by AmidoBlack was washed with TBS for 5 to 10 min and visualized with ChemiDoc™ XRS System (Bio-Rad). After washing with TBS for 1 min, membrane was blocked with TBS-T (TBS + 0.1% Tween 20) and 5% dried milk for 1 h, washed 3 times with TBS-T for 5 min and incubated with 5 mL of primary antibody (diluted in TBS-T with 5% BSA). After incubation, the membrane was washed 3 times with TBS-T for

10 min, blocked with TBS-T (TBS + 0.1% Tween 20) and 5% dried milk for 1 h and incubated with 5 mL of secondary antibody HRP-conjugated (diluted in blocking buffer) against the species of the primary antibody (SantaCruz - Dallas, Texas, USA) for 1 h and 30 min at RT. Membrane was then washed 3 times with TBS-T for 10 min and WesternBright Sirius reagent (Advansta – San Jose, California, USA) was used as chemiluminescent substrate. Signal was acquired in ChemiDoc™ XRS System (Bio-Rad). After band detection, the membrane was washed with TBS for 1 min and stripped with 2% NaOH for 8 min, H_2O for 5 min, PBS for 5 min and 2 times with TBS-T for 5 min before being blocked again and then incubated with another primary antibody. Sequences of immunoblotting and striping were used until all the proteins of interest were detected. The antibodies, species and dilutions are listed in Table 2. Due to the reduced n evaluated, no densitometry was performed.

Table 4.2 List of antibodies used in Western Blot

Antibody	Species	Dilution
Anti-amyloidβ-6E10	Mouse	1:5000
Anti-S100b	Rabbit	1:750
Anti-β-Actin	Mouse	1:5000
Anti-mouse	Rabbit	1:5000
Anti-rabbit	Goat	1:5000

4.8.Immunohistochemistry analysis of slice cultures

The fixes slices were placed in coverslips and surrounded by a liquid blocker-PAP pen. Each slice was incubated for 3 h in blocking solution – 1nM Hepes, 2% normal horse serum, 10% fetal bovine serum, 1% BSA and 0.25% Triton X-100 in HBSS, in low orbital rotation at an orbital shaker. After removal of the blocking solution, each slice was incubated 2 overnights at 4°C with 75 µL of each primary antibody, Anti-Iba-1 rabbit (Wako – Richmond, Virginia, USA, D 1:250), Anti-GFAP mouse (SIGMA, D 1:100) and Anti-NeuN mouse (Millipore - Burlington, Massachusetts, USA , D 1:100), diluted in blocking buffer. The slices were then washed 3 times with 100 µL of PBS and 0.01% Triton X-100 for 20 min (low orbital rotation) and incubated overnight at 4°C with 100 µL of the respective secondary antibody (Invitrogen) diluted 1:500 in blocking buffer – Goat anti-rabbit conjugated with Alexa Fluor Plus 594 and Goat anti-mouse conjugated with Alexa Fluor Plus 488. Slices were then washed 3 times with 100 µL of PBS and 0.01% Triton X-100 for 20 min (low orbital rotation), incubated with DAPI diluted 1:1000 in PBS for 5 min (to stain cell nucleus), washed 3 times with 100 µL of PBS for 1 min and mounted with FluoroMount (Southern Biotech - Birmingham, Alabama, USA) medium. After 15 min, coverslips were stored at 4°C until visualization at the Confocal microscope (Confocal Point Scanning Microscope Zeiss LSM 710 META).

4.9.Statistical analysis

Results of, at least, three different experiments were expressed as mean ± SEM. Significant differences between groups were determined by ordinary one-way ANOVA with Dunnett's and Sidak's multiple comparisons post-tests, using GraphPad PRISM 8.0 (GraphPad Software, San Diego, California, USA), considering a minimal criterion of $P<0.05$ as statistically significant.

5.Results and Discussion

Unfortunately, the lockdown and restrictions imposed by the ongoing COVID-19 pandemic led to a reduction in the number of independent experiments and volume of experimental work. Therefore, I here present preliminary results that will need further confirmation.

5.1.Recombinant protein expression

5.1.1.Expression and purification of S100B

To investigate whether S100B could prevent $A\beta_{42}$ neurotoxicity or further potentiate it, the two proteins were recombinantly expressed in *E. coli* and purified. Firstly, for S100B, a bacterial growth of 8L (two batches) of *E. coli* expressing S100B was prepared, from which 19,34 g of cells were obtained after centrifugation. Afterwards, these cells were resuspended, the cellular wall was disrupted, and cells were then ultracentrifuged. The protein fraction from *E. coli* containing S100B was then separated using a hydrophobic interaction chromatography (HIC) (Fig. 5.1.1.1A) equilibrated with a buffer containing Ca^{2+}. Proteins that did not bind to the resin were eluted during the initial column wash - peak 1 of Fig. 5.1.1.1A and lane 3 of Fig. 5.1.1.1B. Since calcium-bound S100B remained in the column after the initial wash, the protein was eluted using a buffer containing a chelating agent (EDTA) - peak 2 of Fig. 5.1.1.1A and lane 4 of Fig. 5.1.1.1B. In its dimeric form, S100B has around 21.5 kDa (red rectangle in Fig. 5.1.1.1B), thus the protein was successfully separated, although some protein was also lost during the initial wash in the unbound fraction. To further purify S100B, the fraction corresponding to this protein – peak 2 of Fig. 5.1.1.1A – was loaded into a size exclusion chromatography (SEC) (Fig.

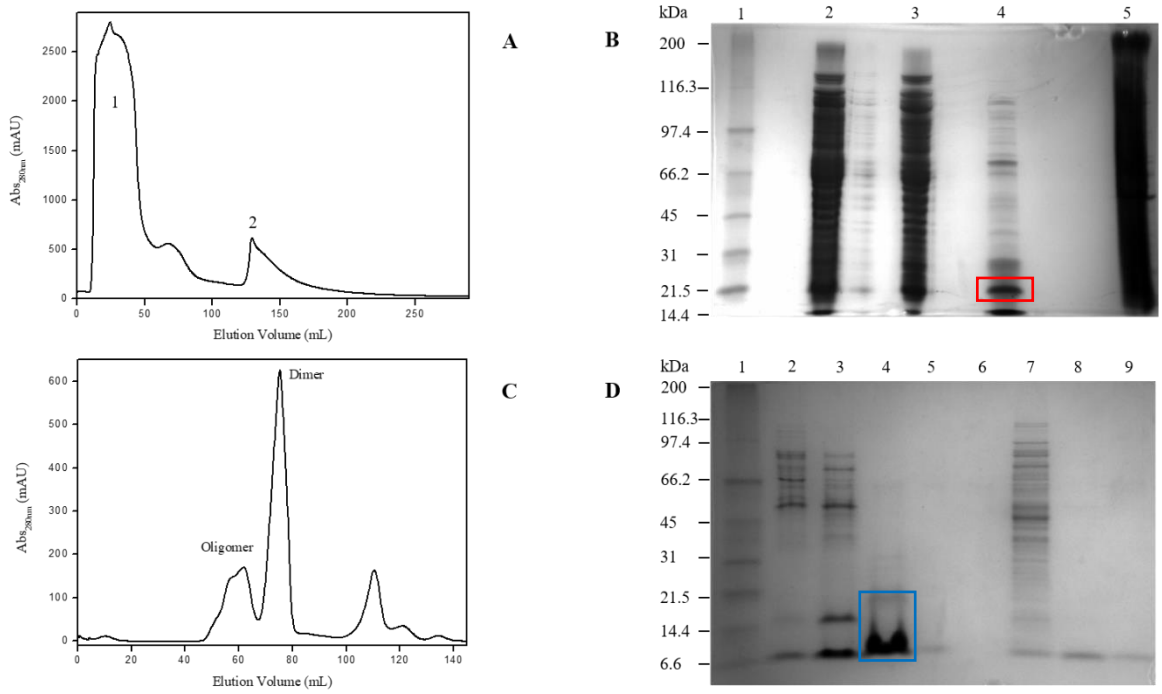

Figure 5.1.1.1 S100B purification process. S100B was expressed in *E. coli* and purified using hydrophobic interaction chromatography (HIC) followed by size exclusion chromatography (SEC). **(A)** HIC Chromatogram. S100B was loaded into a column previously equilibrated with phenylsepharose buffer A – 50 mM Tris-HCl pH 7.6 with 5 mM CaCl2. 0.5 mM DTT. All unbound proteins were washed and S100B was eluted with phenylsepharose buffer B – 50 mM Tris-HCl pH 7.6 with 10 mM EDTA, with a flow of 5 mL/min. **(B)** SDS-PAGE after HIC. **1** - Molecular markers; **2** - After ultracentrifugation supernatant with buffer A; **3** - Unbound fraction of HIC, everything that does not bound to the column; **4** - Protein fraction collected after eluting with buffer B, containing the S100B protein; **5** - Pellet after ultracentrifugation. (**C**) SEC Chromatogram. Dimer form of S100B was obtained by loading the sample in the column and eluting it with a flow of 1 mL/min with 20 mM Tris-HCl pH 7.6 with 150 mM NaCl and 0.5 mM DTT to promote dimer peak appearance. Fractions of 2 mL were collected. (**D**) SDS-PAGE after SEC. **1** - Molecular markers; **2-6** - Different fractions collected during SEC; **7-9** - Flow Through of the 3 different concentrations steps performed during the S100B purification.

5.1.1.1C), equilibrated with a buffer containing DTT to promote dimer peak appearance. Proteins were thus separated according to their molecular mass, where species with higher molecular weight eluted faster than those with lower molecular weight. Therefore, S100B oligomers eluted first – Fig. 5.1.1.1C and lanes 2 and 3 of Fig. 5.1.1.1D, followed by S100B dimers - Fig. 5.1.1.1C and lane 4 of Fig. 5.1.1.1D. The fraction correspondent to dimeric S100B (blue rectangle in Fig. 5.1.1.1D) was prepared according to Materials and Methods before being loaded into another SEC, previously equilibrated in buffer containing H_2O chelex to obtain the Apo form of dimeric S100B. We obtained 54.52 mg of purified Apo S100B from this process, with a yield of 6.82 mg/ L of culture.

5.1.2.Expression and purification of Amyloid β 42

As with S100B, a bacterial growth of 4L of *E. coli* expressing $A\beta_{42}$ was prepared. However, differing from S100B, *E. coli* expressed $A\beta_{42}$ in inclusion bodies, therefore we isolated, washed and solubilized the inclusion bodies as described in Materials and Methods. Afterwards, $A\beta_{42}$ was purified using an ion exchange chromatography, and indeed the peptide was eluted with a high ionic strength buffer, although some $A\beta_{42}$ was lost during this process (red rectangle in lanes 4-6 of Fig. 5.1.2.1). The purified peptide was then concentrated sequentially through centrifugation filters, first with a cut-off of 30 kDa and afterwards with a cut-off of 3 kDa – lane 8 of Fig. 5.1.2.1. We obtained 9.78 mg of purified $A\beta_{42}$ from this process, with a yield of 2.45 mg/L of culture.

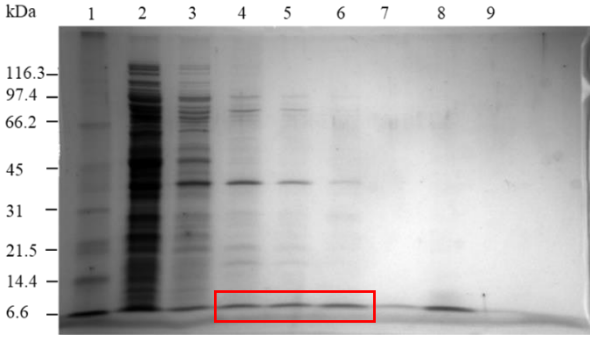

Figure 5.1.2.1 Aβ purification process. Aβ was expressed in *E. coli* and purified using an ion exchange chromatography. SDS-PAGE of Aβ purification. **1** – Molecular markers; **2-3** - The supernatants obtained in the beginning of the purification; **4-6** – fractions collected after increasing ionic strength of the elution buffer; **7** - Supernatant of the 30 kDa cut-off concentration; **8** - fraction corresponding to purified Aβ42; **9** – Flow through of the 3 kDa cut-off concentration.

5.2.$A\beta_{42}$ increases S100B levels in OHSC

To evaluate whether S100B could prevent or exacerbate $A\beta_{42}$ neurotoxicity, organotypic hippocampal slice cultures were exposed to (5 µM) S100B, (0.5, 1 and 2 µM) $A\beta_{42}$ or both at 6 DIV for 24h. Then, the ex vivo model was characterized in terms of $A\beta_{42}$ (Fig. 5.2.1) and S100B (Fig. 5.2.2) levels in both tissue and culture media, as well as their gene expression in slices (Fig. 5.2.2C). The representative blots showed that even though slices were exposed to $A\beta_{42}$, the monomeric form from this peptide was not detected in the slices but instead $A\beta_{42}$ was mainly present in the form of 50 kDa oligomers (Fig. 5.2.1A), whereas in the culture medium, both monomeric $A\beta_{42}$ and a 25 kDa oligomeric form could be observed (Fig. 5.2.1B). The reduced number of experimental replicates and lack of internal controls prevented a quantitative analysis of the observed bands. Nevertheless, the blots seem to suggest increased levels of $A\beta_{42}$ for the higher concentrations incubated in both slices and media, with a slight decrease when slices were co-incubated with both $A\beta_{42}$ and S100B.

Next, the levels of S100B in both slices and culture medium were determined (Fig. 5.2.2). The results clearly showed that upon incubation with S100B, the levels of this protein increase in both tissue and culture medium (Fig. 5.2.2A-B). Additionally, it seemed that $A\beta_{42}$ incubation is able to elicit S100B expression in the slice and an increase of its levels in both tissue and media when in coincubation conditions. However, S100B gene expression analysis showed no differences from control (Fig. 5.2.2C), suggesting that S100B gene expression must have occurred in previous time-points or that protein differences are indicative of S100B sequestration at the extracellular compartment by $A\beta_{42}$, which is in accordance with recent *in vitro* studies where an interaction between S100B and $A\beta_{42}$ was established [1].

Previous studies using rat hippocampal slices also showed increased $A\beta_{42}$ in the slices through immunohistochemistry, as early as 24h [250] or 2-3 days [251] after treatment of slices with $A\beta_{42}$. Additionally, in these studies, higher $A\beta_{42}$ concentrations resulted in higher $A\beta_{42}$ immunoreactivity inside the slices, thus supporting our findings. Furthermore, due to said interaction between S100B and $A\beta_{42}$ *in vitro* [1], the slight decrease of $A\beta_{42}$ levels in coincubation conditions could also be indicative of an interaction between these two molecules and maintenance in cell media.

Concerning S100B, previous studies using cerebellar slice cultures have demonstrated the presence of S100B at the slices [204], as was also observed here using hippocampal slices. However, in contrast to our findings, the same study showed that the exposure of cerebellar slices to S100B increased its own mRNA expression, which was not the case in our hippocampal slices. These results suggest that S100B has a different expression profile depending on the brain region studied, which is supported by recent findings showing that S100B mRNA expression is indeed present in all brain regions, with the highest expression profile in the cerebellum and cortex [192].

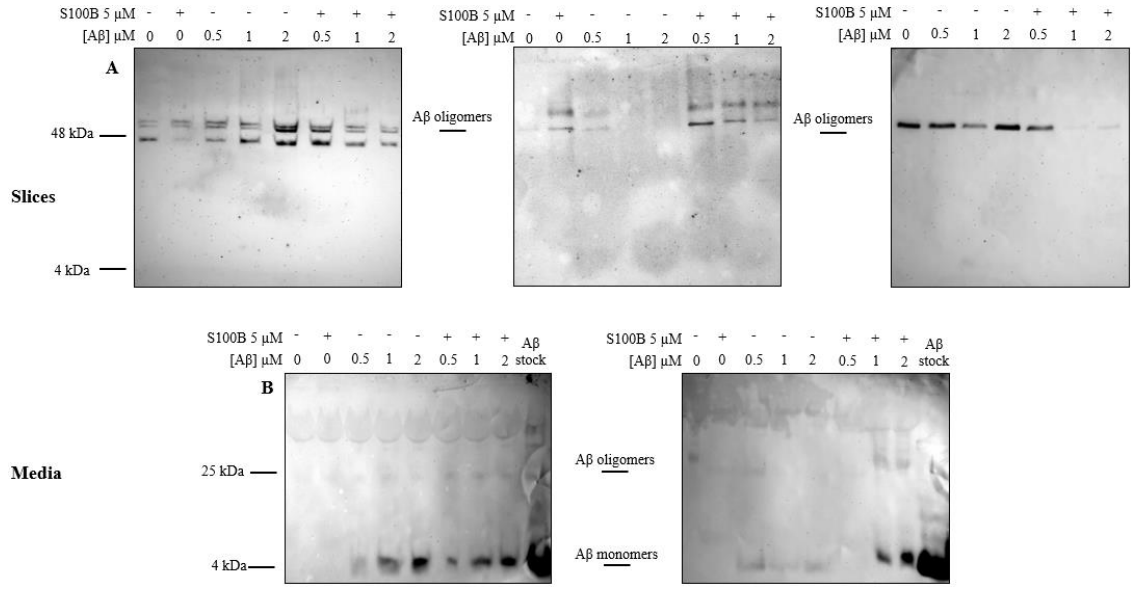

Figure 5.2.1 Aβ levels in OHSC. Organotypic hippocampal slice cultures were exposed to (5 µM) S100B, (0.5, 1 and 2 µM) Aβ or both at 6 DIV for 24h. Aβ levels were visualized by Western Blot in the slices **(A)** from three independent experiments, and in the Media **(B)** from two independent experiments.

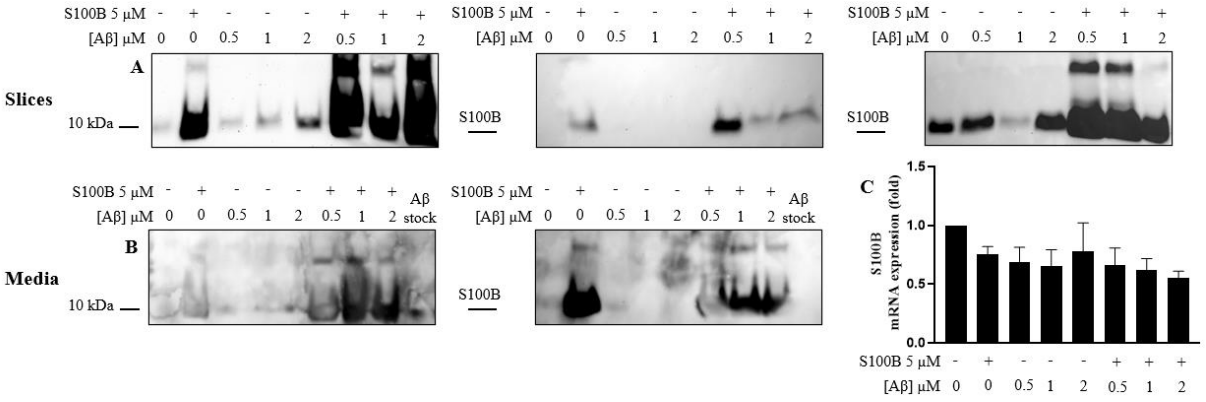

Figure 5.2.2 S100B levels in OHSC. Organotypic hippocampal slice cultures were exposed to (5 µM) S100B, (0.5, 1 and 2 µM) Aβ or both at 6 DIV for 24h. S100B levels were visualized by Western Blot in the slices **(A)** from three independent experiments, and in the Media **(B)** from two independent experiments. Relative S100B gene expression **(C)** was determined by qRealTime-PCR and normalized to β-Actin gene expression. qRealTime-PCR results are mean ± SEM from seven **(C)** independent experiments. One-way ANOVA with Dunnett's and Sidak's multiple comparisons post-tests did not reveal a statistically significant difference between relative S100B gene expression in the conditions tested in comparison with control.

5.3.Aβ$_{42}$ does not affect neuronal viability in OHSC

Following these results, we sought to understand whether this increase in protein levels had an effect at the cellular level, namely in neuronal viability. Therefore, following incubation, slices were stained for NeuN and the level of positive neuronal nuclei determined within the *Cornus Ammonis*, or CA, region of the hippocampus, since no positivity was observed for the *Dentate Gyrus*, DG, region as shown in the representative images (Fig. 5.3.1A). Although we could detect different CA areas, which may be due to slice culture variability, in terms of neuronal loss, no statistically significant differences were observed for any condition (Fig. 5.3.1B), suggesting that neither Aβ$_{42}$ or S100B induce neurotoxicity in this model when incubated only for 24h.

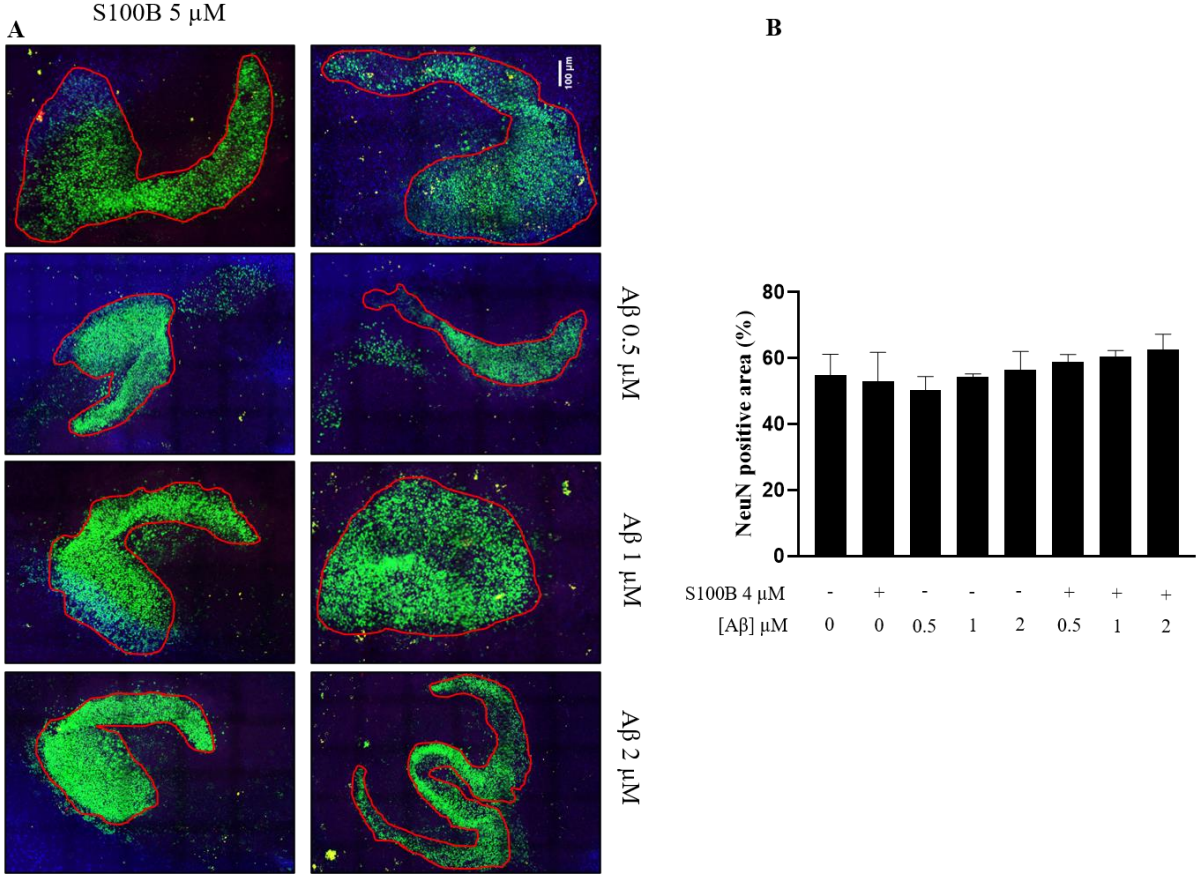

Figure 5.3.1 OHSC neuronal response to Aβ and S100B mediated toxicity. Organotypic hippocampal slice cultures were exposed to (5 µM) S100B, (0.5, 1 and 2 µM) Aβ$_{42}$ or both at 6 DIV for 24h. **(A)** Representative results of one experiment are shown. Nuclei were stained with DAPI (blue) and neurons with NeuN (green). The *Cornus Ammonis* (CA) region of the hippocampus is highlighted in red. **(B)** Area percentage of NeuN positive cells in the hippocampus, following S100B and/or Aβ treatment. Results are mean ± SEM from three independent experiments. One-way ANOVA with Dunnett's or Sidak's multiple comparisons post-tests did not reveal statistically significant differences between the different conditions. Scale bar represents 100 µm.

The Aβ-induced neuronal toxicity in hippocampal slice cultures is a controversial topic. Most studies using OHSC and Aβ$_{42}$, or other forms of the peptide such as Aβ$_{25-35}$ and Aβ$_{40}$, did not find a pronounced neuronal loss, despite Aβ having entered the slices, as also observed here, even after 5 days of Aβ treatment [251-258], suggesting that indeed longer incubation periods might be needed in order to detect Aβ-mediated neuronal loss. In contrast, some earlier findings have shown neuronal toxicity 24 to 48h following treatment of hippocampal slices with high Aβ concentrations [259-261], while others only demonstrate cellular damage mediated by Aβ [240, 262], thus demonstrating the variability of these cultures when exposed to the peptide.

In the case of S100B, its effects on neuronal toxicity have been shown to vary depending on the protein concentration. When in nanomolar concentrations, S100B has been shown to protect neuroblastomas against Aβ$_{25-35}$ induced neuronal apoptosis, but to exacerbate the neurotoxic effect of

the peptide when in micromolar concentrations [201], as opposed to what was observed in slices in coincubations conditions. Additionally, S100B has also been shown to induce neuronal death in neuron-astrocytes co-cultures [263], and since microglia is absent in these models, but is present in the model used in this project, this could perhaps indicate that microglia cells protect neurons against $A\beta_{42}$ and S100B mediated neuronal toxicity. Nevertheless, it remains to be studied whether longer coincubation periods, with the same or higher concentrations, of both alarmins exerts an effect in neuronal viability.

5.4. Altered glial reactivity in OHSC following $A\beta_{42}$ and S100B exposure

Knowing that $A\beta_{42}$ and S100B function as alarmins, we wondered whether glial cells would become reactive in their presence. Therefore, glial cell reactivity was evaluated in slices (Fig. 5.4.1).

First, astrogliosis was evaluated recurring to the increased expression of the astrocyte-specific marker GFAP, usually upregulated when astrocytes became reactive. Exposure of hippocampal slices to S100B or Aβ did not seem to alter the overall astroglia positive area in the whole slice, or in the CA region or DG region of the hippocampus (Fig. 5.4.2C), although slices treated with Aβ 2µM showed a much less GFAP-positive astrocytes than the other conditions in the CA region. Concerning the DG, the elevated variability did not allow any conclusive data.

Microgliosis was evaluated recurring to the increased expression of the microglia-specific marker Iba-1, upregulated in reactive microglia. In contrast with what was seen for astrogliosis, exposure of slices to S100B, Aβ or both seemed to induce microgliosis in the whole slice, which was more pronounced after treatment with S100B, Aβ 0.5 and 2µM or both of these conditions in conjunction (Fig. 5.4.2D). In the CA region of the hippocampus, there was a more pronounced effect for Aβ 2µM (Fig. 5.4.2D). Concerning the DG region, there seemed to be an increased microglia reactivity in slices exposed to S100B and Aβ, where crescent Aβ concentrations appeared to induce an increasingly higher microglial reactivity (Fig. 5.4.2D). Interestingly, co-incubation of slices with S100B and different Aβ concentrations revealed a reduced Iba-1 positive area, and therefore of reactive microglia (Fig. 5.4.2D), suggesting that microglia of the DG may be more sensitive to those stimuli.

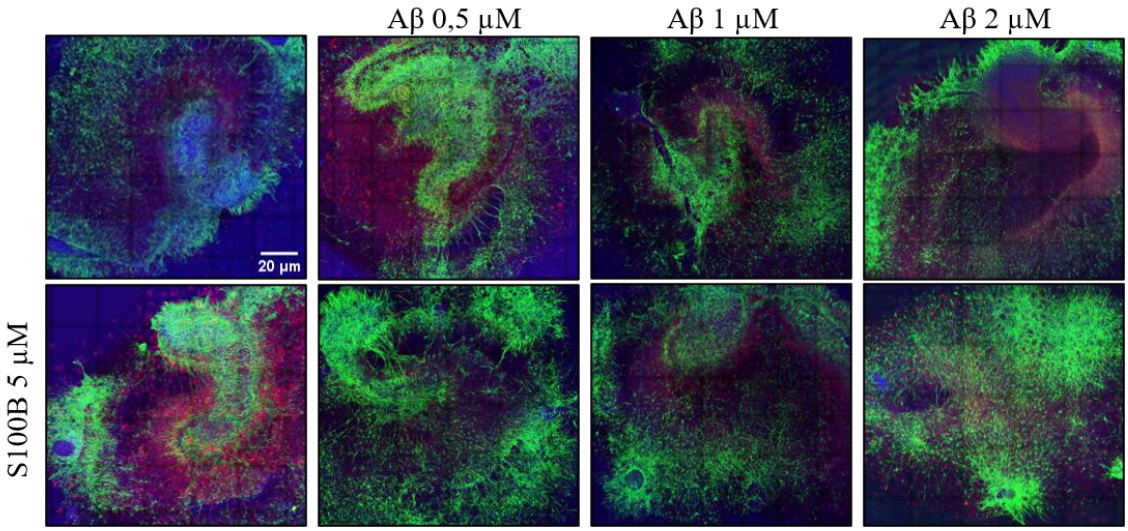

Figure 5.4.1 Altered glial reactivity in OHSC exposed to S100B and $A\beta_{42}$. Organotypic hippocampal slice cultures were exposed to (5 µM) S100B, (0.5, 1 and 2 µM) Aβ or both at 6 DIV for 24h. Representative images of one experiment are shown. OHSC were immunostained to identify reactive astrocytes expressing GFAP (green), reactive microglia expressing Iba-1 (red) and stained with DAPI to detect nuclei (blue). Scale bar represents 20 µm.

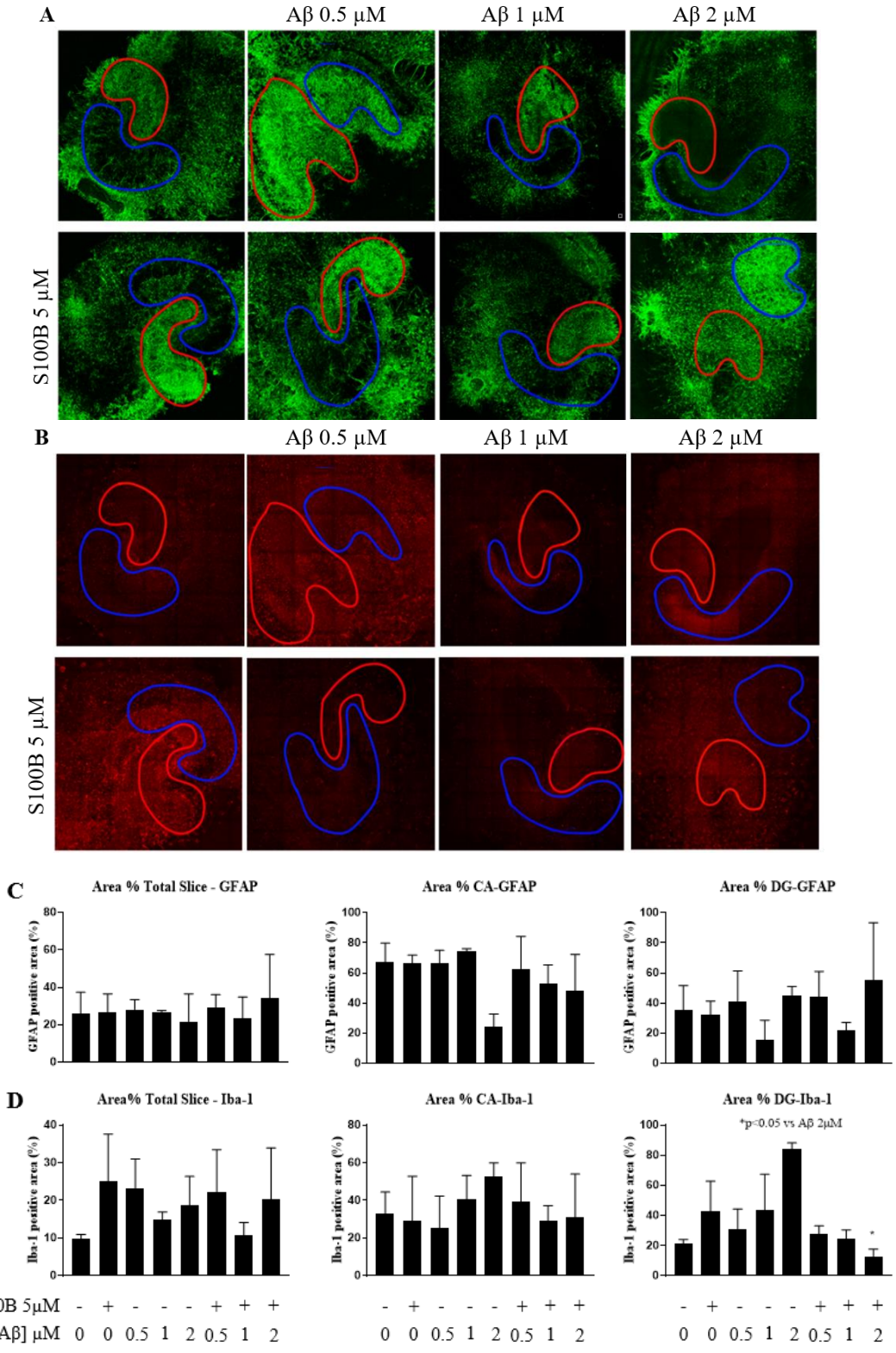

Figure 5.4.2 Altered glial reactivity in hippocampal slices after exposure to S100B and Aβ$_{42}$. Organotypic hippocampal slice cultures were exposed to (5 µM) S100B, (0.5, 1 and 2 µM) Aβ or both at 6 DIV for 24h. Representative images of one experiment are shown. OHSC were immunostained to identify **(A)** reactive astrocytes expressing GFAP (green) and **(B)** reactive microglia expressing Iba-1 (red). Hippocampal regions CA and DG are delineated in red and blue, respectively. **(C)** Area percentage of GFAP positive cells corresponding to the Total slice, CA and DG regions of the hippocampus, after treatment with S100B and/or Aβ$_{42}$. **(D)** Area percentage of Iba-1 positive cells corresponding to the Total slice, CA and DG regions of the hippocampus, after treatment with S100B and/or Aβ. Results are mean ± SEM from three independent experiments. One-way ANOVA with Dunnett's or Sidak's multiple comparisons post-tests revealed a statistically significant difference in the Iba-1 positive area of the DG between S100B 5µM + Aβ 2µM and Aβ 2µM.

Concerning the reactive astrocyte area, and excluding the DG region due to high variability, our results are in contrast with previous studies, where 10 μM of $A\beta_{25-35}$ appeared to promote glial activation in hippocampal slices of wild-type mice [264], or with the general consensus that reactive astrocytes colocalize in the periphery of amyloid plaques in AD, participating in the degradation of the peptide [6], which indicates that low concentrations of $A\beta_{42}$ used here for a reduced time period are potentially not sufficient to induce a profound astrocyte reactivity. Additionally, the astrocytes from the CA region, in slices incubated with $A\beta_{42}$ 2μM may have died, thus explaining the low GFAP immunoreactivity.

Similarly, the absence of an exacerbated astrocytic response in conditions with S100B also goes against previous results, as recent findings reported the colocalization of S100B with reactive astrocytes expressing GFAP in cerebellar slice cultures exposed to S100B [204], which was further shown to function via the S100B-RAGE axis [204], also supported by studies in primary cell lines [265]. Nevertheless, the specific expression of S100B in the various brain regions could account for the differential effect of S100B between these same regions [192]. For instance, astrocytes from the cerebellum could be more prone to express S100B than those from hippocampus upon insult, as S100B shows the highest expression in the cerebellum [192], therefore, showing a higher reactivity capacity than those from the hippocampus.

The Aβ-mediated altered microglia reactivity seen here is in accordance with previous studies, where Aβ immunoreactivity was detected mainly inside microglia cells 2-3 days [251] or 7 days [258] after incubation of slices with the peptide, a process though as beneficial since no neuronal death was detected in slices [258]. Indeed, depletion of microglia resulted in plaque deposition and Aβ-induced neuronal death [258], hence the engulfment of Aβ by microglia appears to actually be required for neuronal survival in OHSC. Interestingly, one study also reported Aβ immunoreactivity in microglia of the CA region of the hippocampus [250], as also seen here mainly for Aβ 2μM. This may be correlated with an increased expression of the complement protein C1q, shown to be related with the phagocytic activity of microglia [266]. This could thus indicate that microglia are one of the reasons why $A\beta_{42}$ did not affect neuronal viability (apart from the incubation periods) in this study.

In contrast, the altered microglial reactivity of the DG region could be linked to other process, rather than the phagocytosis of $A\beta_{42}$ by microglia, as $A\beta_{42}$ was recently found to preferentially induce the degeneration of this region via intracellular zinc dysregulation [267], increasing cellular death, which would activate microglia phagocytic activity of apoptotic cells, therefore altering its reactivity, supporting the results obtained here for the DG region. Nevertheless, further immunohistochemistry experiments should seek to understand whether microglia become reactive due to $A\beta_{42}$ mediated phagocytosis, due to $A\beta_{42}$ mediated cell death, or even both.

Although the majority of studies involving S100B-mediated microglia activation have been performed in other models besides OHSC, they have shown that S100B also affects microglia through a RAGE-dependent interaction [268], modulating microglia migration via chemokine release and microglia activation via NF-κB signaling [269], thus supporting the results obtained here for the whole slice and DG region in slices incubated with S100B. Interestingly, the decreased microglia reactivity, seen in this region, in coincubation conditions, could indicate that S100B might be able to protect the DG against an overt activation of microglia induced by $A\beta_{42}$. Indeed, Hagmeyer et al. have established a possible neuroprotective role for S100B tied to its zinc-buffering activity in the brain [209], which should be able to rescue the zinc dysregulation induced by $A\beta_{42}$ seen by Tamano et al. in the DG [267], thereby rescuing the microglia reactivity in this region.

5.5.S100B prevent $A\beta_{42}$-induced expression of IL-1β in OHSC

Having detected an altered glial reactivity in slices exposed to S100B and $A\beta_{42}$, we next evaluated the inflammatory response looking of gene expression of inflammatory molecules and of the receptor for S100B and Aβ.

Overall, our results suggested a tendency for an increased proinflammatory cytokine mRNA expression, namely TNF-α and IL-1β in slices exposed to $A\beta_{42}$ when compared to control, reaching significant values for $A\beta_{42}$ 2μM (Fig. 5.5.1). On other hand, co-incubation of both S100B and $A\beta_{42}$ seemed to decrease IL-1β mRNA expression in comparison to $A\beta_{42}$ alone, although the same was not observed for TNF-α mRNA expression (Fig. 5.5.1). Furthermore, in spite of a slight increase in IL-10 mRNA expression in slices exposed to S100B or $A\beta_{42}$ 0.5 μM alone, the remaining conditions did not appear to modify this anti-inflammatory cytokine mRNA expression (Fig. 5.5.1). Concerning RAGE mRNA expression the incubation of slices with the various conditions seemed to decrease RAGE mRNA expression, when compared to the control (Fig. 5.5.1), which may be due to its engagement by the increased availability of its ligands and consequent regulatory feed-back.

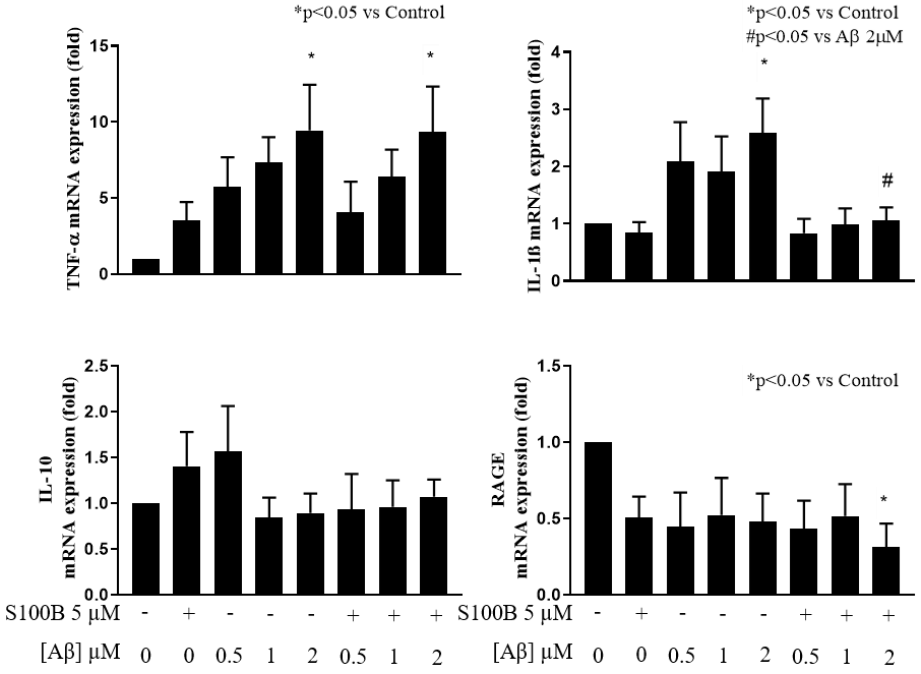

Figure 5.5.1 Regulation of inflammatory gene expression in OHSC exposed to S100B and $A\beta_{42}$. Organotypic hippocampal slice cultures were exposed to (5 μM) S100B, (0.5, 1 and 2 μM) Aβ or both at 6 DIV for 24h. Relative gene expression levels of inflammatory markers - TNF-α, IL-1β, IL-10 and RAGE were determined by qRealTime-PCR and normalized to β-Actin gene expression. Results are mean ± SEM from seven independent experiments. One-way ANOVA with Dunnett's or Sidak's multiple comparisons post-tests revealed a statistically significant difference between Aβ 2μM and S100B 5μM + Aβ 2μM vs control for TNF-α, between S100B 5μM + Aβ 2μM vs Aβ 2μM and S100B 5μM + Aβ 2μM vs control for IL-1β, and between S100B 5μM + Aβ 2μM vs control for RAGE mRNA expression.

As stated in the introduction section, several studies using primary cell lines have uncovered the link between glial cells, Aβ and inflammation [119, 128]. Although previous reports found increased TNF-α and IL-1β levels in microglia and astrocytes from primary cell lines exposed to Aβ oligomers [270], a recent study in OHSC demonstrated that the microglial engulfment of the peptide did not correlate with microglia activation, and therefore no significant differences of IL-6 or TNF-α levels were detected in slices exposed to $A\beta_{42}$ [258], as opposed to the TNF-α mRNA expression observed here. Recent findings also demonstrated that this model is able to reproduce the NLRP3 inflammasome activation when treated with LPS, hence resulting in IL-1β production [271], thus it is possible that Aβ may be inducing inflammasome activation and therefore IL-1β expression in this experimental model, supporting the increased IL-1β mRNA expression found here.

S100B, acting as an alarmin, has been previously shown in primary cultures [265] and more recently in cerebellar slice cultures [204], to induce an inflammatory response in astrocytes and microglia from primary cultures, through a RAGE-dependent interaction [269], increasing TNF-α and IL-1β mRNA expression. These data are in accordance to the results obtained here for TNF-α, but not IL-1β mRNA expression. Interestingly however, S100B was able to prevent the increased IL-1β mRNA expression detected after treatment of slices with $A\beta_{42}$, and although the same was not observed for TNF-α mRNA

expression, this could indicate a possible mechanism by which S100B inhibits the $A\beta_{42}$-mediated NLRP3 activation, which is also in accordance with the rescue of microglia reactivity in slices treated with both alarmins, observed in the DG.

Regarding IL-10, the slight increase in this cytokine mRNA expression seen after treatment of S100B or Aβ 0.5μM might indicate the beginning of an anti-inflammatory response by microglia.

The possible regulatory feedback, observed in conditions with S100B, regarding RAGE mRNA expression is not in accordance with previous findings, where exposure of micromolar S100B levels in cerebellar slice cultures or primary astrocytes upregulated this receptor mRNA and protein expression [204, 265]. Thus, when OHSC model is exposed to excessive levels of S100B and $A\beta_{42}$, it may downregulate RAGE mRNA expression, possibly as a mechanism that prevents the over activation of inflammatory pathways.

Altogether, the work presented here suggests that S100B partially protects slices from Aβ-induced microglia reactivity in the DG region, while also preventing Aβ-induced IL-1β, but not TNF-α increased mRNA expression, without altering neuronal viability.

6. Concluding remarks

The main goal of this thesis was to investigate whether S100B could prevent $A\beta_{42}$ neurotoxicity or further potentiate it in OHSCs. Indeed, the importance of S100B as a proinflammatory cytokine in the brain has been known for several years, having a key role not only in AD but also in other neurodegenerative diseases, affecting all the CNS cells. In the scope of AD, recent findings established a unique chaperone-like function for S100B as a suppressor of Aβ aggregation *in vitro*, while also showing its neuroprotective effects against Aβ-induced toxicity in SH-S5Y5 cells. Therefore, the dual effect of S100B remained to be elucidated in a more complex cellular environment. Here, we used OHSCs, a model that reproduces the hippocampus architecture and cellular connections of the *in vivo* brain.

Our results suggested that S100B was able to partially reduce the microglia reactivity in the DG region of slices exposed to $A\beta_{42}$, while also preventing the increased IL-1β mRNA expression induced by the peptide, indicating a potential neuroprotective effect of S100B. Although we know that *in vitro*, S100B is able to bind $A\beta_{42}$ and inhibit its aggregation mechanism [1], the model used in this project did not allow the confirmation of this interaction in *ex vivo*. Nonetheless, this interaction, if it is occurring inside the slices, could be detected via coimmunostain of both S100B and $A\beta_{42}$, and would then reduce microglia reactivity induced by $A\beta_{42}$, either through impairment of $A\beta_{42}$ phagocytosis, or through prevention of cytotoxic processes mediated by the peptide, which would then reduce the inflammatory cytokines released from reactive microglia. Since we did not observe a reduction of TNF-α mRNA expression in coincubation conditions, the result of this interaction or prevention of cytotoxic processes, appeared to only affect the induction of IL-1β mRNA expression. Furthermore, in contrast to previous findings, neither S100B nor $A\beta_{42}$ were able to induce neuronal death after a 24h incubation, suggesting the time of exposure was not enough to alter neuronal viability, which could potentially indicate some degree of microglia surveillance maintained neuronal survival. Therefore, longer incubation periods might pose a challenge to the homeostatic equilibrium of the slice, which in turn could suffice to alter neuronal viability, thus allowing the study of the possible neuroprotective role of S100B over $A\beta_{42}$-induced neuronal toxicity. Lastly, the decreased RAGE mRNA expression here detected could be interpretated as another potential defense mechanism against increased alarmins concentrations in the hippocampus, although further studies should investigate whether RAGE protein expression is also reduced in these conditions.

To further establish the role of S100B as a neuroprotector against $A\beta_{42}$-induced toxicity in this model, future experiments should seek to understand whether microglia protects neurons through $A\beta_{42}$ phagocytosis, or if indeed S100B is blocking this phagocytosis through an interaction with $A\beta_{42}$. Alternatively, the altered glial reactivity found in some of the experiments needs to be confirmed with a greater experimental n. Moreover, it would also be interesting to examine evidence of amyloid pathology, such amyloid fibrils/plaques in longer incubation periods, or explore whether S100B is able

to suppress and delay the $A\beta_{42}$ aggregation *ex vivo*. If these hypotheses prove to be false, future studies should then ascertain the presence of $A\beta_{42}$ inside neurons and investigate which mechanisms could lead to neuronal death.

Altogether, we expect these findings to provide some insight on the possible role of S100B as a neuroprotector against Aβ-induced toxicity, and open new paths to study suppressors of amyloid pathology in OHSCs.

References

1. Cristovao, J.S., et al., *The neuronal S100B protein is a calcium-tuned suppressor of amyloid-beta aggregation.* Science Advances, 2018. **4**(6).
2. Braak, H. and E. Braak, *Neuropathological stageing of Alzheimer-related changes.* Acta Neuropathol, 1991. **82**(4): p. 239-59.
3. Drummond, E. and T. Wisniewski, *Alzheimer's disease: experimental models and reality.* Acta Neuropathol, 2017. **133**(2): p. 155-175.
4. Cuello, A.C., *Early and Late CNS Inflammation in Alzheimer's Disease: Two Extremes of a Continuum?* Trends Pharmacol Sci, 2017. **38**(11): p. 956-966.
5. Haass, C. and D.J. Selkoe, *Soluble protein oligomers in neurodegeneration: lessons from the Alzheimer's amyloid beta-peptide.* Nat Rev Mol Cell Biol, 2007. **8**(2): p. 101-12.
6. DeTure, M.A. and D.W. Dickson, *The neuropathological diagnosis of Alzheimer's disease.* Mol Neurodegener, 2019. **14**(1): p. 32.
7. Ruggeri, F.S., et al., *AFM-Based Single Molecule Techniques: Unraveling the Amyloid Pathogenic Species.* Curr Pharm Des, 2016. **22**(26): p. 3950-70.
8. Doens, D. and P.L. Fernandez, *Microglia receptors and their implications in the response to amyloid beta for Alzheimer's disease pathogenesis.* J Neuroinflammation, 2014. **11**: p. 48.
9. Wang, Y.J., H.D. Zhou, and X.F. Zhou, *Clearance of amyloid-beta in Alzheimer's disease: progress, problems and perspectives.* Drug Discov Today, 2006. **11**(19-20): p. 931-8.
10. Patterson, C., et al., *Diagnosis and treatment of dementia: 1. Risk assessment and primary prevention of Alzheimer disease.* CMAJ, 2008. **178**(5): p. 548-56.
11. Michetti, F., et al., *The S100B story: from biomarker to active factor in neural injury.* J Neurochem, 2019. **148**(2): p. 168-187.
12. Esposito, Z., et al., *Amyloid beta, glutamate, excitotoxicity in Alzheimer's disease: are we on the right track?* CNS Neurosci Ther, 2013. **19**(8): p. 549-55.
13. Blennow, K., et al., *Amyloid biomarkers in Alzheimer's disease.* Trends Pharmacol Sci, 2015. **36**(5): p. 297-309.
14. Barage, S.H. and K.D. Sonawane, *Amyloid cascade hypothesis: Pathogenesis and therapeutic strategies in Alzheimer's disease.* Neuropeptides, 2015. **52**: p. 1-18.
15. Citron, M., *Strategies for disease modification in Alzheimer's disease.* Nature Reviews Neuroscience, 2004. **5**(9): p. 677-685.
16. Duyckaerts, C., B. Delatour, and M.C. Potier, *Classification and basic pathology of Alzheimer disease.* Acta Neuropathol, 2009. **118**(1): p. 5-36.
17. Perl, D.P., *Neuropathology of Alzheimer's disease.* Mt Sinai J Med, 2010. **77**(1): p. 32-42.
18. Apostolova, L.G., et al., *Hippocampal atrophy and ventricular enlargement in normal aging, mild cognitive impairment (MCI), and Alzheimer Disease.* Alzheimer Dis Assoc Disord, 2012. **26**(1): p. 17-27.
19. Serrano-Pozo, A., et al., *Neuropathological alterations in Alzheimer disease.* Cold Spring Harb Perspect Med, 2011. **1**(1): p. a006189.
20. Thal, D.R., et al., *Phases of A beta-deposition in the human brain and its relevance for the development of AD.* Neurology, 2002. **58**(12): p. 1791-800.
21. Wolfe, M.S., *The role of tau in neurodegenerative diseases and its potential as a therapeutic target.* Scientifica (Cairo), 2012. **2012**: p. 796024.
22. Binder, L.I., A. Frankfurter, and L.I. Rebhun, *The distribution of tau in the mammalian central nervous system.* J Cell Biol, 1985. **101**(4): p. 1371-8.
23. Dixit, R., et al., *Differential regulation of dynein and kinesin motor proteins by tau.* Science, 2008. **319**(5866): p. 1086-9.
24. Weingarten, M.D., et al., *A protein factor essential for microtubule assembly.* Proc Natl Acad Sci U S A, 1975. **72**(5): p. 1858-62.
25. Martin, L., X. Latypova, and F. Terro, *Post-translational modifications of tau protein: implications for Alzheimer's disease.* Neurochem Int, 2011. **58**(4): p. 458-71.

26. Morishima-Kawashima, M., et al., *Proline-directed and non-proline-directed phosphorylation of PHF-tau.* J Biol Chem, 1995. **270**(2): p. 823-9.
27. Alonso, A., et al., *Hyperphosphorylation induces self-assembly of tau into tangles of paired helical filaments/straight filaments.* Proc Natl Acad Sci U S A, 2001. **98**(12): p. 6923-8.
28. Rankin, C.A., Q. Sun, and T.C. Gamblin, *Tau phosphorylation by GSK-3beta promotes tangle-like filament morphology.* Mol Neurodegener, 2007. **2**: p. 12.
29. Zhu, X., et al., *Activation of p38 kinase links tau phosphorylation, oxidative stress, and cell cycle-related events in Alzheimer disease.* J Neuropathol Exp Neurol, 2000. **59**(10): p. 880-8.
30. Wilquet, V. and B. De Strooper, *Amyloid-beta precursor protein processing in neurodegeneration.* Curr Opin Neurobiol, 2004. **14**(5): p. 582-8.
31. Babu, M.M., *The contribution of intrinsically disordered regions to protein function, cellular complexity, and human disease.* Biochem Soc Trans, 2016. **44**(5): p. 1185-1200.
32. Michaels, T.C.T., et al., *Chemical Kinetics for Bridging Molecular Mechanisms and Macroscopic Measurements of Amyloid Fibril Formation.* Annu Rev Phys Chem, 2018. **69**: p. 273-298.
33. Galvagnion, C., et al., *Lipid vesicles trigger alpha-synuclein aggregation by stimulating primary nucleation.* European Biophysics Journal with Biophysics Letters, 2015. **44**: p. S101-S101.
34. Tornquist, M., et al., *Secondary nucleation in amyloid formation.* Chem Commun (Camb), 2018. **54**(63): p. 8667-8684.
35. Meisl, G., et al., *Differences in nucleation behavior underlie the contrasting aggregation kinetics of the Abeta40 and Abeta42 peptides.* Proc Natl Acad Sci U S A, 2014. **111**(26): p. 9384-9.
36. Sowade, R.F. and T.R. Jahn, *Seed-induced acceleration of amyloid-beta mediated neurotoxicity in vivo.* Nat Commun, 2017. **8**(1): p. 512.
37. Morales, R., et al., *Titration of biologically active amyloid-beta seeds in a transgenic mouse model of Alzheimer's disease.* Sci Rep, 2015. **5**: p. 9349.
38. Hardy, J.A. and G.A. Higgins, *Alzheimer's disease: the amyloid cascade hypothesis.* Science, 1992. **256**(5054): p. 184-5.
39. Lin, Y.T., et al., *APOE4 Causes Widespread Molecular and Cellular Alterations Associated with Alzheimer's Disease Phenotypes in Human iPSC-Derived Brain Cell Types.* Neuron, 2018. **98**(6): p. 1141-1154 e7.
40. Reitz, C., *Alzheimer's disease and the amyloid cascade hypothesis: a critical review.* Int J Alzheimers Dis, 2012. **2012**: p. 369808.
41. Gendron, T.F. and L. Petrucelli, *The role of tau in neurodegeneration.* Mol Neurodegener, 2009. **4**: p. 13.
42. Xin, S.-H., et al., *Clearance of Amyloid Beta and Tau in Alzheimer's Disease: from Mechanisms to Therapy.* Neurotoxicity Research, 2018. **34**(3): p. 733-748.
43. Van Eldik, L.J., et al., *Glia Proinflammatory Cytokine Upregulation as a Therapeutic Target for Neurodegenerative Diseases: Function-Based and Target-Based Discovery Approaches*, in *Neuroinflammation in Neuronal Death and Repair*. 2007. p. 277-296.
44. Martinez-Vicente, M. and A.M. Cuervo, *Autophagy and neurodegeneration: when the cleaning crew goes on strike.* The Lancet Neurology, 2007. **6**(4): p. 352-361.
45. Vilchez, D., I. Saez, and A. Dillin, *The role of protein clearance mechanisms in organismal ageing and age-related diseases.* Nat Commun, 2014. **5**: p. 5659.
46. Simonovitch, S., et al., *Impaired Autophagy in APOE4 Astrocytes.* J Alzheimers Dis, 2016. **51**(3): p. 915-27.
47. Iwata, N., et al., *Identification of the major Abeta1-42-degrading catabolic pathway in brain parenchyma: suppression leads to biochemical and pathological deposition.* Nat Med, 2000. **6**(2): p. 143-50.
48. Yasojima, K., et al., *Reduced neprilysin in high plaque areas of Alzheimer brain: a possible relationship to deficient degradation of beta-amyloid peptide.* Neurosci Lett, 2001. **297**(2): p. 97-100.

49. Madani, R., et al., *Lack of neprilysin suffices to generate murine amyloid-like deposits in the brain and behavioral deficit in vivo.* J Neurosci Res, 2006. **84**(8): p. 1871-8.
50. El-Amouri, S.S., et al., *Neprilysin: an enzyme candidate to slow the progression of Alzheimer's disease.* Am J Pathol, 2008. **172**(5): p. 1342-54.
51. Kurochkin, I.V. and S. Goto, *Alzheimer's beta-amyloid peptide specifically interacts with and is degraded by insulin degrading enzyme.* FEBS Lett, 1994. **345**(1): p. 33-7.
52. Farris, W., et al., *Insulin-degrading enzyme regulates the levels of insulin, amyloid beta-protein, and the beta-amyloid precursor protein intracellular domain in vivo.* Proc Natl Acad Sci U S A, 2003. **100**(7): p. 4162-7.
53. Cook, D.G., et al., *Reduced Hippocampal Insulin-Degrading Enzyme in Late-Onset Alzheimer's Disease Is Associated with the Apolipoprotein E-ε4 Allele.* The American Journal of Pathology, 2003. **162**(1): p. 313-319.
54. Lee, C.Y. and G.E. Landreth, *The role of microglia in amyloid clearance from the AD brain.* J Neural Transm (Vienna), 2010. **117**(8): p. 949-60.
55. Nakanishi, A., et al., *Amyloid beta directly interacts with NLRP3 to initiate inflammasome activation: identification of an intrinsic NLRP3 ligand in a cell-free system.* Inflamm Regen, 2018. **38**: p. 27.
56. Hickman, S.E. and J. El Khoury, *TREM2 and the neuroimmunology of Alzheimer's disease.* Biochem Pharmacol, 2014. **88**(4): p. 495-8.
57. Jonsson, T., et al., *Variant of TREM2 associated with the risk of Alzheimer's disease.* N Engl J Med, 2013. **368**(2): p. 107-16.
58. Cheng-Hathaway, P.J., et al., *The Trem2 R47H variant confers loss-of-function-like phenotypes in Alzheimer's disease.* Mol Neurodegener, 2018. **13**(1): p. 29.
59. Arancio, O., et al., *RAGE potentiates Abeta-induced perturbation of neuronal function in transgenic mice.* EMBO J, 2004. **23**(20): p. 4096-105.
60. Takuma, K., et al., *RAGE-mediated signaling contributes to intraneuronal transport of amyloid-beta and neuronal dysfunction.* Proc Natl Acad Sci U S A, 2009. **106**(47): p. 20021-6.
61. Sturchler, E., et al., *Site-specific blockade of RAGE-Vd prevents amyloid-beta oligomer neurotoxicity.* J Neurosci, 2008. **28**(20): p. 5149-58.
62. Zhao, Z., et al., *Central role for PICALM in amyloid-beta blood-brain barrier transcytosis and clearance.* Nat Neurosci, 2015. **18**(7): p. 978-87.
63. van Assema, D.M. and B.N. van Berckel, *Blood-Brain Barrier ABC-transporter P-glycoprotein in Alzheimer's Disease: Still a Suspect?* Curr Pharm Des, 2016. **22**(38): p. 5808-5816.
64. Deane, R., et al., *RAGE mediates amyloid-beta peptide transport across the blood-brain barrier and accumulation in brain.* Nat Med, 2003. **9**(7): p. 907-13.
65. Wolfe, K.J. and D.M. Cyr, *Amyloid in neurodegenerative diseases: friend or foe?* Semin Cell Dev Biol, 2011. **22**(5): p. 476-81.
66. Olzscha, H., et al., *Amyloid-like aggregates sequester numerous metastable proteins with essential cellular functions.* Cell, 2011. **144**(1): p. 67-78.
67. Banerjee, S., et al., *Tau protein- induced sequestration of the eukaryotic ribosome: Implications in neurodegenerative disease.* Sci Rep, 2020. **10**(1): p. 5225.
68. Mattson, M.P., K.J. Tomaselli, and R.E. Rydel, *Calcium-destabilizing and neurodegenerative effects of aggregated beta-amyloid peptide are attenuated by basic FGF.* Brain Res, 1993. **621**(1): p. 35-49.
69. Behl, C., et al., *Hydrogen peroxide mediates amyloid beta protein toxicity.* Cell, 1994. **77**(6): p. 817-27.
70. Loo, D.T., et al., *Apoptosis is induced by beta-amyloid in cultured central nervous system neurons.* Proc Natl Acad Sci U S A, 1993. **90**(17): p. 7951-5.
71. Yaar, M., et al., *Binding of beta-amyloid to the p75 neurotrophin receptor induces apoptosis. A possible mechanism for Alzheimer's disease.* J Clin Invest, 1997. **100**(9): p. 2333-40.
72. Lorenzo, A., et al., *Amyloid beta interacts with the amyloid precursor protein: a potential toxic mechanism in Alzheimer's disease.* Nat Neurosci, 2000. **3**(5): p. 460-4.

73. Yan, S.D., et al., *RAGE and Alzheimer's disease: a progression factor for amyloid-beta-induced cellular perturbation?* J Alzheimers Dis, 2009. **16**(4): p. 833-43.
74. Yan, S.D., et al., *RAGE and amyloid-beta peptide neurotoxicity in Alzheimer's disease.* Nature, 1996. **382**(6593): p. 685-91.
75. Yuan, J. and B.A. Yankner, *Apoptosis in the nervous system.* Nature, 2000. **407**(6805): p. 802-9.
76. Swerdlow, R.H., *Mitochondria and cell bioenergetics: increasingly recognized components and a possible etiologic cause of Alzheimer's disease.* Antioxid Redox Signal, 2012. **16**(12): p. 1434-55.
77. Flannery, P.J. and E. Trushina, *Mitochondrial Dysfunction in Alzheimer's Disease and Progress in Mitochondria-Targeted Therapeutics.* Current Behavioral Neuroscience Reports, 2019. **6**(3): p. 88-102.
78. Wang, X., et al., *Oxidative stress and mitochondrial dysfunction in Alzheimer's disease.* Biochim Biophys Acta, 2014. **1842**(8): p. 1240-7.
79. Cheng, Y. and F. Bai, *The Association of Tau With Mitochondrial Dysfunction in Alzheimer's Disease.* Front Neurosci, 2018. **12**: p. 163.
80. Moreira, P.I., et al., *Mitochondrial dysfunction is a trigger of Alzheimer's disease pathophysiology.* Biochim Biophys Acta, 2010. **1802**(1): p. 2-10.
81. McKenna, M.C., *Glutamate metabolism in primary cultures of rat brain astrocytes: rationale and initial efforts toward developing a compartmental model.* Adv Exp Med Biol, 2003. **537**: p. 317-41.
82. Rosenberg, P.A. and E. Aizenman, *Hundred-fold increase in neuronal vulnerability to glutamate toxicity in astrocyte-poor cultures of rat cerebral cortex.* Neurosci Lett, 1989. **103**(2): p. 162-8.
83. Danysz, W. and C.G. Parsons, *Alzheimer's disease, beta-amyloid, glutamate, NMDA receptors and memantine--searching for the connections.* Br J Pharmacol, 2012. **167**(2): p. 324-52.
84. Wang, R. and P.H. Reddy, *Role of Glutamate and NMDA Receptors in Alzheimer's Disease.* J Alzheimers Dis, 2017. **57**(4): p. 1041-1048.
85. Rudy, C.C., et al., *The role of the tripartite glutamatergic synapse in the pathophysiology of Alzheimer's disease.* Aging Dis, 2015. **6**(2): p. 131-48.
86. Lacor, P.N., et al., *Abeta oligomer-induced aberrations in synapse composition, shape, and density provide a molecular basis for loss of connectivity in Alzheimer's disease.* J Neurosci, 2007. **27**(4): p. 796-807.
87. De Felice, F.G., et al., *Abeta oligomers induce neuronal oxidative stress through an N-methyl-D-aspartate receptor-dependent mechanism that is blocked by the Alzheimer drug memantine.* J Biol Chem, 2007. **282**(15): p. 11590-601.
88. Biasiotto, G., et al., *Iron and Neurodegeneration: Is Ferritinophagy the Link?* Mol Neurobiol, 2016. **53**(8): p. 5542-74.
89. Bartzokis, G., et al., *In vivo evaluation of brain iron in Alzheimer's disease and normal subjects using MRI.* Biol Psychiatry, 1994. **35**(7): p. 480-7.
90. Falangola, M.F., et al., *Histological co-localization of iron in Abeta plaques of PS/APP transgenic mice.* Neurochem Res, 2005. **30**(2): p. 201-5.
91. Rogers, J.T., et al., *An iron-responsive element type II in the 5'-untranslated region of the Alzheimer's amyloid precursor protein transcript.* J Biol Chem, 2002. **277**(47): p. 45518-28.
92. Liu, B., et al., *Iron promotes the toxicity of amyloid beta peptide by impeding its ordered aggregation.* J Biol Chem, 2011. **286**(6): p. 4248-56.
93. Li, Y., et al., *Biometal Dyshomeostasis and Toxic Metal Accumulations in the Development of Alzheimer's Disease.* Front Mol Neurosci, 2017. **10**: p. 339.
94. Vaz, F.N.C., et al., *The Relationship Between Copper, Iron, and Selenium Levels and Alzheimer Disease.* Biol Trace Elem Res, 2018. **181**(2): p. 185-191.
95. Jin, L., et al., *Copper inducing Abeta42 rather than Abeta40 nanoscale oligomer formation is the key process for Abeta neurotoxicity.* Nanoscale, 2011. **3**(11): p. 4746-51.
96. Lovell, M.A., et al., *Copper, iron and zinc in Alzheimer's disease senile plaques.* J Neurol Sci, 1998. **158**(1): p. 47-52.

97. Kim, A.C., S. Lim, and Y.K. Kim, *Metal Ion Effects on Abeta and Tau Aggregation.* Int J Mol Sci, 2018. **19**(1).
98. Guo, J., et al., *Kinetic Insights into Zn(2+)-Induced Amyloid beta-Protein Aggregation Revealed by Stopped-Flow Fluorescence Spectroscopy.* J Phys Chem B, 2017. **121**(16): p. 3909-3917.
99. Mannini, B., et al., *Stabilization and Characterization of Cytotoxic Abeta40 Oligomers Isolated from an Aggregation Reaction in the Presence of Zinc Ions.* ACS Chem Neurosci, 2018. **9**(12): p. 2959-2971.
100. Solomonov, I., et al., *Zn2+-Abeta40 complexes form metastable quasi-spherical oligomers that are cytotoxic to cultured hippocampal neurons.* J Biol Chem, 2012. **287**(24): p. 20555-64.
101. Crouch, P.J., et al., *Restored degradation of the Alzheimer's amyloid-beta peptide by targeting amyloid formation.* J Neurochem, 2009. **108**(5): p. 1198-207.
102. Wang, C.Y., et al., *Zinc overload enhances APP cleavage and Abeta deposition in the Alzheimer mouse brain.* PLoS One, 2010. **5**(12): p. e15349.
103. Kinney, J.W., et al., *Inflammation as a central mechanism in Alzheimer's disease.* Alzheimers Dement (N Y), 2018. **4**: p. 575-590.
104. Jack, C.R., et al., *Tracking pathophysiological processes in Alzheimer's disease: an updated hypothetical model of dynamic biomarkers.* The Lancet Neurology, 2013. **12**(2): p. 207-216.
105. De Strooper, B. and E. Karran, *The Cellular Phase of Alzheimer's Disease.* Cell, 2016. **164**(4): p. 603-15.
106. Eikelenboom, P., et al., *Neuroinflammation - an early event in both the history and pathogenesis of Alzheimer's disease.* Neurodegener Dis, 2010. **7**(1-3): p. 38-41.
107. Rodriguez-Vieitez, E., et al., *Diverging longitudinal changes in astrocytosis and amyloid PET in autosomal dominant Alzheimer's disease.* Brain, 2016. **139**(Pt 3): p. 922-36.
108. Parachikova, A., et al., *Inflammatory changes parallel the early stages of Alzheimer disease.* Neurobiol Aging, 2007. **28**(12): p. 1821-33.
109. Janelsins, M.C., et al., *Early correlation of microglial activation with enhanced tumor necrosis factor-alpha and monocyte chemoattractant protein-1 expression specifically within the entorhinal cortex of triple transgenic Alzheimer's disease mice.* J Neuroinflammation, 2005. **2**: p. 23.
110. Heneka, M.T., et al., *Focal glial activation coincides with increased BACE1 activation and precedes amyloid plaque deposition in APP[V717I] transgenic mice.* J Neuroinflammation, 2005. **2**: p. 22.
111. Ferretti, M.T., et al., *Intracellular Abeta-oligomers and early inflammation in a model of Alzheimer's disease.* Neurobiol Aging, 2012. **33**(7): p. 1329-42.
112. Hanzel, C.E., et al., *Neuronal driven pre-plaque inflammation in a transgenic rat model of Alzheimer's disease.* Neurobiol Aging, 2014. **35**(10): p. 2249-62.
113. Akiyama, H., *Inflammatory response in Alzheimer's disease.* Tohoku J Exp Med, 1994. **174**(3): p. 295-303.
114. Krabbe, G., et al., *Functional impairment of microglia coincides with Beta-amyloid deposition in mice with Alzheimer-like pathology.* PLoS One, 2013. **8**(4): p. e60921.
115. Heneka, M.T., et al., *Neuroinflammation in Alzheimer's disease.* The Lancet Neurology, 2015. **14**(4): p. 388-405.
116. Kato, S., et al., *Confocal observation of senile plaques in Alzheimer's disease: senile plaque morphology and relationship between senile plaques and astrocytes.* Pathol Int, 1998. **48**(5): p. 332-40.
117. Wang, X., et al., *Resolution of inflammation is altered in Alzheimer's disease.* Alzheimers Dement, 2015. **11**(1): p. 40-50 e1-2.
118. Augusto-Oliveira, M., et al., *What Do Microglia Really Do in Healthy Adult Brain?* Cells, 2019. **8**(10).
119. Ennerfelt, H.E. and J.R. Lukens, *The role of innate immunity in Alzheimer's disease.* Immunol Rev, 2020.

120. Lui, H., et al., *Progranulin Deficiency Promotes Circuit-Specific Synaptic Pruning by Microglia via Complement Activation.* Cell, 2016. **165**(4): p. 921-35.
121. Hickman, S., et al., *Microglia in neurodegeneration.* Nat Neurosci, 2018. **21**(10): p. 1359-1369.
122. Bachiller, S., et al., *Microglia in Neurological Diseases: A Road Map to Brain-Disease Dependent-Inflammatory Response.* Front Cell Neurosci, 2018. **12**: p. 488.
123. Grabert, K., et al., *Microglial brain region-dependent diversity and selective regional sensitivities to aging.* Nat Neurosci, 2016. **19**(3): p. 504-16.
124. Hemonnot, A.L., et al., *Microglia in Alzheimer Disease: Well-Known Targets and New Opportunities.* Front Aging Neurosci, 2019. **11**: p. 233.
125. Griffin, W.S., et al., *Brain interleukin 1 and S-100 immunoreactivity are elevated in Down syndrome and Alzheimer disease.* Proc Natl Acad Sci U S A, 1989. **86**(19): p. 7611-5.
126. Heneka, M.T., et al., *NLRP3 is activated in Alzheimer's disease and contributes to pathology in APP/PS1 mice.* Nature, 2013. **493**(7434): p. 674-8.
127. Keren-Shaul, H., et al., *A Unique Microglia Type Associated with Restricting Development of Alzheimer's Disease.* Cell, 2017. **169**(7): p. 1276-1290 e17.
128. Liddelow, S.A., S.E. Marsh, and B. Stevens, *Microglia and Astrocytes in Disease: Dynamic Duo or Partners in Crime?* Trends Immunol, 2020. **41**(9): p. 820-835.
129. Bohlen, C.J., et al., *Diverse Requirements for Microglial Survival, Specification, and Function Revealed by Defined-Medium Cultures.* Neuron, 2017. **94**(4): p. 759-773 e8.
130. Mishra, A., et al., *Astrocytes mediate neurovascular signaling to capillary pericytes but not to arterioles.* Nat Neurosci, 2016. **19**(12): p. 1619-1627.
131. Perez-Nievas, B.G. and A. Serrano-Pozo, *Deciphering the Astrocyte Reaction in Alzheimer's Disease.* Front Aging Neurosci, 2018. **10**: p. 114.
132. Winkler, E.A., A.P. Sagare, and B.V. Zlokovic, *The pericyte: a forgotten cell type with important implications for Alzheimer's disease?* Brain Pathol, 2014. **24**(4): p. 371-86.
133. Bell, R.D., et al., *Apolipoprotein E controls cerebrovascular integrity via cyclophilin A.* Nature, 2012. **485**(7399): p. 512-6.
134. Allen, N.J., *Astrocyte regulation of synaptic behavior.* Annu Rev Cell Dev Biol, 2014. **30**: p. 439-63.
135. Hong, S., et al., *Complement and microglia mediate early synapse loss in Alzheimer mouse models.* Science, 2016. **352**(6286): p. 712-716.
136. Gomez-Arboledas, A., et al., *Phagocytic clearance of presynaptic dystrophies by reactive astrocytes in Alzheimer's disease.* Glia, 2018. **66**(3): p. 637-653.
137. Iram, T., et al., *Astrocytes from old Alzheimer's disease mice are impaired in Abeta uptake and in neuroprotection.* Neurobiol Dis, 2016. **96**: p. 84-94.
138. Liu, C.C., et al., *Astrocytic LRP1 Mediates Brain Abeta Clearance and Impacts Amyloid Deposition.* J Neurosci, 2017. **37**(15): p. 4023-4031.
139. Zhao, J., T. O'Connor, and R. Vassar, *The contribution of activated astrocytes to Abeta production: implications for Alzheimer's disease pathogenesis.* J Neuroinflammation, 2011. **8**: p. 150.
140. Sadleir, K.R., et al., *Presynaptic dystrophic neurites surrounding amyloid plaques are sites of microtubule disruption, BACE1 elevation, and increased Abeta generation in Alzheimer's disease.* Acta Neuropathol, 2016. **132**(2): p. 235-256.
141. Orre, M., et al., *Isolation of glia from Alzheimer's mice reveals inflammation and dysfunction.* Neurobiol Aging, 2014. **35**(12): p. 2746-2760.
142. Boisvert, M.M., et al., *The Aging Astrocyte Transcriptome from Multiple Regions of the Mouse Brain.* Cell Rep, 2018. **22**(1): p. 269-285.
143. Sekar, S., et al., *Alzheimer's disease is associated with altered expression of genes involved in immune response and mitochondrial processes in astrocytes.* Neurobiol Aging, 2015. **36**(2): p. 583-91.
144. Zamanian, J.L., et al., *Genomic analysis of reactive astrogliosis.* J Neurosci, 2012. **32**(18): p. 6391-410.

145. Liddelow, S.A. and B.A. Barres, *Reactive Astrocytes: Production, Function, and Therapeutic Potential.* Immunity, 2017. **46**(6): p. 957-967.
146. Lian, H., et al., *NFkappaB-activated astroglial release of complement C3 compromises neuronal morphology and function associated with Alzheimer's disease.* Neuron, 2015. **85**(1): p. 101-115.
147. Rahpeymai, Y., et al., *Complement: a novel factor in basal and ischemia-induced neurogenesis.* EMBO J, 2006. **25**(6): p. 1364-74.
148. Mattson, M.P. and M.K. Meffert, *Roles for NF-kappaB in nerve cell survival, plasticity, and disease.* Cell Death Differ, 2006. **13**(5): p. 852-60.
149. Liu, F., et al., *Truncation and activation of calcineurin A by calpain I in Alzheimer disease brain.* J Biol Chem, 2005. **280**(45): p. 37755-62.
150. Dineley, K.T., et al., *Acute inhibition of calcineurin restores associative learning and memory in Tg2576 APP transgenic mice.* Neurobiol Learn Mem, 2007. **88**(2): p. 217-24.
151. Norris, C.M., et al., *Calcineurin triggers reactive/inflammatory processes in astrocytes and is upregulated in aging and Alzheimer's models.* J Neurosci, 2005. **25**(18): p. 4649-58.
152. Merlini, M., et al., *Vascular beta-amyloid and early astrocyte alterations impair cerebrovascular function and cerebral metabolism in transgenic arcAbeta mice.* Acta Neuropathol, 2011. **122**(3): p. 293-311.
153. Hawkes, C.A., et al., *Perivascular drainage of solutes is impaired in the ageing mouse brain and in the presence of cerebral amyloid angiopathy.* Acta Neuropathol, 2011. **121**(4): p. 431-43.
154. Wilcock, D.M., M.P. Vitek, and C.A. Colton, *Vascular amyloid alters astrocytic water and potassium channels in mouse models and humans with Alzheimer's disease.* Neuroscience, 2009. **159**(3): p. 1055-69.
155. Hawkes, C.A., et al., *Failure of perivascular drainage of beta-amyloid in cerebral amyloid angiopathy.* Brain Pathol, 2014. **24**(4): p. 396-403.
156. Xu, Z., et al., *Deletion of aquaporin-4 in APP/PS1 mice exacerbates brain Abeta accumulation and memory deficits.* Mol Neurodegener, 2015. **10**: p. 58.
157. Rodriguez, J.J., et al., *Complex and differential glial responses in Alzheimer's disease and ageing.* Curr Alzheimer Res, 2016. **13**(4): p. 343-58.
158. Meraz-Rios, M.A., et al., *Inflammatory process in Alzheimer's Disease.* Front Integr Neurosci, 2013. **7**: p. 59.
159. Murgas, P., B. Godoy, and R. von Bernhardi, *Abeta potentiates inflammatory activation of glial cells induced by scavenger receptor ligands and inflammatory mediators in culture.* Neurotox Res, 2012. **22**(1): p. 69-78.
160. Coraci, I.S., et al., *CD36, a class B scavenger receptor, is expressed on microglia in Alzheimer's disease brains and can mediate production of reactive oxygen species in response to beta-amyloid fibrils.* Am J Pathol, 2002. **160**(1): p. 101-12.
161. Godoy, B., et al., *Scavenger receptor class A ligands induce secretion of IL1beta and exert a modulatory effect on the inflammatory activation of astrocytes in culture.* J Neuroimmunol, 2012. **251**(1-2): p. 6-13.
162. Yang, C.N., et al., *Mechanism mediating oligomeric Abeta clearance by naive primary microglia.* Neurobiol Dis, 2011. **42**(3): p. 221-30.
163. Hickman, S.E., E.K. Allison, and J. El Khoury, *Microglial dysfunction and defective beta-amyloid clearance pathways in aging Alzheimer's disease mice.* J Neurosci, 2008. **28**(33): p. 8354-60.
164. El Khoury, J.B., et al., *CD36 mediates the innate host response to beta-amyloid.* J Exp Med, 2003. **197**(12): p. 1657-66.
165. Ricciarelli, R., et al., *CD36 overexpression in human brain correlates with beta-amyloid deposition but not with Alzheimer's disease.* Free Radic Biol Med, 2004. **36**(8): p. 1018-24.
166. Bamberger, M.E., et al., *A cell surface receptor complex for fibrillar beta-amyloid mediates microglial activation.* J Neurosci, 2003. **23**(7): p. 2665-74.
167. Stewart, C.R., et al., *CD36 ligands promote sterile inflammation through assembly of a Toll-like receptor 4 and 6 heterodimer.* Nat Immunol, 2010. **11**(2): p. 155-61.

168. Lien, E., et al., *Toll-like receptor 4 imparts ligand-specific recognition of bacterial lipopolysaccharide.* J Clin Invest, 2000. **105**(4): p. 497-504.
169. Fassbender, K., et al., *The LPS receptor (CD14) links innate immunity with Alzheimer's disease.* FASEB J, 2004. **18**(1): p. 203-5.
170. Liu, Y., et al., *LPS receptor (CD14): a receptor for phagocytosis of Alzheimer's amyloid peptide.* Brain, 2005. **128**(Pt 8): p. 1778-89.
171. Walter, S., et al., *Role of the toll-like receptor 4 in neuroinflammation in Alzheimer's disease.* Cell Physiol Biochem, 2007. **20**(6): p. 947-56.
172. Jana, M., C.A. Palencia, and K. Pahan, *Fibrillar amyloid-beta peptides activate microglia via TLR2: implications for Alzheimer's disease.* J Immunol, 2008. **181**(10): p. 7254-62.
173. Liu, S., et al., *TLR2 is a primary receptor for Alzheimer's amyloid beta peptide to trigger neuroinflammatory activation.* J Immunol, 2012. **188**(3): p. 1098-107.
174. Halle, A., et al., *The NALP3 inflammasome is involved in the innate immune response to amyloid-beta.* Nat Immunol, 2008. **9**(8): p. 857-65.
175. Sheedy, F.J., et al., *CD36 coordinates NLRP3 inflammasome activation by facilitating intracellular nucleation of soluble ligands into particulate ligands in sterile inflammation.* Nat Immunol, 2013. **14**(8): p. 812-20.
176. Lue, L.F., et al., *Involvement of microglial receptor for advanced glycation endproducts (RAGE) in Alzheimer's disease: identification of a cellular activation mechanism.* Exp Neurol, 2001. **171**(1): p. 29-45.
177. Origlia, N., et al., *Receptor for advanced glycation end product-dependent activation of p38 mitogen-activated protein kinase contributes to amyloid-beta-mediated cortical synaptic dysfunction.* J Neurosci, 2008. **28**(13): p. 3521-30.
178. Fang, F., et al., *RAGE-dependent signaling in microglia contributes to neuroinflammation, Abeta accumulation, and impaired learning/memory in a mouse model of Alzheimer's disease.* FASEB J, 2010. **24**(4): p. 1043-55.
179. Maccioni, R.B., et al., *The role of neuroimmunomodulation in Alzheimer's disease.* Ann N Y Acad Sci, 2009. **1153**: p. 240-6.
180. Hu, J., et al., *Amyloid-beta peptide activates cultured astrocytes: morphological alterations, cytokine induction and nitric oxide release.* Brain Res, 1998. **785**(2): p. 195-206.
181. Pena, L.A., C.W. Brecher, and D.R. Marshak, *beta-Amyloid regulates gene expression of glial trophic substance S100 beta in C6 glioma and primary astrocyte cultures.* Brain Res Mol Brain Res, 1995. **34**(1): p. 118-26.
182. Li, C., et al., *Astrocytes: implications for neuroinflammatory pathogenesis of Alzheimer's disease.* Curr Alzheimer Res, 2011. **8**(1): p. 67-80.
183. Koistinaho, M., et al., *Apolipoprotein E promotes astrocyte colocalization and degradation of deposited amyloid-beta peptides.* Nat Med, 2004. **10**(7): p. 719-26.
184. Haan, M.N., et al., *The role of APOE epsilon4 in modulating effects of other risk factors for cognitive decline in elderly persons.* JAMA, 1999. **282**(1): p. 40-6.
185. Yang, Z. Han, and J.J. Oppenheim, *Alarmins and immunity.* Immunol Rev, 2017. **280**(1): p. 41-56.
186. Kerkhoff, C., Y. Radon, and H. Flaßkamp, *Alarmins*, in *Encyclopedia of Inflammatory Diseases*. 2014. p. 1-12.
187. Said-Sadier, N. and D.M. Ojcius, *Alarmins, inflammasomes and immunity.* Biomed J, 2012. **35**(6): p. 437-49.
188. Chen, G.Y. and G. Nunez, *Sterile inflammation: sensing and reacting to damage.* Nat Rev Immunol, 2010. **10**(12): p. 826-37.
189. Heneka, M.T., D.T. Golenbock, and E. Latz, *Innate immunity in Alzheimer's disease.* Nat Immunol, 2015. **16**(3): p. 229-36.
190. Youm, Y.H., et al., *Canonical Nlrp3 inflammasome links systemic low-grade inflammation to functional decline in aging.* Cell Metab, 2013. **18**(4): p. 519-32.

191. Cristovao, J.S. and C.M. Gomes, *S100 Proteins in Alzheimer's Disease.* Front Neurosci, 2019. **13**: p. 463.
192. Hagmeyer, S., et al., *Distribution and Relative Abundance of S100 Proteins in the Brain of the APP23 Alzheimer's Disease Model Mice.* Front Neurosci, 2019. **13**: p. 640.
193. Venegas, C. and M.T. Heneka, *Danger-associated molecular patterns in Alzheimer's disease.* J Leukoc Biol, 2017. **101**(1): p. 87-98.
194. Sheng, J.G., R.E. Mrak, and W.S. Griffin, *S100 beta protein expression in Alzheimer disease: potential role in the pathogenesis of neuritic plaques.* J Neurosci Res, 1994. **39**(4): p. 398-404.
195. Vaneldik, L.J. and W.S.T. Griffin, *S100-Beta Expression in Alzheimers-Disease - Relation to Neuropathology in Brain-Regions.* Biochimica Et Biophysica Acta-Molecular Cell Research, 1994. **1223**(3): p. 398-403.
196. Donato, R., et al., *S100B's double life: intracellular regulator and extracellular signal.* Biochim Biophys Acta, 2009. **1793**(6): p. 1008-22.
197. Van Eldik, L.J., et al., *Neurotrophic activity of S-100 beta in cultures of dorsal root ganglia from embryonic chick and fetal rat.* Brain Res, 1991. **542**(2): p. 280-5.
198. Bhattacharyya, A., et al., *S100 is present in developing chicken neurons and Schwann cells and promotes motor neuron survival in vivo.* J Neurobiol, 1992. **23**(4): p. 451-66.
199. Huttunen, H.J., et al., *Coregulation of neurite outgrowth and cell survival by amphoterin and S100 proteins through receptor for advanced glycation end products (RAGE) activation.* J Biol Chem, 2000. **275**(51): p. 40096-105.
200. Villarreal, A., et al., *S100B alters neuronal survival and dendrite extension via RAGE-mediated NF-kappaB signaling.* J Neurochem, 2011. **117**(2): p. 321-32.
201. Businaro, R., et al., *S100B protects LAN-5 neuroblastoma cells against Abeta amyloid-induced neurotoxicity via RAGE engagement at low doses but increases Abeta amyloid neurotoxicity at high doses.* J Neurosci Res, 2006. **83**(5): p. 897-906.
202. Mrak, R.E. and W.S.T. Griffin, *The role of activated astrocytes and of the neurotrophic cytokine S100B in the pathogenesis of Alzheimer's disease.* Neurobiology of Aging, 2001. **22**(6): p. 915-922.
203. Adami, C., et al., *S100B expression in and effects on microglia.* Glia, 2001. **33**(2): p. 131-42.
204. Santos, G., et al., *Impaired oligodendrogenesis and myelination by elevated S100B levels during neurodevelopment.* Neuropharmacology, 2018. **129**: p. 69-83.
205. Barger, S.W. and L.J. Van Eldik, *S100 beta stimulates calcium fluxes in glial and neuronal cells.* J Biol Chem, 1992. **267**(14): p. 9689-94.
206. Xiong, Z., et al., *Enhanced calcium transients in glial cells in neonatal cerebellar cultures derived from S100B null mice.* Exp Cell Res, 2000. **257**(2): p. 281-9.
207. Brozzi, F., et al., *S100B Protein Regulates Astrocyte Shape and Migration via Interaction with Src Kinase: IMPLICATIONS FOR ASTROCYTE DEVELOPMENT, ACTIVATION, AND TUMOR GROWTH.* J Biol Chem, 2009. **284**(13): p. 8797-811.
208. Chow, S.K., et al., *Amyloid beta-peptide directly induces spontaneous calcium transients, delayed intercellular calcium waves and gliosis in rat cortical astrocytes.* ASN Neuro, 2010. **2**(1): p. e00026.
209. Hagmeyer, S., et al., *Zinc Binding to S100B Affords Regulation of Trace Metal Homeostasis and Excitotoxicity in the Brain.* Frontiers in Molecular Neuroscience, 2018. **10**.
210. Simpson, J.E., et al., *Astrocyte phenotype in relation to Alzheimer-type pathology in the ageing brain.* Neurobiol Aging, 2010. **31**(4): p. 578-90.
211. Petzold, A., et al., *Cerebrospinal fluid S100B correlates with brain atrophy in Alzheimer's disease.* Neurosci Lett, 2003. **336**(3): p. 167-70.
212. Giulian, D., et al., *Interleukin-1 injected into mammalian brain stimulates astrogliosis and neovascularization.* J Neurosci, 1988. **8**(7): p. 2485-90.
213. Sheng, J.G., et al., *In vivo and in vitro evidence supporting a role for the inflammatory cytokine interleukin-1 as a driving force in Alzheimer pathogenesis.* Neurobiol Aging, 1996. **17**(5): p. 761-6.

214. de Souza, D.F., et al., *S100B secretion is stimulated by IL-1beta in glial cultures and hippocampal slices of rats: Likely involvement of MAPK pathway.* J Neuroimmunol, 2009. **206**(1-2): p. 52-7.
215. Mrak, R.E., J.G. Sheng, and W.S. Griffin, *Correlation of astrocytic S100 beta expression with dystrophic neurites in amyloid plaques of Alzheimer's disease.* J Neuropathol Exp Neurol, 1996. **55**(3): p. 273-9.
216. Li, Y., et al., *S100 beta increases levels of beta-amyloid precursor protein and its encoding mRNA in rat neuronal cultures.* J Neurochem, 1998. **71**(4): p. 1421-8.
217. Sheng, J.G., et al., *Overexpression of the neuritotrophic cytokine S100beta precedes the appearance of neuritic beta-amyloid plaques in APPV717F mice.* J Neurochem, 2000. **74**(1): p. 295-301.
218. Roltsch, E., et al., *PSAPP mice exhibit regionally selective reductions in gliosis and plaque deposition in response to S100B ablation.* J Neuroinflammation, 2010. **7**: p. 78.
219. Mori, T., et al., *Overexpression of human S100B exacerbates cerebral amyloidosis and gliosis in the Tg2576 mouse model of Alzheimer's disease.* Glia, 2010. **58**(3): p. 300-14.
220. Baudier, J. and R.D. Cole, *Interactions between the microtubule-associated tau proteins and S100b regulate tau phosphorylation by the Ca2+/calmodulin-dependent protein kinase II.* J Biol Chem, 1988. **263**(12): p. 5876-83.
221. Sidoryk-Wegrzynowicz, M., et al., *Astrocytes in mouse models of tauopathies acquire early deficits and lose neurosupportive functions.* Acta Neuropathol Commun, 2017. **5**(1): p. 89.
222. Esposito, G., et al., *S100B induces tau protein hyperphosphorylation via Dickopff-1 up-regulation and disrupts the Wnt pathway in human neural stem cells.* J Cell Mol Med, 2008. **12**(3): p. 914-27.
223. Li, X., X. Bao, and R. Wang, *Experimental models of Alzheimer's disease for deciphering the pathogenesis and therapeutic screening (Review).* Int J Mol Med, 2016. **37**(2): p. 271-83.
224. Macias, M.P., et al., *A cellular model of amyloid precursor protein processing and amyloid-beta peptide production.* J Neurosci Methods, 2014. **223**: p. 114-22.
225. Barbati, A.C., et al., *Culture of primary rat hippocampal neurons: design, analysis, and optimization of a microfluidic device for cell seeding, coherent growth, and solute delivery.* Biomed Microdevices, 2013. **15**(1): p. 97-108.
226. Timmerman, R., S.M. Burm, and J.J. Bajramovic, *An Overview of in vitro Methods to Study Microglia.* Front Cell Neurosci, 2018. **12**: p. 242.
227. Das, A., et al., *Transcriptome sequencing reveals that LPS-triggered transcriptional responses in established microglia BV2 cell lines are poorly representative of primary microglia.* J Neuroinflammation, 2016. **13**(1): p. 182.
228. Melief, J., et al., *Characterizing primary human microglia: A comparative study with myeloid subsets and culture models.* Glia, 2016. **64**(11): p. 1857-68.
229. Israel, M.A., et al., *Probing sporadic and familial Alzheimer's disease using induced pluripotent stem cells.* Nature, 2012. **482**(7384): p. 216-20.
230. Foveau, B., et al., *Stem Cell-Derived Neurons as Cellular Models of Sporadic Alzheimer's Disease.* J Alzheimers Dis, 2019. **67**(3): p. 893-910.
231. Humpel, C., *Organotypic vibrosections from whole brain adult Alzheimer mice (overexpressing amyloid-precursor-protein with the Swedish-Dutch-Iowa mutations) as a model to study clearance of beta-amyloid plaques.* Front Aging Neurosci, 2015. **7**: p. 47.
232. Mendes, N.D., et al., *Free-floating adult human brain-derived slice cultures as a model to study the neuronal impact of Alzheimer's disease-associated Abeta oligomers.* J Neurosci Methods, 2018. **307**: p. 203-209.
233. Beach, R.L., S.L. Bathgate, and C.W. Cotman, *Identification of cell types in rat hippocampal slices maintained in organotypic cultures.* Brain Res, 1982. **255**(1): p. 3-20.
234. Humpel, C., *Organotypic brain slice cultures: A review.* Neuroscience, 2015. **305**: p. 86-98.
235. Croft, C.L., et al., *Organotypic brain slice cultures to model neurodegenerative proteinopathies.* Mol Neurodegener, 2019. **14**(1): p. 45.

236. Staal, J.A., et al., *Characterization of cortical neuronal and glial alterations during culture of organotypic whole brain slices from neonatal and mature mice.* PLoS One, 2011. **6**(7): p. e22040.
237. del Rio, J.A., et al., *Proliferation and differentiation of glial fibrillary acidic protein-immunoreactive glial cells in organotypic slice cultures of rat hippocampus.* Neuroscience, 1991. **43**(2-3): p. 335-47.
238. Hailer, N.P., J.D. Jarhult, and R. Nitsch, *Resting microglial cells in vitro: analysis of morphology and adhesion molecule expression in organotypic hippocampal slice cultures.* Glia, 1996. **18**(4): p. 319-31.
239. Harrigan, M.R., et al., *Beta amyloid is neurotoxic in hippocampal slice cultures.* Neurobiol Aging, 1995. **16**(5): p. 779-89.
240. Frozza, R.L., et al., *A comparative study of beta-amyloid peptides Abeta1-42 and Abeta25-35 toxicity in organotypic hippocampal slice cultures.* Neurochem Res, 2009. **34**(2): p. 295-303.
241. Xu, K., et al., *Glial fibrillary acidic protein is necessary for mature astrocytes to react to beta-amyloid.* Glia, 1999. **25**(4): p. 390-403.
242. Daria, A., et al., *Young microglia restore amyloid plaque clearance of aged microglia.* EMBO J, 2017. **36**(5): p. 583-603.
243. Dawson, T.M., T.E. Golde, and C. Lagier-Tourenne, *Animal models of neurodegenerative diseases.* Nat Neurosci, 2018. **21**(10): p. 1370-1379.
244. Sinnige, T., et al., *Biophysical studies of protein misfolding and aggregation in in vivo models of Alzheimer's and Parkinson's diseases.* Q Rev Biophys, 2020. **49**: p. e22.
245. Hsiao, K., et al., *Correlative memory deficits, Abeta elevation, and amyloid plaques in transgenic mice.* Science, 1996. **274**(5284): p. 99-102.
246. Oakley, H., et al., *Intraneuronal beta-amyloid aggregates, neurodegeneration, and neuron loss in transgenic mice with five familial Alzheimer's disease mutations: potential factors in amyloid plaque formation.* J Neurosci, 2006. **26**(40): p. 10129-40.
247. Oddo, S., et al., *Triple-transgenic model of Alzheimer's disease with plaques and tangles: intracellular Abeta and synaptic dysfunction.* Neuron, 2003. **39**(3): p. 409-21.
248. Botelho, H.M., G. Fritz, and C.M. Gomes, *Analysis of S100 oligomers and amyloids.* Methods Mol Biol, 2012. **849**: p. 373-86.
249. Walsh, D.M., et al., *A facile method for expression and purification of the Alzheimer's disease-associated amyloid beta-peptide.* FEBS J, 2009. **276**(5): p. 1266-81.
250. Fan, R. and A.J. Tenner, *Complement C1q expression induced by Abeta in rat hippocampal organotypic slice cultures.* Exp Neurol, 2004. **185**(2): p. 241-53.
251. Harris-White, M.E., et al., *Effects of transforming growth factor-beta (isoforms 1-3) on amyloid-beta deposition, inflammation, and cell targeting in organotypic hippocampal slice cultures.* J Neurosci, 1998. **18**(24): p. 10366-74.
252. Malouf, A.T., *Effect of beta amyloid peptides on neurons in hippocampal slice cultures.* Neurobiol Aging, 1992. **13**(5): p. 543-51.
253. Bruce, A.J., B. Malfroy, and M. Baudry, *beta-Amyloid toxicity in organotypic hippocampal cultures: protection by EUK-8, a synthetic catalytic free radical scavenger.* Proc Natl Acad Sci U S A, 1996. **93**(6): p. 2312-6.
254. Baskys, A. and Y. Adamchik, *Neuroprotective effects of extracellular glutamate are absent in hippocampal organotypic cultures treated with the amyloid peptide Abeta(25-35).* Brain Res, 2001. **907**(1-2): p. 188-94.
255. Vincent, V.A., S.P. Selwood, and G.M. Murphy, Jr., *Proinflammatory effects of M-CSF and A beta in hippocampal organotypic cultures.* Neurobiol Aging, 2002. **23**(3): p. 349-62.
256. Kim, H.J., et al., *Selective neuronal degeneration induced by soluble oligomeric amyloid beta protein.* FASEB J, 2003. **17**(1): p. 118-20.
257. Tardito, D., et al., *Long-term soluble Abeta1-40 activates CaM kinase II in organotypic hippocampal cultures.* Neurobiol Aging, 2007. **28**(9): p. 1388-95.

258. Richter, M., et al., *The neuroprotective role of microglial cells against amyloid beta-mediated toxicity in organotypic hippocampal slice cultures.* Brain Pathol, 2020. **30**(3): p. 589-602.
259. Itagaki, S., et al., *Relationship of microglia and astrocytes to amyloid deposits of Alzheimer disease.* J Neuroimmunol, 1989. **24**(3): p. 173-82.
260. Allen, Y.S., P.H. Devanathan, and G.P. Owen, *Neurotoxicity of beta-amyloid protein: cytochemical changes and apoptotic cell death investigated in organotypic cultures.* Clin Exp Pharmacol Physiol, 1995. **22**(5): p. 370-1.
261. Suh, E.C., et al., *A beta 25-35 induces presynaptic changes in organotypic hippocampal slice cultures.* Neurotoxicology, 2008. **29**(4): p. 691-9.
262. Nassif, M., et al., *Beta-amyloid peptide toxicity in organotypic hippocampal slice culture involves Akt/PKB, GSK-3beta, and PTEN.* Neurochem Int, 2007. **50**(1): p. 229-35.
263. Hu, J., A. Ferreira, and L.J. Van Eldik, *S100beta induces neuronal cell death through nitric oxide release from astrocytes.* J Neurochem, 1997. **69**(6): p. 2294-301.
264. Orellana, J.A., et al., *Amyloid beta-induced death in neurons involves glial and neuronal hemichannels.* J Neurosci, 2011. **31**(13): p. 4962-77.
265. Villarreal, A., et al., *S100B protein activates a RAGE-dependent autocrine loop in astrocytes: implications for its role in the propagation of reactive gliosis.* J Neurochem, 2014. **131**(2): p. 190-205.
266. Diaz-Aparicio, I. and A. Sierra, *C1q is related to microglial phagocytosis in the hippocampus in physiological conditions.* Matters, 2019.
267. Tamano, H., et al., *Preferential Neurodegeneration in the Dentate Gyrus by Amyloid β1–42-Induced Intracellular Zn2+Dysregulation and Its Defense Strategy.* Molecular Neurobiology, 2020. **57**(4): p. 1875-1888.
268. Sorci, G., et al., *S100B Protein, a Damage-Associated Molecular Pattern Protein in the Brain and Heart, and Beyond.* Cardiovascular Psychiatry and Neurology, 2010. **2010**: p. 1-13.
269. Bianchi, R., I. Giambanco, and R. Donato, *S100B/RAGE-dependent activation of microglia via NF-kappaB and AP-1 Co-regulation of COX-2 expression by S100B, IL-1beta and TNF-alpha.* Neurobiol Aging, 2010. **31**(4): p. 665-77.
270. Hughes, C., et al., *Beta amyloid aggregates induce sensitised TLR4 signalling causing long-term potentiation deficit and rat neuronal cell death.* Commun Biol, 2020. **3**(1): p. 79.
271. Hoyle, C., et al., *Hallmarks of NLRP3 inflammasome activation are observed in organotypic hippocampal slice culture.* Immunology, 2020. **161**(1): p. 39-52.
272. Croft, C.L. and W. Noble, *Preparation of organotypic brain slice cultures for the study of Alzheimer's disease.* F1000Res, 2018. **7**: p. 592.
273. Gotz, J. and L.M. Ittner, *Animal models of Alzheimer's disease and frontotemporal dementia.* Nat Rev Neurosci, 2008. **9**(7): p. 532-44.